

## **The voltage-gated proton channel HVCN1 modulates mitochondrial ROS production and inflammatory response in macrophages**

Emami-Shahri, Nia

For additional information about this publication click this link.

<http://qmro.qmul.ac.uk/jspui/handle/123456789/8036>

Information about this research object was correct at the time of download; we occasionally make corrections to records, please therefore check the published record when citing. For more information contact [scholarlycommunications@qmul.ac.uk](mailto:scholarlycommunications@qmul.ac.uk)

**The voltage-gated proton channel HVCN1 modulates  
mitochondrial ROS production and inflammatory response in  
macrophages**

**Nia Emami-Shahri**

**Thesis submitted to Queen Mary, University of London in fulfilment of  
the requirements for the degree of Doctor of Philosophy**

**Centre for Cancer and Inflammation**

**Barts Cancer Institute – a CRUK Centre for Excellence**

**Queen Mary, University of London**

**3<sup>rd</sup> floor, John Vane Science Centre**

**Charterhouse Square**

**London EC1M 6BQ**

## **STATEMENT OF ORIGINALITY**

I, Nia Emami-Shahri, confirm that the research included within this thesis is my own work or that where it has been carried out in collaboration with, or supported by others, that this is duly acknowledged below and my contribution indicated. Previously published material is also acknowledged below.

I attest that I have exercised reasonable care to ensure that the work is original, and does not to the best of my knowledge break any UK law, infringe any third party's copyright or other Intellectual Property Right, or contain any confidential material.

I accept that the College has the right to use plagiarism detection software to check the electronic version of the thesis.

I confirm that this thesis has not been previously submitted for the award of a degree by this or any other university.

The copyright of this thesis rests with the author and no quotation from it or information derived from it may be published without the prior written consent of the author.

Signature:

Date

## ABSTRACT

It is clear that the voltage-gated proton channel HVCN1 plays an essential role in a range of cell types, in particular immune cells. Previous published work has confirmed the existence of proton channels in both murine and human macrophages. However, the role of HVCN1 in macrophages has not been investigated. Given that the current literature on voltage-gated proton channels in immune cells has found HVCN1 to be involved in several cellular processes (such as the respiratory burst and signalling events) it is important to establish its functional role in macrophages, which are a crucial constituent of the immune system.

The aim of my thesis was to investigate the function of voltage-gated proton channels in macrophages with the use of mice with a disrupting mutation within the *Hvcn1* gene, which results in HVCN1 loss. In particular, I wanted to address how *Hvcn1*<sup>-/-</sup> macrophages responded to LPS activation. I hypothesised that HVCN1 regulates the respiratory burst of macrophages and that it potentially modulates mitochondrial ROS production, and in doing so, may affect several functional aspects of macrophage biology.

I show here that the voltage-gated proton channel, HVCN1, regulates phagocytic respiratory burst, modulates the mitochondrial ROS production and inflammatory response of macrophages. These cells also showed clear signs of mitochondrial defect as they had attenuated mitochondrial respiration. *Hvcn1*<sup>-/-</sup> macrophages had elevated basal levels of mitochondrial ROS, which resulted in the enhanced activation of the redox-sensitive MAPK and NF-κB signaling pathways. This caused

*Hvcn1*<sup>-/-</sup> macrophages to produce increased cytokine production following LPS activation. Our findings provide a new perspective for voltage-gated proton channels in immune cells and, more generally, in macrophage biology.

## **ACKNOWLEDGEMENTS**

Special thanks to my supervisor, Prof. Thorsten Hagemann, for his support and encouragement during my PhD. I am also thankful to my second supervisor, Dr. Melania Capasso, for her scientific guidance and support throughout the years.

I am eternally indebted to Dr. Eleni Maniati, Dr. Cristina Ghirelli, Lily Keane and Monica Canosa for their incredible friendship, unwavering support, and advice.

A special thank you to Richard Thompson for his help and expertise with animals; to Rozita Roshani for her kindness and help with the confocal imaging; and to Emily Mclean-Inglis for her help and encouragement.

I wish also to thank all current and previous members of the Centre for Cancer and Inflammation in particular: Maud Bossard, Juliana Candido, Gemma Everitt, Ganga Gopinathan and Ela Hondares.

Thank you to Anthony White, words cannot express my love and gratitude towards you. For your incredible love, support and patience. This is as much your thesis as it is mine because you lived through it with me.

An enormous thank you to my wonderful sister, Nilo Emami, for your love and support throughout this journey. Also, for your constant encouragement and for teaching me not to fear the unknown.

Last, but certainly not least, thank you to my amazing mother and father who are the most loving and patient parents. For their unwavering support and belief in me.

## TABLE OF CONTENTS

STATEMENT OF ORIGINALITY	ii
ABSTRACT	iii-iv
ACKNOWLEDGEMENTS	v-vi
TABLE OF CONTENTS	vii-xiii
LIST OF FIGURES	xiii-xv
LIST OF TABLES	xvi
ABBREVIATIONS	xvii-xxii
<b>1 CHAPTER ONE: INTRODUCTION</b>	<b>21</b>
<b>CHAPTER ONE: INTRODUCTION</b>	<b>21</b>
<b>1.1 THE IMMUNE SYSTEM</b>	<b>22</b>
<b>1.2 MONONUCLEAR PHAGOCYTE SYSTEM</b>	<b>25</b>
<b>1.3 CELLULAR ORIGINS OF TISSUE-RESIDENT MACROPHAGES</b>	<b>28</b>
<b>1.4 MACROPHAGE ACTIVATION</b>	<b>32</b>
1.4.1 CLASSICAL MACROPHAGE ACTIVATION	32
1.4.2 ALTERNATIVE MACROPHAGE ACTIVATION	33
1.4.3 REGULATORY MACROPHAGE ACTIVATION	37
<b>1.5 MACROPHAGES IN TISSUE HOMEOSTASIS</b>	<b>39</b>
<b>1.6 MACROPHAGES IN TISSUE INJURY</b>	<b>41</b>
<b>1.7 MACROPHAGES IN DISEASE</b>	<b>43</b>
<b>1.8 VOLTAGE-GATED PROTON CHANNELS</b>	<b>45</b>
<b>1.9 THE ROLE OF HVCN1 IN IMMUNE CELLS</b>	<b>48</b>
1.9.1 POLYMORPHONUCLEAR LEUKOCYTES	48
1.9.1.1 NEUTROPHILS	48
1.9.1.2 EOSINOPHILS	49
1.9.1.3 BASOPHILS	51
1.9.2 MONONUCLEAR LEUKOCYTES	51
1.9.2.1 B CELLS	51
1.9.2.2 T CELLS	54
1.9.2.3 DENDRITIC CELLS	55
1.9.2.4 MACROPHAGES	56
<b>1.10 CELLULAR METABOLISM</b>	<b>58</b>

1.10.1	GLYCOLYSIS	59
1.10.2	OXIDATIVE PHOSPHORYLATION	61
<b>1.11</b>	<b>IMMUNOMETABOLISM</b>	<b>64</b>
1.11.1	GRANULOCYTES	64
1.11.2	DENDRITIC CELLS	65
1.11.3	T CELLS	66
1.11.4	B CELLS	67
1.11.5	MACROPHAGES	67
<b>1.12</b>	<b>REDOX REGULATION OF CELLULAR SIGNALLING</b>	<b>68</b>
1.12.1	SOURCES OF REACTIVE OXYGEN SPECIES	68
1.12.2	ANTIOXIDANT SYSTEMS AND REGULATION OF MITOCHONDRIAL ROS	72
1.12.3	REDOX SIGNALLING	74
<b>1.13</b>	<b>THESIS AIMS</b>	<b>77</b>
<b>2</b>	<b>CHAPTER TWO: MATERIALS AND METHODS</b>	<b>79</b>
<b>2.1</b>	<b>TRANSGENIC ANIMALS</b>	<b>80</b>
<b>2.2</b>	<b>TISSUE CULTURE</b>	<b>81</b>
2.2.1	GENERATION OF BONE MARROW-DERIVED MACROPHAGES	81
<b>2.3</b>	<b>PROTEIN ANALYSIS</b>	<b>82</b>
2.3.1	PROTEIN EXTRACTION	82
2.3.2	PROTEIN QUANTIFICATION	82
2.3.3	WESTERN BLOT	83
2.3.4	ENZYME-LINKED IMMUNOSORBENT ASSAY (ELISA)	87
<b>2.4</b>	<b>NUCEIC ACIDS</b>	<b>89</b>
2.4.1	TOTAL RNA ISOLATION	89
2.4.2	RNA QUANTIFICATION AND QUALITY CONTROL	90
2.4.3	CDNA SYNTHESIS	90
2.4.4	QUANTITATIVE REAL TIME POLYMERASE CHAIN REACTION (QRT-PCR)	91
<b>2.5</b>	<b>CELLULAR BIOENERGETICS</b>	<b>94</b>
2.5.1	XF CELL TECHNOLOGY	94
2.5.2	XF CELL ASSAY	95
<b>2.6</b>	<b>FLOW CYTOMETRY</b>	<b>97</b>
2.6.1	MITOCHONDRIAL BIOMASS	97
2.6.2	INTRACELLULAR ROS LEVELS	98
2.6.3	PHAGOCYTOSIS	98
2.6.4	MITOCHONDRIAL MEMBRANE POTENTIAL	99
<b>2.7</b>	<b>CHEMILUMINESCENCE</b>	<b>101</b>
2.7.1	ATP LEVELS	101
<b>2.8</b>	<b>CONFOCAL MICROSCOPY - IMMUNOFLUORESCENCE</b>	<b>102</b>
<b>2.9</b>	<b>STATISTICAL ANALYSIS</b>	<b>104</b>
<b>3</b>	<b>CHAPTER THREE: ELEVATED BASAL ROS AND ATTENUATED RESPIRATORY BURST IN <i>HVCN1</i><sup>-/-</sup> MACROPHAGES</b>	<b>105</b>
<b>3.1</b>	<b>INTRODUCTION</b>	<b>106</b>
<b>3.2</b>	<b>AIMS</b>	<b>108</b>
3.2.1	EXPRESSION OF HVCN1 IN MACROPHAGES	109
3.2.2	ELEVATED BASAL ROS LEVELS IN <i>Hvcn1</i> <sup>-/-</sup> MACROPHAGES	113
3.2.3	ATTENUATED REGULATION OF MITOCHONDRIAL ROS PRODUCTION	119
3.2.4	IMPAIRED RESPIRATORY BURST IN <i>Hvcn1</i> <sup>-/-</sup> MACROPHAGES	124
3.2.5	HVCN1 IS LOCALISED ON THE PLASMA MEMBRANE IN MACROPHAGES	128
<b>3.3</b>	<b>CHAPTER DISCUSSION</b>	<b>130</b>

---

<b>4</b>	<b><u>CHAPTER FOUR: ATTENUATED MITOCHONDRIAL RESPIRATION AND DIMINISHED SPARE RESPIRATORY CAPACITY IN <i>HVCN1</i><sup>-/-</sup> MACROPHAGES</u></b>	<b>133</b>
<b>4.1</b>	<b>INTRODUCTION</b>	<b>134</b>
<b>4.2</b>	<b>AIMS</b>	<b>136</b>
4.2.1	ATTENUATED MITOCHONDRIAL RESPIRATION IN <i>Hvcn1</i> <sup>-/-</sup> MACROPHAGES	137
4.2.2	DECREASED ATP LEVELS IN <i>Hvcn1</i> <sup>-/-</sup> MACROPHAGES	140
4.2.3	DIMINISHED SPARE RESPIRATORY CAPACITY IN <i>Hvcn1</i> <sup>-/-</sup> MACROPHAGES	145
<b>4.3</b>	<b>CHAPTER DISCUSSION</b>	<b>147</b>
<b>5</b>	<b><u>CHAPTER FIVE: ENHANCED REDOX SIGNALLING AND INFLAMMATORY CYTOKINE PRODUCTION IN <i>HVCN1</i><sup>-/-</sup> MACROPHAGES</u></b>	<b>150</b>
<b>5.1</b>	<b>INTRODUCTION</b>	<b>151</b>
<b>5.2</b>	<b>AIMS</b>	<b>154</b>
5.2.1	ENHANCED REDOX SIGNALLING IN <i>Hvcn1</i> <sup>-/-</sup> MACROPHAGES	155
5.2.2	INCREASED INFLAMMATORY CYTOKINE PRODUCTION IN <i>Hvcn1</i> <sup>-/-</sup> MACROPHAGES	163
<b>5.3</b>	<b>CHAPTER DISCUSSION</b>	<b>165</b>
<b>6</b>	<b><u>CHAPTER SIX: DISCUSSION</u></b>	<b>168</b>
<b>7</b>	<b><u>CHAPTER SEVEN: REFERENCES</u></b>	<b>181</b>

## LIST OF FIGURES

Figure 1-1 Innate and adaptive immune cell interactions .....	24
Figure 1-2 Macrophage activation states .....	36
Figure 1-3 Structure of the HVCN1 protein .....	46
Figure 1-4 The glycolysis pathway .....	61
Figure 1-5 Oxidative phosphorylation and the electron transport chain. ....	63
Figure 1-6 The phagocytic respiratory burst.....	69
Figure 1-7 Mitochondrial ROS production.....	71
Figure 3-1 <i>Hvcn1</i> is not expressed in <i>Hvcn1</i> <sup>-/-</sup> macrophages.....	109
Figure 3-2 HVCN1 expressed in WT macrophages and knocked out in <i>Hvcn1</i> <sup>-/-</sup> macrophages. ....	110
Figure 3-3 Bone marrow progenitor and macrophage yield.....	111
Figure 3-4 Microscopic images of WT and <i>Hvcn1</i> <sup>-/-</sup> macrophages.. ....	112
Figure 3-5 Increased basal ROS levels in <i>Hvcn1</i> <sup>-/-</sup> macrophages.....	113
Figure 3-6 Mito-TEMPO and Apocynin titration.....	115
Figure 3-7 Mito-TEMPO and Apocynin do not affect cell viability. ....	116
Figure 3-8 Mito-TEMPO and Apocynin do not affect mitochondrial respiration.....	117

Figure 3-9 Mito-TEMPO reduces basal ROS levels in WT and *Hvcn1*<sup>-/-</sup> macrophages.  
 ..... 118

Figure 3-10 Comparable SOD2 protein levels in untreated and activated  
 macrophages. .... 120

Figure 3-11 Comparable SOD2 fold change in untreated and activated macrophages.  
 ..... 121

Figure 3-12 Lowered mitochondrial membrane potential in *Hvcn1*<sup>-/-</sup> macrophages.  
 ..... 123

Figure 3-13 Impaired respiratory burst in *Hvcn1*<sup>-/-</sup> macrophages..... 125

Figure 3-14 Impaired respiratory burst in *Hvcn1*<sup>-/-</sup> macrophages (relative levels).....  
 ..... 125

Figure 3-15 Apocynin does not affect the viability of LPS-stimulated macrophages.  
 ..... 126

Figure 3-16 Phagocytic capacity of steady state and activated *Hvcn1*<sup>-/-</sup> macrophages  
 is not impaired. .... 127

Figure 3-17 HVCN1 does not co-localise with the mitochondria or the endoplasmic  
 reticulum. .... 129

Figure 4-1 Attenuated mitochondrial respiration in *Hvcn1*<sup>-/-</sup> macrophages. .... 138

Figure 4-2 Increased glycolysis in activated *Hvcn1*<sup>-/-</sup> macrophages. .... 139

Figure 4-3 Attenuated ATP levels in untreated and activated *Hvcn1*<sup>-/-</sup> macrophages.  
 ..... 141

Figure 4-4 Comparable mitochondrial biomass in WT and *Hvcn1*<sup>-/-</sup> macrophages. . 142

Figure 4-5 HVCN1 loss does not affect protein expression of ETC complexes. .... 143

Figure 4-6 HVCN1 loss does not affect fold change of ETC complexes. .... 144

Figure 4-7 Diminished spare respiratory capacity in *Hvcn1*<sup>-/-</sup> macrophages. .... 146

Figure 5-0 LPS activation of the NF-κB signalling pathway.. .... 153

Figure 5-1 Enhanced MAPK signalling in *Hvcn1*<sup>-/-</sup> macrophages in response to LPS.  
 ..... 156

Figure 5-2 Enhanced NF-κB signalling in *Hvcn1*<sup>-/-</sup> macrophages in response to LPS..  
 ..... 157

Figure 5-3 Densitometry analysis of phosphorylation events in WT and *Hvcn1*<sup>-/-</sup>  
 macrophages ..... 160

Figure 5-4 Apocynin does not significantly affect cell signalling in macrophages in  
 response to LPS ..... 161

Figure 5-5 Densitometry analysis of phosphorylation events in WT and *Hvcn1*<sup>-/-</sup>  
 macrophages. .... 162

Figure 5-6 Mitochondrial ROS are involved in LPS-induced cytokine production in  
 macrophages. .... 164



---

## LIST OF TABLES

Table 1-1 Distinct locations and functions of tissue macrophages. ....	29
Table 2-1 Primary antibodies used for Western Blot. ....	86
Table 2-2 Secondary antibodies used for Western Blot. ....	86
Table 2-3 Primers used for qRT-PCR. ....	92
Table 2-4 Compounds used for the XF assay. ....	96
Table 2-5 Primary antibodies used for immunofluorescence. ....	103
Table 2-6 Secondary antibodies used for immunofluorescence. ....	103

## ABBREVIATIONS

ADP adenosine diphosphate

Ala alanine

APCs antigen presenting cells

ATP adenosine triphosphate

BCA bichinonic acid

BCR B cell receptor

BMDCs bone marrow-derived dendritic cells

BMDMs bone marrow-derived macrophages

BTS b cell-specific tetraspanning molecule

Ca<sup>2+</sup> calcium ion

[Ca<sup>2+</sup>]<sub>i</sub> intracellular calcium

CCL chemokine C-C motif ligand

CCR chemokine C-C motif receptor

CD cluster of differentiation

cDNA complementary deoxyribonucleic acid

CDP common DC progenitors

Cl<sup>-</sup> chloride ion

CNS central nervous system

DCs dendritic cells

DMEM Dulbecco's modified Eagle's medium

DNA deoxyribonucleic acid

DPI dyphenylene iodonium

ECAR extracellular acidification rate

ECL enhanced chemiluminescence

ECM extracellular matrix

ERKs extracellular signal-regulated kinases

ETC electron transport chain

F1,6-BP fructose 1,6-bisphosphate

FADH<sub>2</sub> flavine adenine dinucleotide

FBS fetal bovine serum

G6P glucose 6-phosphate

GADP glyceraldehyde 3-phosphate

GM-CSF granulocyte/macrophage-colony stimulating factor

GMPs granulocyte-macrophage progenitors

GPx glutathione peroxidase

GR glutathione reductase

GSH glutathione

GSSG glutathione disulfide

H<sup>+</sup> hydrogen ion/proton

[H<sup>+</sup>]<sub>i</sub> intracellular hydrogen/proton

H<sub>2</sub>O<sub>2</sub> hydrogen peroxide

HI heat-inactivated

His histidine

HMDMs human monocyte-derived macrophages

HOCl hypochlorous acid

HRP horseradish peroxidase

HSCs hematopoietic stem cells

HVCN1 human voltage-gated proton channel 1

IFN interferon

Ig immunoglobulin

TGF tumour growth factor

IκB inhibitor of κB

IKK I $\kappa$ B kinase

IL interleukin

JNK c-Jun N-terminal kinase

K<sup>+</sup> potassium ion

LPS lipopolysaccharide

M-CSF macrophage-colony stimulating factor

MAPK mitogen-activated protein kinase

MHC major histocompatibility complex

MMPs matrix metalloproteases

MPS mononuclear phagocyte system

MPs myeloid progenitors

Na<sup>2+</sup> sodium ion

NADPH nicotinamide adenine dinucleotide phosphate

NF- $\kappa$ b nuclear factor kappa-light-chain-enhancer of activated B cells

NK natural killer

NO nitric oxide

O<sup>2-</sup> superoxide

OCR oxygen consumption rate

OXPHOS oxidative phosphorylation

PAMPs pathogen-associated molecular pattern

PBS phosphate buffered saline

pDCs plasmacytoid dendritic cells

PDGF platelet-derived growth factor

PFK phosphofructokinase

PGI phosphoglucose isomerase

pH power of hydrogen

[pH]<sub>i</sub> intracellular pH

P<sub>i</sub> inorganic phosphate

PMA phorbol 12-myristate 13-acetate

PPP pentose phosphate pathway

PRRs pattern recognition receptors

Prx peroxiredoxin

PTEN phosphatase and tensin homolog

PTP1b protein-tyrosine phosphatase 1b

qPCR quantitative polymerase chain reaction

RA rheumatoid arthritis

RANKL receptor activator of nuclear kappa B ligand

RIPA radioimmunoprecipitation assay

RNA ribonucleic acid

ROS reactive oxygen species

SDS sodium dodecyl sulphate

PVDF polyvinylidene fluoride

SOD superoxide dismutase

TBS tris buffered saline

TCA tricarboxylic acid cycle

T<sub>H</sub> helper T cell

TLRs toll-like receptors

TNF tumour necrosis factor

T<sub>reg</sub> regulatory T cell

VEGF vascular endothelial growth factor

Zn<sup>2+</sup> zinc ion

## **CHAPTER ONE: INTRODUCTION**

## 1.1 THE IMMUNE SYSTEM

The immune system has continuously been evolved to efficiently detect, isolate and eliminate infectious agents. The two arms of the immune system, innate and adaptive, work together in order to successfully deal with those agents (Parkin and Cohen, 2001).

The innate immune system provides an acute and robust response to pathogenic challenge as well as tissue damage. It relies on a limited number of receptors that can detect pathogens, known as pattern recognition receptors (PPRs) (Lee and Kim, 2007). These receptors recognise conserved microbial molecules that are characteristic of large groups of pathogens and are known as pathogen-associated molecular patterns (PAMPs) (Beutler, 2004). The cells involved in the innate immune system include macrophages, dendritic cells (DCs), mast cells, neutrophils, eosinophils, basophils, natural killer (NK) cells and NK T cells. The cells of the innate immune system rapidly generate an inflammatory response upon encountering pathogens (Turvey and Broide, 2010). Moreover, these cells are crucial for activating and amplifying the adaptive immune system (Figure ). Antigen-presenting cells (APCs) phagocytose antigen and then display a fragment of the antigen, which is bound to major histocompatibility complex (MHC) class II, on their plasma membrane. This allows cells of the adaptive immune system, such as T cells, to recognise and interact with the presented antigen and thus becomes activated (Trombetta and Mellman, 2005).

The cells of the innate immune system are limited by the range of PAMPs that they can recognise. In addition, pathogens have the ability to mutate in order to evade host detection. This has propelled the evolution of the adaptive immune system (Cooper and Alder, 2006). Cells of the adaptive immune system include T cells and antibody-producing B cells. The full response of the adaptive immune system is less rapid as it is mounted towards specific antigens. This allows the system to generate a life-long ‘immunological memory’ and thus a swifter response is produced upon re-exposure to those individual antigens (Dempsey et al., 2003). B cells activation can occur either through binding of antigen or through the actions of helper T cells. This allows B cells to mature into antibody-secreting plasma cells (Figure ). T cells, however, are dependent on antigen presentation by APCs (via MHC II) or any other cell type via MHC I (Figure 1 - 1) (Bonilla and Oettgen, 2010).

Whilst this is the trademark of the immune system, it is also crucial to maintaining homeostasis. The system faces constant exposure to a range of other foreign agents (environmental, dietary, toxins etc.) and to the high turnover of cells, which includes both those that are of an apoptotic and necrotic nature (Sirisinha, 2011). An active immune response to these homeostatic procedures would be both wasteful and detrimental to the host. That is why the immune system has evolved in such a way to allow maintenance procedures to occur in the absence of an immune assault (Crimeen-Irwin et al., 2005).

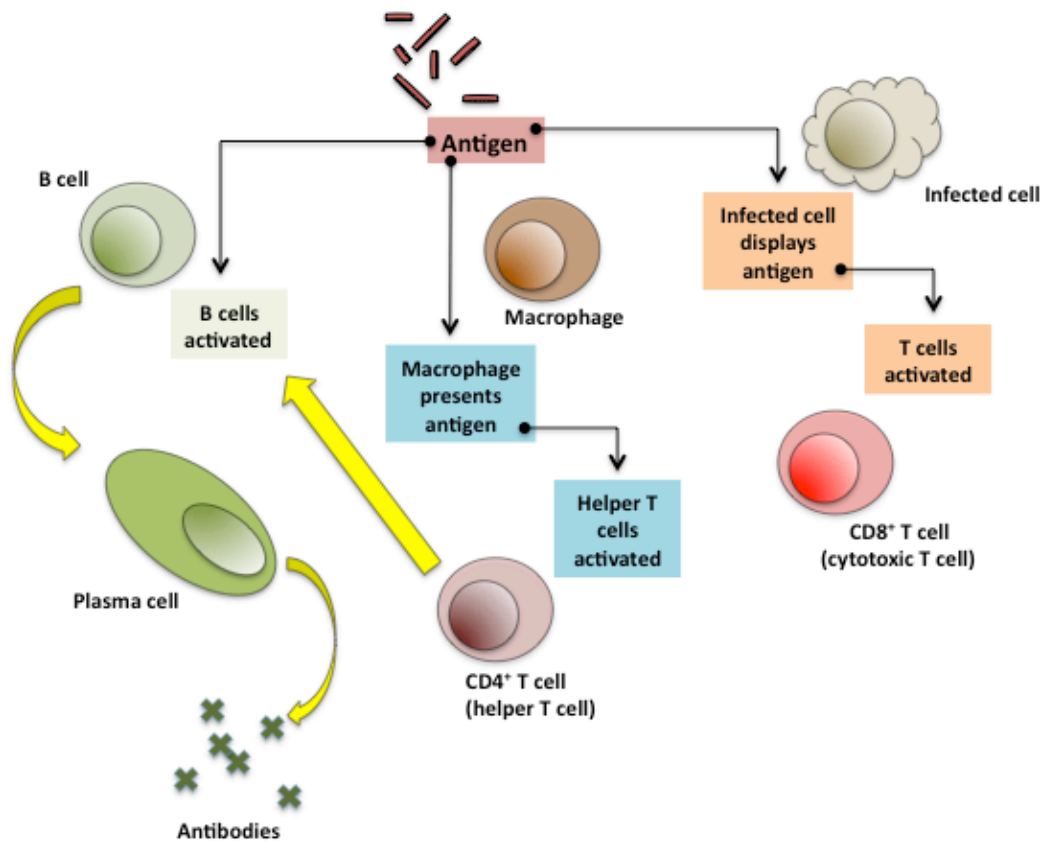


**Figure 1 - 1 Innate and adaptive immune cell interactions**

APCs ingest antigens that are then bound to MHC II and presented to T cell, which activates these cells. T cells can also recognise antigens presented on MHC I on other cell types, such as epithelial cells. B cells can act as APCs and bind antigen, but need co-stimulation in the form of TLR activation in order for themselves to be activated. They can also be activated though the actions of helper T cells. Both activation mechanisms induce the maturation of B cells into plasma cells, the antibody-producing cells of the adaptive immune system. Adapted from (Chaplin, 2010).

## 1.2 MONONUCLEAR PHAGOCYTE SYSTEM

Elie Metchnikoff first described macrophages in the 19<sup>th</sup> century. Macrophages were originally classified as reticular cells, a type of phagocytes that were part of the reticuloendothelia system (Kaufmann, 2008). The system also included endothelial cells, monocytes and histiocytes. It was believed that reticular cells and endothelia shared a common tissue origin owing to initial studies on phagocytic activity (Hashimoto et al., 2011). However, functional and morphological differences were discovered between endothelial cells and macrophages, which led to the rejection of the reticuloendothelial system. Since then, it has been recognised that macrophages are present in virtually every tissue of the body. Tissue macrophages show great heterogeneity, which is attributed to their different anatomical locations. This heterogeneity is due to the specialised functions performed by those macrophages (Gordon and Taylor, 2005).

A seminal study in 1968 provided evidence that distinct populations of macrophages were derived from monocytes in the circulation (van Furth and Cohn, 1968). This concept established the early mononuclear phagocyte system (MPS) (van Furth et al., 1972). The idea of the MPS as such a strict linear model was disputed by others who found evidence for macrophage proliferation in the tissues (Melnicoff et al., 1988) and the existence of macrophages in the early yolk sac (Naito et al., 1996). The MPS includes monocytes, macrophages and DCs. The MPS has been found to be crucial in numerous host functions that are relevant in infection, inflammation, autoimmunity, organ transplantation and cancer (Wynn et al., 2013). All blood cell types are generated from hematopoietic stem cells (HSCs). Successive commitment

steps from the HSCs give rise to common myeloid progenitors (MPs), granulocyte-macrophage progenitors (GMPs) and macrophage/DC progenitors (Fogg et al., 2006). It is thought that cells are committed to the mononuclear phagocyte lineage at the MDP stage, where the fates of other cell types (lymphoid, erythrocyte, megakaryocyte and granulocyte) have already been precluded (Iwasaki and Akashi, 2007). MDPs differentiate into monocytes (Ly6C<sup>-</sup> and Ly6C<sup>+</sup>) or common DC progenitors (CDP). The majority of lymphoid and non-lymphoid tissue DCs, such as plasmacytoid DCs (pDCs), are derived from CDPs (Naik et al., 2007). In comparison, monocytes can differentiate into macrophages/DCs or participate as effector cells in immune responses. Monocytes are generally found in the bone marrow, circulation and spleen. They can migrate into tissues to replenish resident myeloid cell populations under both physiological and pathophysiological situations (Auffray et al., 2009).

In humans, monocytes have been found to show morphological heterogeneity in terms of size and granularity. This apparent heterogeneity led to studies that identified differential expression of surface markers that gave rise to the recognition of monocyte subsets (Ziegler-Heitbrock et al., 1993). The two main subsets are based on the expression of cluster of differentiation (CD) 14 (which forms part of the receptor for lipopolysaccharide [LPS]) and CD16, also known as Fc receptor  $\gamma$ RIII. Classical monocytes are described as CD14<sup>high</sup>CD16<sup>-</sup> whilst non-classical monocytes are identified as CD14<sup>low</sup>CD16<sup>+</sup>. Each subset shows distinct expression of a range of other receptors, in particular the chemokine receptors. For example, classical monocytes express CC-chemokine receptor (CCR) 2, whereas the non-classical subset

expresses CX3CR1. During inflammation classical monocytes invade tissue through interaction of CCR2/CCL2 in a VCAM1-dependent manner. In contrast, non-classical monocytes invade through interaction of CX3CR1/CCL3 in an ICAM1-dependent manner (Weber et al., 2000).

### 1.3 CELLULAR ORIGINS OF TISSUE-RESIDENT MACROPHAGES

The importance of macrophages in the innate immune system has been recognised for decades. Macrophages are often the first type of cell to encounter a pathogen or foreign substance. They have the ability to ingest pathogens and particles via phagocytosis, one of their most distinctive properties (Wynn et al., 2013). Macrophages can detect these pathogens using a number of PRRs such as the toll-like receptors (TLRs). In addition, they have an arsenal of antimicrobial effector mechanisms to eliminate pathogens including oxidation, antimicrobial peptides and enzymatic degradation (Rees, 2010). Macrophages are also important in amplifying the adaptive immune response through their antigen-presenting abilities (Bonilla and Oettgen, 2010).

Tissue-resident macrophage populations can be found in the majority of tissues in the body (Table 1 - 1). There is great heterogeneity in the tissue-resident macrophages and this is important as they perform specific functions in the tissues that they occupy in order to maintain homeostasis. The microanatomical niches that tissue-resident macrophages are positioned in allow them to provide defence against pathogens, aid in tissue repair after tissue injury and maintain tissue homeostasis through clearance of apoptotic/necrotic cells (Elliott and Ravichandran, 2010).

As previously described, the foundational dogma states that tissue-resident macrophages are constitutively replenished by circulating monocytes in the adult. However, recent findings into the origin of tissue-resident macrophage populations have found evidence that challenges this model.

Tissue	Cell type	Function
<b>Central nervous system</b>	Microglia	Neural survival, immune surveillance
<b>Bone</b>	Osteoclasts	Bone resorption
	Bone marrow macrophages	Support erythropoeisis
<b>Gastrointestinal tract</b>	Intestinal macrophages	Intestinal homeostasis
<b>Liver</b>	Kupffer cells	Clearance of microorganisms, cell debris and aged erythrocytes
<b>Lung</b>	Alveolar macrophages	Immune surveillance
<b>Serosal tissue</b>	Peritoneal macrophages	Immune surveillance
	Pleural macrophages	
<b>Skin</b>	Dermal macrophages	Immune surveillance
	Langerhans cells	Interaction with T cels
<b>Spleen</b>	Marginal zone macrophages	Immune surveillance of the circulation
	Metallophilic macrophages	Immune surveillance
	Red pulp macrophages	Erythrocyte clearance and iron metabolism
	White pulp macrophages	Clearance of apoptotic cells

**Table 1 - 1 Distinct locations and functions of tissue macrophages.**

Select examples of tissue-resident macrophages and their functions. Adapted from Davies et al. (2013) (Davies et al., 2013)

Embryonic progenitors from the yolk sac have been found to give rise to major macrophage populations, such as the central nervous system (CNS)-resident macrophages (Ginhoux et al., 2010), Kupffer cells, and Langerhans cells (Schulz et al., 2012).

A number of macrophage populations in tissues have also been found to be maintained long-term without the input from hematopoietic stem cells (Hashimoto et al., 2013, Ajami et al., 2007, Yona et al., 2013). Hashimoto et al. used fate-mapping models, such as *Mx1/S100a4-cre x R26<sup>Tomato</sup>*, to find that tissue-resident macrophages expressed minimal levels of tdTomato, which indicates a lack of monocyte contribution to tissue-resident macrophages. This was further confirmed with the use of parabiotic approaches. The authors also used a genotoxic ablation approach to deplete lung macrophages and found that re-population was mainly due to cell proliferation *in situ*. Finally they observed that mice given a bone marrow transplantation of GM-CSF receptor-deficient progenitors still managed to expand their tissue-resident macrophages (Hashimoto et al., 2013).

Recent studies have observed significant macrophage proliferation during tissue stress, such as infection. Jenkins et al. found that during helminth infection very small numbers of monocytes accumulated in the peritoneal cavity of the animals. Despite this there was a significant infiltration of alternatively activated macrophages. They further confirmed this by repeating the experiment and this time giving the animals clodronate-loaded liposomes, which deplete monocytes. They found that this did not affect the number of alternatively activated macrophages in the peritoneal cavity. The authors found that the large increase in macrophages

numbers in the peritoneal cavity were due to local proliferation and highly dependent on IL-4 availability. IL-4-deficient animals infected in the same manner had significantly fewer proliferating macrophages in the cavity (Jenkins et al., 2011).

Notably, the long-held view that monocytes rapidly differentiate into macrophages upon entering tissues is now being revised as recent evidence has shown that monocytes can enter steady-state nonlymphoid organs and re-enter the circulation without differentiating (Jakubzick et al., 2013, Gautier et al., 2012).

## 1.4 MACROPHAGE ACTIVATION

Macrophages display remarkable plasticity and can thus rapidly respond to injury or infection by changing their physiology to adapt to a particular situation (Mosser and Edwards, 2008). The activation phenotype of recruited macrophages is mainly determined by soluble cues generated by the surrounding microenvironment (Figure 1 - 2). Two general macrophage activation phenotypes have been recognised that mirror T helper polarisation ( $T_H1/T_H2$ ): the classically activated (M1) macrophage phenotype and the alternatively activated (M2) macrophage phenotype (Mills et al., 2000). Regulatory macrophages have also been described as a third macrophage phenotype (Gerber and Mosser, 2001).

### 1.4.1 CLASSICAL MACROPHAGE ACTIVATION

Macrophages were originally polarised towards the M1 phenotype with the combination of two signals, interferon (IFN)- $\gamma$  and tumour-necrosis factor (TNF) (O'Shea and Murray, 2008). Bacterial components, such as LPS, in the presence of IFN- $\gamma$  can also lead to classical activation of macrophages. M1 macrophages are characterised by the production of reactive oxygen and nitrogen species, secretion of large amounts of pro-inflammatory cytokines (in particular interleukin [IL]-12) and mediators (Galli et al., 2011). Classically activated macrophages also have an efficient antigen presenting capacity and promote the induction of  $T_H1$  cells through stimulation by IL-12 and interaction with MHC II.

Both innate and adaptive immune cells can produce IFN- $\gamma$  and an important source of IFN- $\gamma$  is provided by NK cells, which produce the cytokine in response to stress and infection. However, NK cells only transiently produce IFN- $\gamma$  and cannot sustain large

populations of classical macrophages. In order to maintain classically activated macrophages and support host defences,  $T_H1$  cells provide the necessary levels of the cytokine (Biswas and Mantovani, 2010).

Whilst the pro-inflammatory cytokines that are produced by classically activated macrophages play a crucial role in host defence, they also have the potential to cause widespread damage to the host tissue by maintaining inflammation through the recruitment of additional inflammatory immune cells (Langrish et al., 2005, Veldhoen et al., 2006). Indeed, classically activated macrophages have been found to have distinct roles in mediating the immunopathology of several autoimmune diseases such as inflammatory bowel disease (Hontecillas et al., 2011) and rheumatoid arthritis (RA) (Szekanecz and Koch, 2007). Therefore, it is vital that the activation of M1 macrophages is tightly regulated.

#### **1.4.2 ALTERNATIVE MACROPHAGE ACTIVATION**

Alternatively activated macrophages were originally described as a population of macrophages responding to the  $T_H2$  cytokine, IL-4 (Stein et al., 1992). It is believed that that IL-4 is one of the first innate cytokines to be released during tissue injury (Loke et al., 2007). Mast cells and basophils are the main early sources of innate IL-4 (Kuroda et al., 2009), although other cell types have also been implicated such as polymorphonuclear neutrophils (Brandt et al., 2000).

Alternatively activated macrophages participate in  $T_H2$ -type immune responses and the signature cytokines found in such a response are IL-4 and IL-13 (Raes et al., 2007). Indeed, it has been shown that the M2 phenotype can be induced *in vitro* in response to IL-4 and/or IL-13. Macrophages treated in such a manner cannot present

antigen to T cells, produce almost no pro-inflammatory cytokines and generate very low levels of reactive oxygen species (ROS) (Edwards et al., 2006).

Alternatively activated macrophages are characterised by high expression of mannose and scavenger receptors, enhanced phagocytic ability, increased production of IL-10 and high arginase activity (Gordon and Taylor, 2005). Arginase allows the conversion of arginine to ornithine, which serves as a precursor to collagen and polyamines, and thus contributes to the production of extracellular matrix related proteins (Kreider et al., 2007). These characteristics imply that the primary function of alternatively activated macrophages is related to wound healing, which is why they are also referred to as “wound-healing macrophages” (Mosser and Edwards, 2008). Indeed, alternatively activated macrophages have the ability to limit inflammation, aid in tissue repair and also exhibit some immunoregulatory functions (Wynn and Barron, 2010).

Similarly to the uncontrolled activity of classically activated macrophages in autoimmune disorders, the actions of alternatively activated macrophages can also be detrimental to the host tissue. In particular, it is the deregulation of their matrix-enhancing activity that has been implicated in disease states such as chronic schistosomiasis (Hesse et al., 2001) and asthma (Munitz et al., 2008). During chronic schistosomiasis, Th2 cytokines IL-4 and IL-13 increase the number of alternatively activated macrophages that cause fibrotic pathology in the form of increased collagen deposition (Barron and Wynn, 2011). Similarly in asthma, alternatively activated macrophages have been found to exacerbate the condition through increased collagen deposition. In addition, alternatively activated macrophages

secrete TGF $\beta$  that causes goblet cells to secrete increased amounts mucus (Hussell and Bell, 2014).

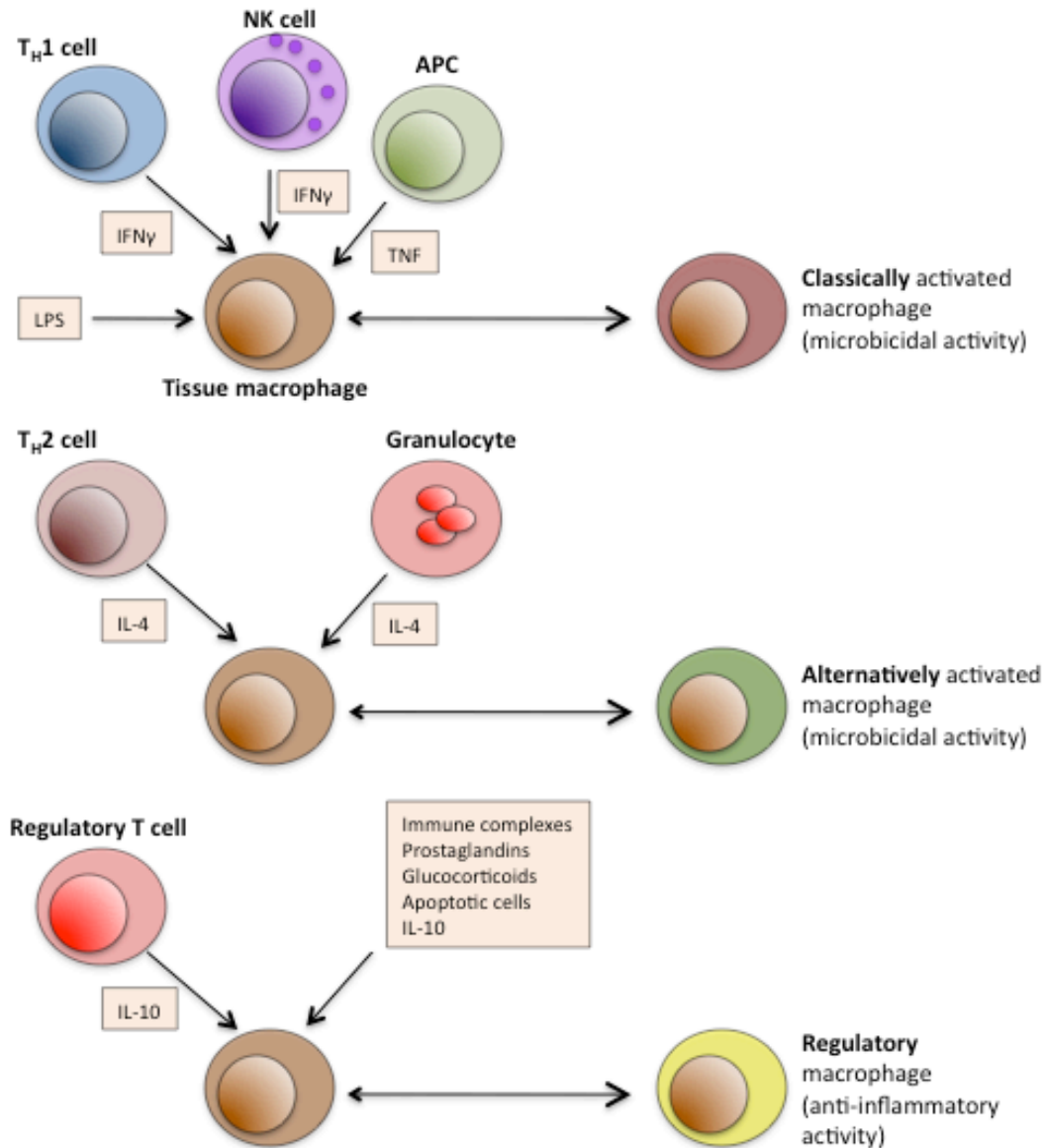


**Figure 1 - 2 Macrophage activation states**

In response to stimuli such as LPS, IFN $\gamma$  and TNF, macrophages become classically activated. This phenotype is associated with pro-inflammatory cytokine production and microbicidal activity. IL-4 secreted by granulocytes can induce alternatively activated macrophages, which are associated with wound-healing activities. Regulatory macrophages are induced in the presence of IL-10 and other anti-inflammatory factors. Adapted from (Mosser and Edwards, 2008).

### 1.4.3 REGULATORY MACROPHAGE ACTIVATION

Regulatory macrophages can be induced by TLR agonists in the presence of immunoglobulin G (Ig)G immune complexes (Gerber and Mosser, 2001), engulfment of apoptotic cells (Erwig and Henson, 2007), prostaglandins (Strassmann et al., 1994) and stimulation by IL-10 (Martinez et al., 2008).

Regulatory macrophages are characterised by their production of IL-10 and tumour growth factor (TGF)- $\beta$ , poor antigen presenting capacity, and induction of T<sub>H</sub>2 and regulatory T cell (T<sub>reg</sub>) responses (Edwards et al., 2006). These characteristics gear regulatory macrophages towards dampening immune responses and inflammation. However, unlike alternatively activated macrophages, regulatory macrophages do not produce extracellular matrix related proteins and have a better antigen presenting ability in comparison (Edwards et al., 2006).

It is believed that there is a spectrum of macrophage activation phenotypes despite the description of distinct subpopulations of macrophages. Macrophages show a high degree of plasticity and have been found to readily change from one functional phenotype to another in response to new environmental cues (Stout et al., 2005). Both injury and pathological conditions are associated with dynamic changes in macrophage phenotypes. Classically activated macrophages are frequently associated with initiating and maintaining inflammation and the macrophage population is found to switch to the alternative activation to resolve inflammation or to lead to a chronic condition. The re-education of what is essentially a terminally

differentiated cell allows macrophages to respond to environmental signals and adapt to the situation at hand (Sica and Mantovani, 2012).

## 1.5 MACROPHAGES IN TISSUE HOMEOSTASIS

One of the most important functions of macrophages is that of immune surveillance, which they are able to perform since they are strategically located throughout the body. They constantly scan their environment for signs of tissue injury or invading pathogens (Lech et al., 2012). Once a danger signal is detected by cell surface receptors and/or phagocytosed it is readily conveyed by macrophages to lymphocytes and other immune cells, which are stimulated by the macrophages to respond (Underhill and Ozinsky, 2002). For example, when a macrophage encounters a pathogen it is ingested and enveloped in a phagosome to quarantine the threat. A lysosome will then fuse with the phagosome in order to destroy the pathogen. The phagolysosome achieves this by releasing ROS and enzymes that damage and digest the pathogen (Aderem and Underhill, 1999). It should be noted that certain pathogens have developed specific mechanisms to prevent their destruction, either through escaping the phagolysosome or neutralising the released enzymes/ROS. *L. monocytogenes* escape by lysing the phagolysosome membrane through the secretion of the enzyme phospholipase C. *S. aureus* neutralises the ROS released by the phagolysosome through its own secretion of catalase and SOD (Rosenberger and Finlay, 2003).

In addition to their vital role in warding off infections, tissue resident macrophages maintain tissue homeostasis by phagocytosing toxins, apoptotic and necrotic cells (Henson and Hume, 2006). For example, in the liver the function of Kupffer cells is to clear erythrocytes, pathogens and toxic materials from the circulation (Bilzer et al., 2006), whereas alveolar macrophages are ideally located in the lung in order to

assist in the removal of allergens (Kirby et al., 2009). Following infection or injury, tissue resident macrophages also maintain tissue homeostasis by suppressing inflammation mediated by inflammatory monocytes (Fujiwara and Kobayashi, 2005).

## 1.6 MACROPHAGES IN TISSUE INJURY

A highly debated question in the macrophage biology field at the moment is whether tissue resident macrophages within any given organ can sufficiently deal with tissue injury or if it is essential to recruit inflammatory monocytes to the tissue to replenish the myeloid numbers (Brancato and Albina, 2011). In many infections and tissue injury situations the resident population of macrophages are overwhelmed and cannot efficiently mediate both defence against pathogens as well as subsequent tissue repair. The foundational dogma thus far has dictated that in situations of tissue injury, monocytes are recruited to the damaged tissue and terminally differentiate into a spectrum of macrophages (Weidenbusch and Anders, 2012).

The increased production of monocytes and neutrophils is driven by tissue stress in the form of both acute and chronic inflammation as well as sterile inflammation (Shi and Pamer, 2011). The processes of production and migration to the site of injury are heavily dependent on cytokines and chemokines such as macrophage –colony stimulating factor (M-CSF), granulocyte/macrophage colony stimulating factor (GM-CSF) and CC-chemokine ligand (CCL)2 (Serbina et al., 2008). As mentioned previously, monocytes are generally thought to adopt two different phenotypes after exiting the bone marrow (Geissmann et al., 2010). Importantly, only the Ly6C<sup>hi</sup> monocyte pool expresses the CCR2 and can thus respond to CCL2. Large pools of LY6C<sup>hi</sup> monocytes are found in the subcapsular red pulp of the spleen and these are readily mobilised to migrate to inflammatory sites (Swirski et al., 2009).

Following tissue injury, the initial macrophages responding to the insult exhibit an inflammatory phenotype in order to be able to efficiently deal with the invading

pathogen (Novak and Koh, 2013). These classically activated macrophages produce large amounts of pro-inflammatory mediators and ROS that drive inflammatory responses forward (Galli et al., 2011). However, an excessive production of pro-inflammatory mediators could lead to collateral tissue damage and it is therefore essential that it be balanced to protect the surrounding tissue. Alternatively activated macrophages and regulatory macrophages are crucial in these settings in order to limit inflammation by antagonising the classically activated macrophage responses, initiate wound healing and restore tissue homeostasis (Sindrilaru et al., 2011). Tissue repair is also aided by macrophage-derived TGF- $\beta$ , which induces differentiation of fibroblasts into myofibroblasts, and production of the immunoregulatory cytokine IL-10 (Gordon and Taylor, 2005).

## 1.7 MACROPHAGES IN DISEASE

Macrophages play important roles in the pathogenesis of many chronic diseases, such as RA (McInnes and Schett, 2011) and fibrosis (Wynn and Barron, 2010). A number of factors control the contribution of the macrophages to the disease state and as such their involvement varies greatly in different stages of the disease.

A great deal of evidence shows that macrophages are intimately involved in the pathogenesis of fibrotic diseases (Wynn and Barron, 2010). In these instances, macrophages are found to produce 'pro-fibrotic' mediators such as TGF $\beta$ 1 (Broekelmann et al., 1991) and platelet-derived growth factor (PDGF) (Nagaoka et al., 1990). These mediators activate local fibroblasts, which regulate extracellular matrix deposition. Increased matrix deposition by these cells leads to fibrosis, which can severely impair the function of the surrounding tissue (Wynn, 2008). Macrophages also produce matrix metalloproteases (MMPs), which are involved in extracellular matrix (ECM) turnover (Wynn and Barron, 2010).

In RA autoantibodies are produced that trigger the activation of macrophages and mast cells through Fc receptor binding, which leads to local inflammation. (McInnes and Schett, 2011). Due to the constant presence of autoantibodies, this leads to the development of chronic inflammation and this causes significant tissue damage (Ma and Pope, 2005). These macrophages produce many of the inflammatory cytokines that are recognised as propagators of autoimmune inflammation, such as IL-18, IL-23 and TNF $\alpha$  (Murray and Wynn, 2011). For example, TNF $\alpha$  production by macrophages triggers cytokine secretion by synovial cells that can lead to the development of chronic polyarthritis (Kawane et al., 2006). A great deal of bone loss is also observed

with RA due to unrestrained osteoclast function. CSF-1 and receptor activator of nuclear factor kappa-B ligand (RANKL) is locally produced in affected tissues and leads to the recruitment and differentiation of monocytes into osteoclasts, which in turn trigger the bone loss (Hamilton, 2008, Dougall et al., 1999).

Macrophages are found in great numbers in tumours and have been associated with pathogenic roles in tumorigenesis (Qian and Pollard, 2010). Studies have shown that macrophages can promote the progression of tumours through the secretion of various mediators such as members of the vascular endothelial growth factor (VEGF) family, which are involved in increasing the vascular density (Murdoch et al., 2008). Macrophages have also been implicated in facilitating tumour metastasis through the regulation of ECM turnover with their production of proteases such as MMPs (Mason and Joyce, 2011). Several studies have highlighted the importance of macrophages in tumorigenesis with the use of tumour xenografts where macrophage ablation, in the form of CSF-1 blockade, led to a decrease in tumour growth (Aharinejad et al., 2004, Paulus et al., 2006).

## 1.8 VOLTAGE-GATED PROTON CHANNELS

Proton currents were originally identified in snail neurons by Thomas and Meech (1982) in the early 1980s and have since been recorded in a variety of cells (Thomas and Meech, 1982); the most recent being mouse eosinophils (Zhu et al., 2013). In 2006, two independent groups discovered the *Human Voltage-gated Channel 1* (*Hvcn1*) gene by clonal studies in mouse (Sasaki et al., 2006) and human (Ramsey et al., 2006). The gene encodes a protein of 273 amino acids, which has a striking resemblance to the voltage-sensing domains of other ion channels. The HVCN1 protein forms the four transmembrane segments (S1-S4) of a voltage-sensing domain observed in other voltage-gated channels (Figure 1 – 3); however, it does not form a pore domain as it lacks the S5-S6 segments (Koch et al., 2008).

Voltage-gated proton channels are extremely selective for protons ( $H^+$ ), with no evident permeability to other cations. Several studies into the structure of the proton channel have provided evidence that it is a dimer, with a separate permeation pathway in each monomer (Hong et al., 2013, Tombola et al., 2010, Musset et al., 2010a). These same studies also showed that the proton channel could function as a monomer with the same functions as the dimer; however, it has been established that the two monomers do not function independently to conduct  $H^+$ . Interestingly, the monomers cooperate during gating and thus increase the voltage sensitivity of the channel two-fold (Qiu et al., 2013).

Small peptides found in toxins from insects and animals can block most ion channels, however, there are no known selective inhibitors of voltage-gated proton channels (Musset et al., 2010b). Despite being non-selective, zinc ( $Zn^{2+}$ ) is the most potent

inhibitor of voltage-gated proton channels (Mahaut-Smith, 1989). Other cations have also been found to be effective (DeCoursey et al. 2007). The HVCN1 protein has two His residues that are accessible by extracellular molecules. Ramsey et al. (2006) showed that by mutating either histidine (His)140 or His193 to alanine (Ala) significantly affected  $Zn^{2+}$  inhibition and the double mutant more or less abolished  $Zn^{2+}$  sensitivity (Ramsey et al., 2006). More recent studies have shed light on the exact mechanism of this inhibition.  $Zn^{2+}$  binds simultaneously to the His residues at the interface between the monomers (Berger and Isacoff, 2011).

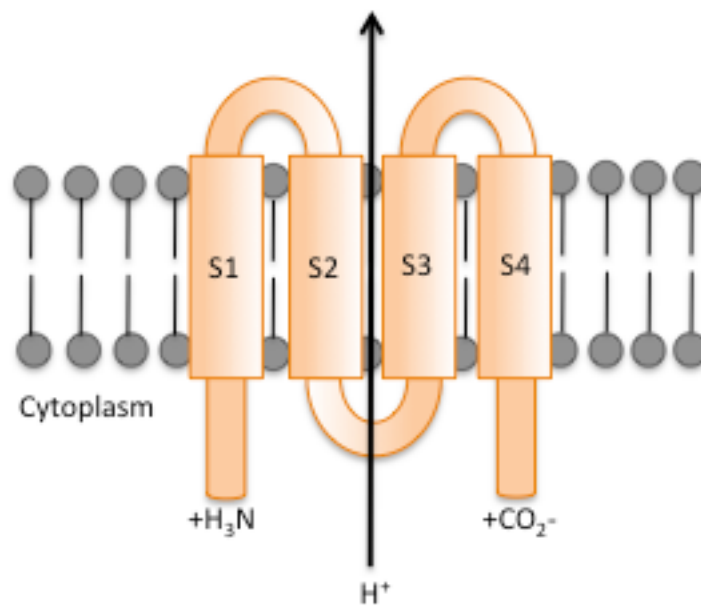


**Figure 1 - 3 Structure of the HVCN1 protein**

The figure shows the four transmembrane segment (S1-S4) structure of HVCN1. The four segments form the pore that allows the extrusion of protons. Adapted from Berger and Isacoff (2011) (Berger and Isacoff, 2011).

Proton channels have been characterized, through electrophysiological studies, to function in the plasma membrane. Other studies have shown evidence for proton channel expression on other organelles as well. One such study used fluorescence ratio imaging to study the factors that contribute to the establishment of the steady state Golgi power of hydrogen (pH) in intact and permeabilised mammalian cells (Vero cells, which are kidney epithelial cells from African green monkey) (Schapiro and Grinstein, 2000). They observed a net loss of  $H^+$  from the Golgi that was neither due to  $H^+$ /cation antiporters or symporters. This  $H^+$  conductive pathway was sensitive to both voltage changes and  $Zn^{2+}$  inhibition, thus suggesting the activity of HVCN1. Okochi et al. (2009) studied phagosomal membrane fractions from neutrophils and used immunoblotting to demonstrate that the fraction contained the subunits of nicotinamide adenine dinucleotide phosphate (NADPH) oxidase (gp91, p22, p47 and p67) as well as HVCN1 (Okochi et al., 2009). Recently, it was shown that voltage-gated proton channels are expressed in intracellular compartment membranes in HeLa cells (Li et al., 2010).

## 1.9 THE ROLE OF HVCN1 IN IMMUNE CELLS

Only a few studies have investigated the phenotypes of immune cells deficient of voltage-gated proton channels. Below is a description of what work has been previously conducted on a particular immune cell type and the findings of those investigations.

### 1.9.1 POLYMORPHONUCLEAR LEUKOCYTES

#### 1.9.1.1 NEUTROPHILS

Decoursey et al. were the first to report the need for proton channels in NADPH oxidase-mediated respiratory burst in phagocytes. Neutrophils were shown to rely on proton channels in order to produce superoxide upon membrane depolarisation. This was evident as the respiratory burst in neutrophils was impaired in the presence of  $Zn^{2+}$  (DeCoursey et al., 2003).

Okochi et al. investigated this further by focusing on the phagosomal compartments, where the superoxide is produced to eliminate pathogens. They were able to confirm that *Hvcn1*<sup>-/-</sup> neutrophils have significantly reduced ROS production upon PMA stimulation. They also found that phagosomal membrane fractions contained NADPH oxidase subunits as well as the HVCN1 protein (Okochi et al., 2009).

Similarly, Ramsey et al. found that proton channels are required for high-level NADPH oxidase-dependent ROS production. The study also wanted to determine whether the impaired respiratory burst observed in *Hvcn1*<sup>-/-</sup> neutrophils would affect bacterial clearance. WT and *Hvcn1*<sup>-/-</sup> BMCs were given live *Staphylococcus aureus*. Both cell types achieved greater than 90% clearance of the bacteria added.

Furthermore, no difference was observed in the phagocytic capacity of both cell types when given fluorescently labelled *S. aureus* or *E. coli*. The study next tested whether this was true in an *in vivo* setting by inoculating the mice with *S. aureus* or *Pseudomonas aeruginosa*. *Hvcn1*<sup>-/-</sup> mice displayed bacterial clearance to the same extent as their WT littermates (Ramsey et al., 2009).

Voltage-gated proton channels have also been found to maintain pH in neutrophils during phagocytosis (Morgan et al., 2009). During the phagocytosis of opsonised zymosan, human neutrophils initially displayed a sharp decrease in intracellular pH (pH<sub>i</sub>) after which a slow recovery to starting pH<sub>i</sub> was achieved. In the presence of Zn<sup>2+</sup> there was an even greater decrease in pH<sub>i</sub>, which was sustained and led to inhibition of the NADH oxidase complex. These observations were mirrored in bone marrow phagocytes from *Hvcn1*<sup>-/-</sup> mice.

A similar study suggested that the acid-extruding role of HVCN1 sustains calcium entry in neutrophils, which in turn controls cell migration (El Chemaly et al., 2010). The study found that *Hvcn1*<sup>-/-</sup> neutrophils produced less superoxide and had a more acidic cytosol than WT mice. The absence of proton channels also greatly reduced the influx of calcium (Ca<sup>2+</sup>) ions, which are important in the regulation of actin depolymerisation. Indeed, impaired actin depolymerisation was observed in *Hvcn1*<sup>-/-</sup> neutrophils as well as a migration defect in these cells.

### 1.9.1.2 EOSINOPHILS

Both human and mouse eosinophils have been found to possess a voltage-gated H<sup>+</sup> conductance (Gordienko et al., 1996, Zhu et al., 2013). Voltage-clamp studies of human eosinophils showed that voltage activation of the membrane resulted in an

outward current. This was sustained even following simultaneous replacement of potassium ( $K^+$ ), sodium ( $Na^+$ ) and chloride ( $Cl^-$ ) with mostly impermeant ions, thus indicating that the conductance was highly selective for  $H^+$  ions. Increasing intracellular  $H^+$  [ $H^+$ ]<sub>i</sub> through acidification of the pipette solution led to augmentation of the  $H^+$  current whilst extracellular application of  $Zn^{2+}$  reversibly inhibited the proton current (Gordienko et al., 1996).

Zhu et al. investigated HVCN1 in regards to eosinophils effector functions in order to further understand its role. The protein expression of HVCN1 was confirmed in mouse eosinophils by both quantitative polymerase chain reaction (qPCR) and immunoblot. Similar to other *Hvcn1*<sup>-/-</sup> immune cells, *Hvcn1*<sup>-/-</sup> mouse eosinophils produced less ROS following phorbol 12-myristate 13-acetate (PMA) stimulation. ROS production was inhibited in both WT and *Hvcn1*<sup>-/-</sup> cells in the presence of either  $Zn^{2+}$  or diphenylene iodonium (DPI). Since migration *in vitro* had been shown to be impaired in *Hvcn1*<sup>-/-</sup> neutrophils due to impaired calcium responses, the authors decided to investigate whether this was true for eosinophils. This was assessed *in vitro* with the use of the eosinophil-specific chemoattractant, eotaxin-1. No differences were observed between WT and *Hvcn1*<sup>-/-</sup> eosinophils in their chemotactic ability towards eotaxin-1. Using a model of peritonitis, injection of thioglycollate medium recruited the same number of eosinophils into the peritoneal cavity in both WT and *Hvcn1*<sup>-/-</sup> mice, suggesting that HVCN1 deficiency does not affect eosinophil migration *in vivo* (Zhu et al., 2013).

### **1.9.1.3 BASOPHILS**

Basophils are closely related to eosinophils and neutrophils, however they do not express the NADPH oxidase. As discussed previously, there is a close link between HVCN1 and NADPH oxidase; therefore, Musset et al. studied the effect of cell activation on proton channels in basophils (Musset et al., 2008). They found that human basophils had functional voltage-gated proton channels that responded to PMA and IgE stimulation, thus suggesting a link between proton channels and activation of basophils by allergens through the IgE receptor. Activation of proton channels by PMA or IgE was inhibited in the presence of  $Zn^{2+}$ . Inhibition of proton channel activation also negatively affected histamine release. With the use of a ratiometric fluorescent dye it was established that IgE activation produced intracellular acidification that was exacerbated with the addition of  $Zn^{2+}$ . The authors thus suggested that proton channels prevent excessive intracellular acidification during IgE-mediated responses and that this might play a role in histamine release.

## **1.9.2 MONONUCLEAR LEUKOCYTES**

### **1.9.2.1 B CELLS**

Voltage-gated proton currents were first described in human peripheral blood B cells (Schilling et al., 2002). Electrophysiological recordings found marked changes in channel expression in lymphocytes following 24h of stimulation with PMA by measuring the proton current. The mean proton current amplitude of PMA-stimulated B cells was halved compared to that of unstimulated cells. Taking into consideration the roughly 30% increase in size following stimulation with PMA meant that the mean  $H^+$  current density of  $CD19^+$  B cells decreased by about 70%.

The authors argued that the function of voltage-gated proton currents in B cells was to repolarise the membrane during superoxide anion production, but offered no functional conclusion to the observed decrease in  $H^+$  current density.

Suenaga et al. (2007) described another similar gene around the same time that the *Hvcn1* gene was discovered (Suenaga et al., 2007). They identified a B cell-specific tetraspanning (BTS) molecule that was found to be involved in B cell development and proliferation. qPCR analysis of various tissues showed that BTS was expressed predominantly in the spleen, in particular in follicular B cells. FLAG-tagged BTS in an immature B cell line suggested that the protein was expressed predominantly within the cells. The authors investigated this further by co-staining with mitochondrial or lysosomal markers, but found no localisation with either organelle.

Functional assays revealed that the growth retardations observed in BTS expressing B cell lines was due inhibition of cell cycle progression and not induction of apoptosis. The authors also identified the N terminus of the BTS to be responsible for its inhibitory function. Upon BCR stimulation with anti-IgM  $F(ab')_2$ , BTS expression was down-regulated. Following on from the *in vitro* data, transgenic mice with high BTS expression were generated to investigate its functions *in vivo*. Similarly, they found inhibition of B cell development in the transgenic mice. It was later discovered that the *BTS* gene and *Hvcn1* gene are one and the same.

Boyd et al. (2009) identified the HVCN1 protein in a shotgun proteomic screen of plasma membrane proteins expressed in purified B cells from mantle cell lymphoma patients (Boyd et al., 2009). However, their qPCR data showed that *Hvcn1* mRNA levels were similar in both normal B and MCL cells. The authors' unpublished

observations hinted at the potential involvement of HVCN1 in class switch recombination in B cells.

Expanding on these previous studies, Capasso et al. (2010) investigated the role of HVCN1 in the initial phase of B cell activation (Capasso et al., 2010). They observed abundant expression in resting naïve and memory B cells, but a downregulation of HVCN1 expression in B cells activated by CD154 in the presence of IL-4. A co-localisation of HVCN1 with the B cell receptor (BCR) following activation was confirmed through confocal microscopy, electron microscopy and subcellular fractionation methods. Internalised BCR co-localised with HVCN1 and late endosomal markers. Extensive co-immunoprecipitation and immunoblot analysis suggested functional interactions between the components of BCR signalling and HVCN1.

The study assessed the ROS generating ability of *Hvcn1*<sup>-/-</sup> B cells in the steady state and after BCR activation. Surprisingly, *Hvcn1*<sup>-/-</sup> B cells had greater levels of ROS at steady state than their wild-type counterpart. Rotenone, an inhibitor of the electron transport chain (ETC), diminished the basal ROS levels of the *Hvcn1*<sup>-/-</sup> B cells to similar amounts found in the wild type cells; however, DPI (an inhibitor of NADPH oxidase) failed to diminish basal ROS levels. The authors thus suggested a mitochondrial source for the differential basal ROS found, but did not explore the significance of this observation further. ROS production was significantly impaired in *Hvcn1*<sup>-/-</sup> B cells following PMA or F(ab')<sub>2</sub> activation and this also impaired local SH2-containing protein tyrosine phosphatase-1 (SHP-1) oxidation, which is crucial for initiation of signalling cascades downstream of the BCR. However, SHP-1 oxidation

was found to be four-fold greater in unstimulated *Hvcn1*<sup>-/-</sup> B cells compared to wild type cells.

This diminished SHP-1 oxidation was shown to have a detrimental effect on BCR downstream signalling. The tyrosine kinase Syk, a crucial SHP-1 target, was activated to a lesser extent in the *Hvcn1*<sup>-/-</sup> B cells. The same was true for activation of Akt, which is heavily involved in cellular metabolism. To this end, mitochondrial respiration and glycolysis was assessed in the B cells and it was observed that after BCR activation *Hvcn1*<sup>-/-</sup> B cells showed lower rates of oxidative phosphorylation and glycolysis compared to their wild type counterparts.

Finally, the authors challenged wild type and *Hvcn1*<sup>-/-</sup> mice with immunogens to assess B cell responses. Whilst they did not find any impairment of B cell development, they did observe defective antibody responses in *Hvcn1*<sup>-/-</sup> mice.

### 1.9.2.2 T CELLS

Schilling et al. (2002) were also the first to describe voltage-gated proton currents in human peripheral blood T cells (Schilling et al., 2002). H<sup>+</sup> currents measured in unstimulated human peripheral blood lymphocytes revealed that the mean H<sup>+</sup> current density in CD19<sup>+</sup> B cells was 100-fold greater than in CD3<sup>+</sup> T cells. However, unlike B cells, PMA-stimulated peripheral blood T cells had a 13-fold increase in H<sup>+</sup> current amplitude. Normalising this to cell capacity meant that T cells increased their H<sup>+</sup> current density 8-fold following PMA stimulation. The implication is that the need for voltage-gated proton channels is much greater after activation. The authors suggested that H<sup>+</sup> channels might be required to maintain an alkaline pH<sub>i</sub> in T cells

during proliferation, antigen presentation and cytokine release as intracellular acidification can inhibit IL-2 release .

More recently, it was shown that mouse T cells express the HVCN1 protein (Sasaki et al., 2013). The same study also found that in the *Hvcn1*<sup>-/-</sup> mice there were a greater proportion of activated T cells (CD4<sup>+</sup>CD44<sup>high</sup> and CD8<sup>+</sup>CD44<sup>high</sup>), both in the steady state and after infection with lymphocytic choriomeningitis virus. However, no difference was observed in the proportion of CD4<sup>+</sup> and CD8<sup>+</sup> T cells in the thymus or the ability of CD4<sup>+</sup> cells to differentiate into Th1/Th17 cells.

The authors investigated ROS production in mouse T cells as T cells have been shown to express a phagocyte-type NADPH oxidase that is activated after T cell receptor stimulation (Jackson et al., 2004). By stimulating CD4<sup>+</sup> and CD8<sup>+</sup> T cells with PMA they observed that the kinetics of superoxide production had two distinct phases or 'peaks' in these cell types. The first 'peak' was reached after 5min and the second 'peak' after 30min. *Hvcn1*<sup>-/-</sup> T cells only managed to produce superoxide for the first phase. The two phases were abolished in the presence of Apocynin (a specific NADPH oxidase inhibitor) in both wild type and *Hvcn1*<sup>-/-</sup> T cells. The authors suggested that HVCN1 is important in the second phase of superoxide production in T cells and not necessary for the first phase. They stressed that further investigations were needed to identify the mechanism by which HVCN1 contributes to ROS production in T cells.

### 1.9.2.3 DENDRITIC CELLS

Szteyn et al. (2012) recently demonstrated the functional expression of HVCN1 in mouse bone marrow-derived DCs (BMDCs) (Szteyn et al., 2012). Whole cell patch-

clamp experiments revealed  $Zn^{2+}$ -sensitive currents that were highly selective for  $H^+$ . Acute treatment of BMDCs with LPS increased HVCN1 channel activity, whereas incubation with LPS for 24h had the opposite effect.  $H^+$  currents, ROS production and *Hvcn1* mRNA levels were all reduced at the later time point; however, HVCN1 protein abundance was not affected.

Ligation of TLR4 by LPS on DCs induces maturation in these cells, which leads to the downregulation of endocytic ability in the fully matured DCs (Zanoni and Granucci, 2010, West et al., 2004). Szteyn et al. (2012) argued that the loss of endocytic ability in mature DCs might be due to the inhibition of  $H^+$  currents observed after 24h with LPS; however, the authors did not address the discrepancy between unaffected HVCN1 protein levels and reduced  $H^+$  currents at 24h post-treatment Szteyn et al. (2012).

#### **1.9.2.4 MACROPHAGES**

The existence of  $H^+$  conductance in macrophages was first shown in a study of murine peritoneal macrophages (Kapus et al., 1993). A suspension of thioglycollate-elicited peritoneal macrophages was used to measure the cytosolic pH fluorimetrically using BCECF. This was conducted in the absence of  $Na^+$  and  $HCO_3^-$  to minimise the activity of other  $H^+$  transporting systems. The cytosols of the cells were acid-loaded and  $pH_i$  was recorded. Recovery of  $pH_i$  was found to be inhibited in the presence of extracellular  $Zn^{2+}$ , thus suggesting the involvement of a  $H^+$  conductive pathway. Patch-clamping of single cells provided further evidence of  $H^+$  currents. These currents were found to be voltage-gated and pH-sensitive.

In a set of similar experiments, Holevinsky et al. (1994) identified  $H^+$  currents in human monocyte-derived macrophages (HMDMs) (Holevinsky et al., 1994). Currents were characterised following an elevation in intracellular  $Ca^{2+}$   $[Ca^{2+}]_i$  using whole-cell voltage clamp recordings.  $[Ca^{2+}]_i$  elevation was achieved by exposing cells to the  $Ca^{2+}$  ionophore, A23187, in the presence of extracellular  $Ca^{2+}$ . The setup of these experiments was chosen as it mimics macrophage activation. Changes in  $[Ca^{2+}]_i$  are closely followed by changes in membrane potential and  $pH_i$ , which are associated with the activation of the respiratory burst and superoxide production in macrophages.

## 1.10 CELLULAR METABOLISM

There are two main stages of catabolic reactions in mammalian cells. Glycolysis is the first stage and occurs in the cytoplasm of the cell. At this stage, adenosine triphosphate (ATP) and NADPH are generated by breaking down glucose and other sugars through a series of enzymatic reactions. A small amount of ATP and NADH are formed through this process, especially in comparison to the catabolic processes that take place within the mitochondria (Lunt and Vander Heiden, 2011).

The second stage is oxidative phosphorylation (OXPHOS) and involves catabolism of pyruvate, the end stage product of glycolysis. Pyruvate molecules are transported into the matrix of mitochondria where they are oxidised in a series of chemical reactions termed the tricarboxylic acid (TCA) cycle (Papa et al., 2012). This process is chemically linked to the last part of cellular respiration, namely the respiratory chain. Protein complexes situated in the intermembrane wall of mitochondria form the electron transport chain (ETC) and facilitate the movement of electrons in redox reactions, which release electrochemical energy that is used to generate ATP. Complete oxidation of glucose in this manner produces large amounts of ATP (Schultz and Chan, 2001).

Cells also have the ability to catabolise other substrates, such as fatty acids through  $\beta$ -oxidation and glutamine through glutaminolysis, which fuel OXPHOS and replenish the TCA cycle (Fennie et al., 2004).

### 1.10.1 GLYCOLYSIS

Glucose is a major source of cellular energy and takes place in all of the cells of the body. The enzymes that are involved in the glycolytic pathway are found in the cytoplasm of the cell. Glycolysis comprises several metabolic reactions by which one molecule of glucose is catabolised to two molecules of pyruvate (Lunt and Vander Heiden, 2011). The pathway is generally divided into two specific phases:

1. Energy investment phase
2. Energy generating phase

In the energy investment phase, glucose is phosphorylated by hexokinase to glucose 6-phosphate (G6P) (Figure 1 - 4). This reaction consumes ATP, but promotes the continuous transport of glucose molecules into the cell by maintaining a low intracellular concentration of glucose (Kim and Dang, 2005). Due to the lack of G6P transporters and the molecule's negative charge it cannot leave cross the plasma membrane through active transport or passive diffusion. Next, another molecule of ATP is consumed to convert G6P to fructose 1,6-bisphosphate (F1,6-BP) through sequential reactions that are catalysed by the enzymes glucose-6-phospho isomerase (PGI), and phosphofructokinase (PFK) (Vander Heiden et al., 2011).

In the energy-yielding phase, F1,6-BP is further converted sequentially into pyruvate through the use of catabolic enzymes and thus generates of four molecules of ATP and two molecules of NADH. This process consumes two adenosine diphosphate (ADP) and two NAD<sup>+</sup> molecules (Fernie et al., 2004). The reactions in the energy-yielding phase occur twice as two molecules of glyceraldehyde 3-phosphate (GADP)

are produced in the energy investment phase and thus there is a net gain of two ATP and two NADPH molecules (Greiner et al., 1994).

Glycolysis can occur in the presence (aerobic) or absence (anaerobic) of oxygen. Anaerobic glycolysis involves the conversion of pyruvate to lactate by the enzyme lactate dehydrogenase (Vander Heiden et al., 2009). This reaction also produces  $\text{NAD}^+$ , which is used to maintain the glycolytic pathway in the absence of oxygen (Brand and Hermfisse, 1997).

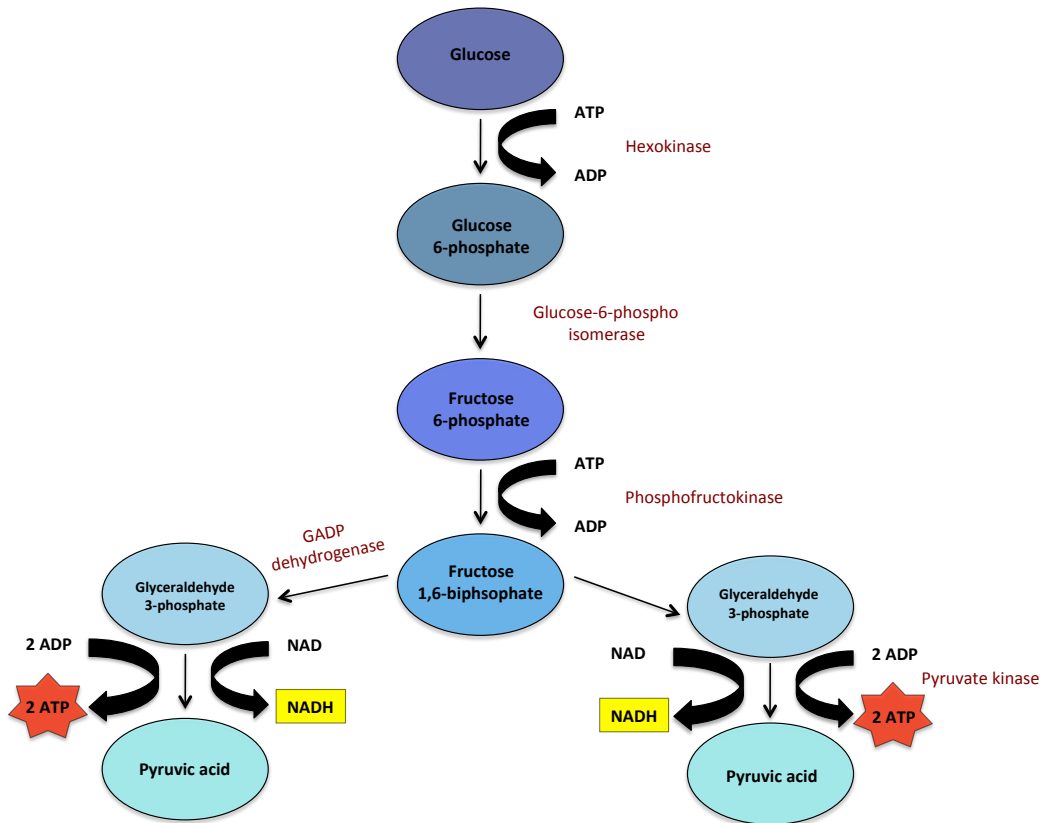


**Figure 1 - 4 The glycolysis pathway**

The figure shows the catabolism of glucose into pyruvic acid. The process uses two ATP molecules, but generates 4 ATP molecules and 2 NADH molecules; thus giving a net gain of two ATP and two NADH. Adapted from Fernie et al. (2004).

### 1.10.2 OXIDATIVE PHOSPHORYLATION

The mitochondria have a four-layered structure, which includes the outer mitochondrial membrane, intermembrane space, inner mitochondrial membrane the matrix (Lenaz and Genova, 2009). Mitochondria generate large amounts of ATP using the process of OXPHOS. The OXPHOS system is located on the inner

mitochondrial membrane and consists of five multiprotein complexes (Figure 1 - 5) (Saraste, 1999). These proteins make up the ETC and include complex I (NADH dehydrogenase), complex II (succinate dehydrogenase), complex III (ubiquinol cytochrome c reductase), complex IV (cytochrome c oxidase), and complex V (ATP synthase) (Fernie et al., 2004). The system also comprises two electron carriers, namely coenzyme Q and cytochrome c. The function of the ETC is the transport of electrons and protons through the inner mitochondrial membrane to allow complex V to produce ATP. All of the complexes, except for complex II, are encoded by the mitochondrial genome (Smeitink et al., 2001).

Electrons enter the ETC through the donation from NADH to complex I and flavin adenine dinucleotide (FADH<sub>2</sub>) to complex II (Papa et al., 2012). The negatively charged electrons pass through the electron carriers and other complexes and thus generate a proton-motive force (Figure 1 - 5). This allows positively charged protons to be pumped from the mitochondrial matrix through complexes I, III and IV into the intermembrane space (Schultz and Chan, 2001). This results in a negative charge in the mitochondrial matrix and a positive charge in the intermembrane space, thus creating a mitochondrial membrane potential across the inner mitochondrial membrane (Echtay et al., 2002). Complex V pumps the protons back into the mitochondrial matrix and in doing so generates ATP from ADP and inorganic phosphate (P<sub>i</sub>) (Schultz and Chan, 2001).

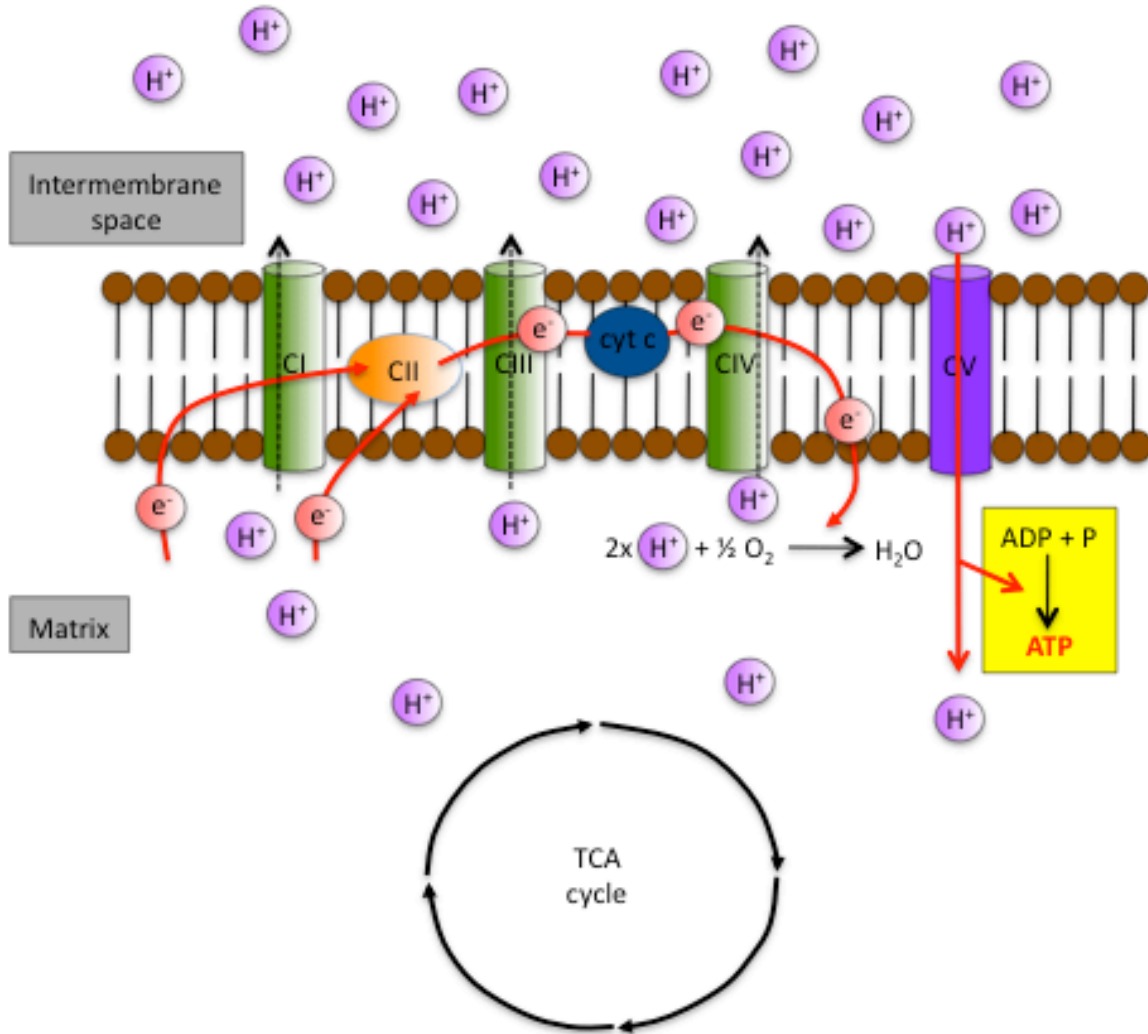


**Figure 1 - 5 Oxidative phosphorylation and the electron transport chain.**

A proton-motive force is generated by electrons passing through the ETC, which causes H<sup>+</sup> to be pumped into the intermembrane space of mitochondria. Complex V (ATP synthase) pumps H<sup>+</sup> back into the matrix of mitochondria and in doing so generates energy that it uses to produce ATP molecules. Adapted from (Ferne et al., 2004).

## **1.11 IMMUNOMETABOLISM**

The field of immune cell metabolism has greatly expanded in recent years, as there has been a greater appreciation and understanding of cross talk between immunity and metabolism (Mathis and Shoelson, 2011). Several studies have focused on the interaction of immune cells with organs that control whole-body metabolism, such as the liver and adipose tissue (Odegaard and Chawla, 2013). Other studies have specifically focused on the regulation of immune responses through metabolic pathways within the immune cells (Pearce and Pearce, 2013).

Cells can utilise distinct metabolic pathways to achieve their metabolic goals; however, these pathways also converge at several levels (Lunt and Vander Heiden, 2011). This is further complicated given that commitment to a particular metabolic fate is influenced by both substrate availability and signalling pathways elicited by extracellular stimuli, such as cytokines and microbial components (Kominsky et al., 2010). Current studies are thus interested in elucidating the process by which immune cells commit to a particular metabolic fate and also the immunological consequences of utilising one pathway over another.

### **1.11.1 GRANULOCYTES**

Myeloid cells are thought to primarily use glycolysis to generate the ATP that they need for cellular processes (Kominsky et al., 2010). Early studies into the metabolism of neutrophils found them to be highly dependent on aerobic glycolysis to generate ATP (Sbarra and Karnovsky, 1959, Valentine and Beck, 1951). Indeed, neutrophils have been found to have little mitochondrial biomass and consume small amounts of oxygen (van Raam et al., 2006). Neutrophils increase their consumption of oxygen

and glucose upon binding of TLR ligands or phagocytosis of particles (Borregaard and Herlin, 1982). This increase in their oxygen consumption rate does not reflect the oxidation of glucose in the mitochondria, rather an increase in the activity of the pentose phosphate pathway (PPP) (Dale et al., 2008). The PPP is an anabolic process that oxidises glucose to produce NADPH and five-carbon sugars such as ribose-5-phosphate, which is used crucial for the synthesis of nucleic acids and nucleotides (Wamelink et al., 2008). As mentioned previously, NADPH is important in the process of the respiratory burst in order to produce ROS to eliminate pathogens (Lambeth, 2004). The few studies that have investigated the metabolism of eosinophils (Sher et al., 1983, Venge et al., 2003) and basophils (Sumbayev et al., 2009) have found these cells to be metabolically similar to neutrophils. It has been suggested that the low mitochondrial activity of granulocytes reflects their terminally differentiated state and their inability to proliferate in the periphery (Pearce and Pearce, 2013).

### **1.11.2 DENDRITIC CELLS**

DCs can be activated by a number of pathogen-associated molecular patterns, such as LPS and double-stranded ribonucleic acid (RNA), which allows them to respond to foreign particles or changes in their microenvironment. DCs play an important part in the immune system as they can prime T cell responses as well as initiate inflammation (Banchereau et al., 2000). Similar to macrophages, DCs can be replenished in the tissues from the monocyte pool during inflammation. Therefore, there are metabolic similarities between monocyte-derived macrophages and DCs (Geissmann et al., 2010). At steady state, DCs largely use mitochondrial respiration to generate energy, but upon activation they switch to glycolysis. This switch

involves the increased expression of the glucose transporter GLUT1 (Krawczyk et al., 2010). The glycolytic switch in DCs can be limited in the presence of IL-10, thus suggesting that glycolytic metabolism is essential for pro-inflammatory effects (Krawczyk et al., 2010). It has been shown in DCs that the decrease in mitochondrial respiration after TLR4 activation was due to inhibition of oxidative phosphorylation by nitric oxide (NO), which constitutes part of the glycolytic shift observed in myeloid cells after activation (Everts et al., 2012). NO achieves this by competing with oxygen to inhibit cytochrome c oxidase, an electron acceptor of the ETC. This is followed by a decrease of glucose into the TCA cycle and an increase in lactate production, thus myeloid cells depend on aerobic glycolysis alone to survive (Everts et al., 2012).

### **1.11.3 T CELLS**

T cells differ from innate immune cells in that they have the ability to proliferate upon activation. Similar to other immune cells, effector T cells also switch to glycolytic metabolism once they have been activated (Jones and Thompson, 2007). However, they also maintain mitochondrial respiration albeit at a lower rate (Fox et al., 2005). It has been shown that other T cell subset use different metabolic processes. Memory T cells rely on mitochondrial fatty acid oxidation over aerobic glycolysis and this is crucial for their development. They also have a greater mitochondrial biomass compared to effector T cells (Pearce et al., 2009). Regulatory T cells have been found to use mitochondrial respiration and fatty acid oxidation both for their development and survival (Michalek et al., 2011). In contrast, aerobic glycolysis is crucial for the generation of T helper 17 cells (Shi et al., 2011). Although there is a growing understanding of metabolic reprogramming in T cells, it remains

unclear exactly why T cell subsets rely on different metabolic phenotypes for their differentiation (Pearce and Pearce, 2013).

#### **1.11.4 B CELLS**

Studies have observed shared metabolic characteristics between B cells and T cells such as a switch to aerobic glycolysis upon activation (Doughty et al., 2006) as well as an increased glucose uptake (Dufort et al., 2007). However, much less is known about the metabolic reprogramming of B cells in comparison. It has been suggested that plasma cells and memory B cells may mirror the metabolic phenotypes of effector T cells and memory T cells, respectively. This could be relevant as the two sets of cells are similar in terms of their lifespan and functional capacity (Pearce et al., 2013).

#### **1.11.5 MACROPHAGES**

Macrophages display a shift towards aerobic glycolysis in response to IFN $\gamma$  or TLR ligands whilst no such effect is observed in response to IL-4 (Rodriguez-Prados et al., 2010). The increased glycolytic flux observed with classically activated macrophages is necessary in order to rapidly trigger microbicidal activity and also to withstand hypoxic microenvironments (Biswas and Mantovani, 2012). In response to IL-4, macrophages polarise towards the alternative phenotype and maintain the OXPHOS metabolism in order to have sustained energy for tissue repair and remodelling. Alternatively activated macrophages also display increased fatty acid oxidation, which is important in controlling membrane fluidity necessary for the processes of phagocytosis (Vats et al., 2006).

## 1.12 REDOX REGULATION OF CELLULAR SIGNALLING

### 1.12.1 SOURCES OF REACTIVE OXYGEN SPECIES

Most ROS are partially reduced forms of molecular oxygen and many oxidative enzymes are capable of generating small amounts of ROS during normal function. Xanthine oxidases, cytochrome P-450, nitric oxide synthases and NADPH-dependent oxidases are amongst the enzymes that can produce ROS (Nathan and Cunningham-Bussel, 2013). Electron leak in the ETC complexes during cellular respiration can also produce ROS (Murphy, 2009). The mitochondria and the NADPH oxidase complex produce the greatest amount of ROS. Whilst mitochondria constantly produce ROS as a by-product of cellular respiration, the NADPH oxidase complex only generates ROS during the respiratory burst in phagocytes (Lambeth, 2004).

The respiratory burst is an example of deliberate generation of ROS and the NADPH oxidase complex catalyses the reaction. Phagocytes are able to distinguish between pathogens and self through the use of specific phagocytic receptors, such as mannose receptors (Aderem and Underhill, 1999). For example, mannose-residues found on pathogens are recognised by mannose receptors on APCs and the binding of the two leads to the mobilisation of the actin cytoskeleton and thus internalisation of the pathogen. The phagocytic cell thus forms a phagosome by fusing its cell membrane around the pathogen as part of the internalisation process. (Lambeth, 2004). Once the pathogen is engulfed, the phagocyte assembles the NADPH oxidase enzymatic complex on its plasma membrane (Figure 1 - 6). The recruited cytosolic components (p40<sup>phox</sup>, p47<sup>phox</sup>, p67<sup>phox</sup> and Rac) are bound by the membrane-bound components, gp91<sup>phox</sup> and p22<sup>phox</sup> (Bylund et al., 2010).

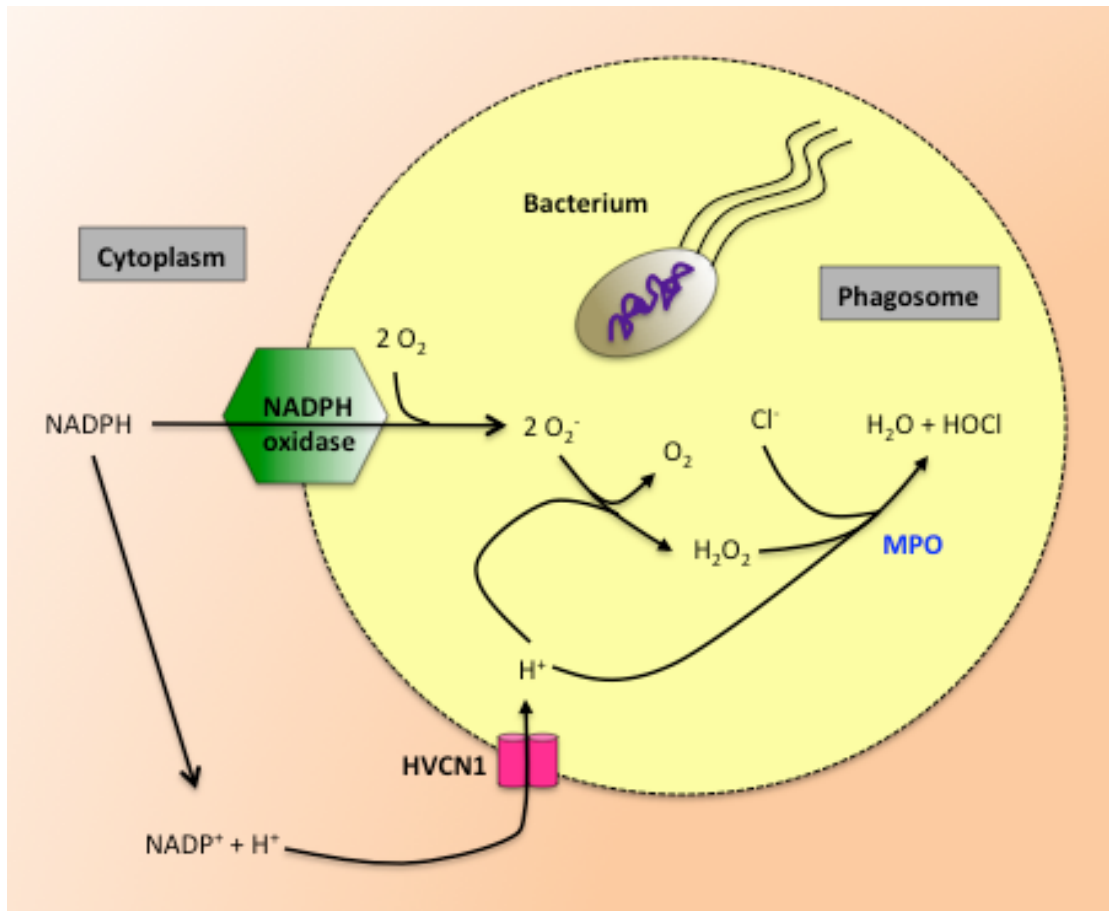


**Figure 1 - 6 The phagocytic respiratory burst.**

The components of the NADPH oxidase complex assemble on the phagosome once a pathogen has been engulfed. The complex catalyses the reduction of O<sub>2</sub> into O<sub>2</sub><sup>-</sup>. HVCN1 provides charge compensation by extruding H<sup>+</sup> into the phagosome. Several potent ROS are generated within the phagosome, such as HOCl. Adapted from (DeCoursey, 2010).

gp91<sup>phox</sup> creates an electron transport chain that passes electrons from intracellular NADPH out to the phagosome that, with the addition of intraphagosomal oxygen, produces superoxide anion (O<sub>2</sub><sup>-</sup>); which is the precursor for several ROS (Babior et

al., 2002). Dismutation of  $O_2^-$  produces hydrogen peroxide ( $H_2O_2$ ) that myeloperoxidases convert to hypochlorous acid (HOCl). The bacteria is thus killed by the high levels of intraphagosomal ROS (Winterbourn, 2008).

The electrogenic activity of translocating electrons to the phagosome by the NADPH oxidase would depolarise the plasma membrane. Depolarisation would give the membrane a positive charge, at which NADPH oxidase would cease to function (Murphy and DeCoursey, 2006). Charge compensation is achieved mainly through voltage-gated proton channels, by diminishing cytosolic acidification caused by the enzyme complex and hexose monophosphate shunt. Cytosolic acidification can also inhibit the action of NADPH oxidase, which has an optimal activity at  $pH_i$  7.5 (Morgan et al., 2009).

Mitochondrial ROS is generated from the ETC, which is located on the inner mitochondrial membrane, during the process of OXPHOS (Murphy, 2009). Whilst the ETC is highly efficient in transporting electrons through the various complexes, there is some leakage of electrons during the process. This leakage takes place at the sites of complex I (Hirst et al., 2008) and complex III (Zhang et al., 1998), which leads to the reduction of  $O_2$  to form  $O_2^-$  (Figure 1 - 7). Approximately 2 % of  $O_2$  consumed by the mitochondria during OXPHOS generates  $O_2^-$ . Complex I leaks  $O_2^-$  into the mitochondrial matrix (Kussmaul and Hirst, 2006) and the  $O_2^-$  leaked from complex III goes into both the mitochondrial matrix and the intermembrane space (Muller et al., 2004).

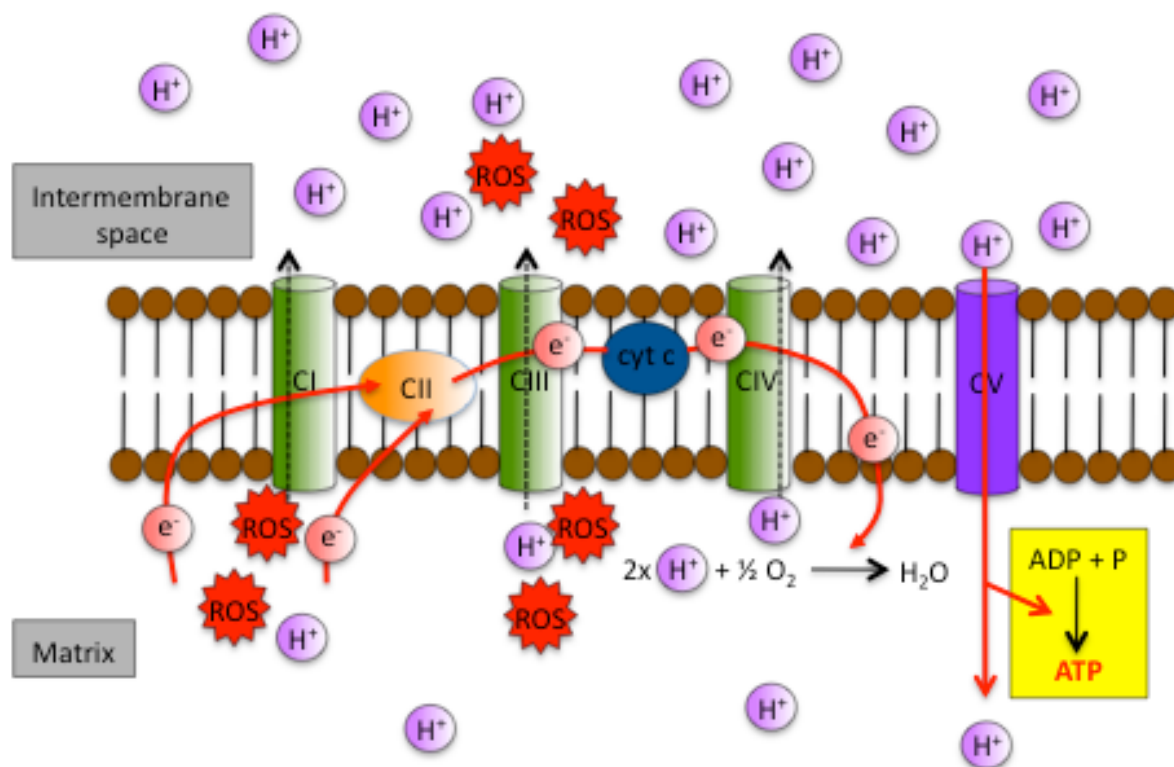


**Figure 1 - 7 Mitochondrial ROS production.**

Electron leaks at Complex I and Complex III allow the reduction of O<sub>2</sub> to occur, which produces O<sub>2</sub><sup>-</sup>. ROS produced at the site of Complex I are released into the matrix of mitochondria. In contrast, ROS produced at the site of Complex III are released into both the mitochondrial matrix and the intermembrane space. Adapted from (Fennie et al., 2004).

### 1.12.2 ANTIOXIDANT SYSTEMS AND REGULATION OF MITOCHONDRIAL ROS

Mitochondrial ROS have high reactivity and toxicity and there are therefore a number of antioxidant enzyme systems that have been evolved by mammalian cells to scavenge ROS as they are generated (Winterbourn, 2008). The mitochondrial antioxidant enzymes are encoded by the nuclear chromosomal genes and are thereafter transported into the mitochondria after protein translation in the cytosol (Handy and Loscalzo, 2012).

One of the most important antioxidant enzyme systems is that of the superoxide dismutase (SOD) family of enzymes. There are three isoforms of SOD including SOD1, SOD2 and SOD3 (Miao and St Clair, 2009). SOD1 can be found in the nucleus, intermembrane space of mitochondria, and the cytosol. SOD2 is only expressed in the mitochondrial matrix, whilst SOD3 is located in the extracellular space (Okado-Matsumoto and Fridovich, 2001). Superoxide that is produced from the ETC during OXPHOS is dismutated into  $H_2O_2$  by SOD1 and SOD2 in the mitochondrial intermembrane space and matrix of the mitochondria, respectively (Cadenas and Davies, 2000). SOD2 is however the most physiologically relevant antioxidant enzyme of the three. This is made evident by the finding that in contrast to the other isoforms, SOD2-deficiency causes early neonatal death in mice (Li et al., 1995).

Glutathione peroxidases (GPx) catalyses the reduction of  $H_2O_2$  into water using reduced glutathione (GSH) as a cofactor. In this process, GSH is oxidised into oxidised glutathione (GSSG) (Winterbourn, 2008). The majority of GPx is found in the cytosol, but some can be found in both the matrix and intermembrane space of

mitochondria (Mari et al., 2009). NADPH can be used as a substrate to recycle GSSG back into GSH with the help of the enzyme glutathione reductase (GR). This antioxidant enzyme system is therefore highly dependent on the bioavailability of NADPH pools (Mari et al., 2013). Genetically engineered GPx knockout mice have been found to be phenotypically normal and to have a normal lifespan, thus indicating that these enzymes are not critical for survival (Muller et al., 2007).

Peroxiredoxins (Prx) are another family of antioxidant enzymes and they regulate the levels of peroxides (Wood et al., 2003). Peroxides are compounds that contain  $O_2^{2-}$ , such as  $H_2O_2$ , or an oxygen-oxygen single bond. Prx is located in the mitochondrial matrix as well as the cytosol. Certain cytokines, such as TNF, can induce the production of peroxides and therefore Prx mediate signal transduction through their regulation of the peroxide pools (Rhee et al., 2000).

Catalase is a heme-containing enzyme that reduces  $H_2O_2$  to water. It uses NADPH as a cofactor, which supplies electrons to the reaction to prevent the inactivation of the enzyme by  $H_2O_2$  (Kirkman et al., 1999). NADPH has also been found to stabilise the enzyme complex and optimise its activity. Catalase is highly efficient at reducing  $H_2O_2$ , however it is not believed to play a central role in modulating ROS levels as the enzyme is mainly found in the peroxisomes (Li et al., 2013).

### 1.12.3 REDOX SIGNALLING

Until recently, ROS were thought to exclusively cause damaging effects on cellular proteins and lack a physiological function. However, ROS are now appreciated to function as signalling molecules that can modulate cellular processes through redox-dependent signalling (Sena and Chandel, 2012). Early investigations showed that hydrogen peroxide was required for growth factor, mitogen-activated protein kinase (MAPK) and nuclear factor kappa-light-chain-enhancer of activated B cells (NF- $\kappa$ B) signalling (Finkel, 1998). These were followed by reports that suggested that hydrogen peroxide could inhibit phosphatases by cysteine oxidation, thus providing a potential biochemical mechanism for ROS as signalling molecules (Rhee et al., 2000). Recent studies have shown that mitochondrial ROS can activate c-Jun N-terminal kinase (JNK) (Kamata et al., 2005) and NF- $\kappa$ B signalling pathways.

A great deal of evidence indicates that ROS can regulate signalling pathways by causing reversible protein modifications. Hydrogen peroxide oxidation of cysteine groups can alter the deoxyribonucleic acid (DNA) binding activity of transcription factors, protein-protein interactions and affect the catalytic activity of enzymes (Brandes et al., 2009). Phosphatases are particularly susceptible to regulation by ROS as they possess a reactive cysteine in their catalytic domains. These enzymes inhibit protein kinases through the processes of dephosphorylation, thus oxidation of their cysteine residue inhibits the enzymatic activity of phosphatases (Janssen-Heininger et al., 2008). Some notable examples of susceptible phosphatases are protein tyrosine phosphatase 1b (PTP1b) (Lee et al., 1998), phosphatase and tensin homolog (PTEN) (Kwon et al., 2004) and MAPK phosphatases (Levinthal and Defranco, 2005).

MAPKs are crucial for relaying extracellular signals to the nucleus and accomplish this through a number of phosphorylation events, which are negatively regulated by MAPK phosphatases (Cargnello and Roux, 2011). Three subgroups of MAPKs exist: the extracellular signal regulated kinases (ERKs), the JNKs, and the p38 MAPKs. MAPKs are involved in several cellular functions such as cell survival, differentiation and inflammatory responses (Boutros et al., 2008). A number of studies have demonstrated ROS-induced MAPK activation and this is further evident as antioxidants have been shown to inhibit MAPK activation after cell stimulation (Ding et al., 2010). ROS have also been indicated in the pro-inflammatory cytokine production of macrophages through their activation of MAPKs (Kasahara et al., 2011, Emre et al., 2007).

The NF- $\kappa$ B signalling pathway plays a highly important role in the immune system as it regulates the expression of a number of genes involved in inflammation such as those for cytokines and growth factors (Li and Verma, 2002). The members of the NF- $\kappa$ B family are found in the cytoplasm of cells bound to I $\kappa$ B family proteins. This prevents the NF- $\kappa$ B proteins to translocate to the nucleus, thus inhibiting activation of the pathway (Hayden and Ghosh, 2004). NF- $\kappa$ B signalling can occur through a classical or alternative pathway. In the classical pathway of NF- $\kappa$ B activation, stimulation of the TLR4, for example, activates the I $\kappa$ B kinase (IKK)  $\beta$  complex. This in turn phosphorylates I $\kappa$ B proteins, which are targeted for degradation by the ubiquitin ligases. In the case of the alternative activation, IKK $\alpha$  phosphorylates the p100 NF- $\kappa$ B protein, which is processed by the proteasome (Bonizzi and Karin, 2004). Several novel mechanisms have been reported for ROS-induced NF- $\kappa$ B activation

such as tyrosine phosphorylation of I $\kappa$ B, activation of IKK and serine phosphorylation of p65 (Takada et al., 2003). Studies have shown that ROS can regulate the production of cytokines, such as TNF, in macrophages through its actions on the NF- $\kappa$ B signalling pathway (Rose et al., 2000) (Bulua et al., 2011).

### 1.13 THESIS AIMS

It is clear that the voltage-gated proton channel HVCN1 plays an essential role in a range of cell types, in particular immune cells. Previous published work has confirmed the existence of proton channels in both murine and human macrophages. However, the role of HVCN1 in macrophages has not been investigated. Given that the current literature on voltage-gated proton channels in immune cells has found HVCN1 to be involved in several cellular processes (such as the respiratory burst and signalling events) it is important to establish its functional role in macrophages, which are a crucial constituent of the immune system.

The aim of my thesis was to investigate the function of voltage-gated proton channels in macrophages with the use of mice with a disrupting mutation within the *Hvcn1* gene, which results in HVCN1 loss. In particular, I wanted to address how *Hvcn1*<sup>-/-</sup> macrophages responded to LPS activation. I hypothesised that HVCN1 regulates the respiratory burst of macrophages and that it potentially modulates mitochondrial ROS production, and in doing so, may affect several functional aspects of macrophage biology. The specific aims of the present work were:

1. Elucidate the involvement of HVCN1 in the ROS producing processes of macrophages
2. Determine the subcellular localisation of HVCN1 in macrophages and investigate its potential functional role in regards to its specific location.
3. Assess the impact of HVCN1-deficiency on the metabolic processes of macrophages.

4. Investigate cell signalling pathways in order to gain insight into other potential cellular functions associated with HVCN1 loss.
5. Study characteristic macrophage functions to gain a global understanding of the role of voltage-gated proton channels in these cells.

My thesis provides a novel perspective on the role of voltage-gated proton channels in immune cells and more generally on macrophage biology.

## **CHAPTER TWO: MATERIALS AND METHODS**

## 2.1 TRANSGENIC ANIMALS

C57BL/6 mice were purchased from Charles River (Canterbury, UK) aged 6-8 weeks and *Hvcn1*<sup>-/-</sup> mice were bred in-house on a C57BL/6 background. *Hvcn1*<sup>-/-</sup> mice were generated in the lab of David Clapham and backcrossed against C57BL/6 mice for 8 generations. *Hvcn1*<sup>-/-</sup> mice were screened by genomic PCR using primers specific for *Hvcn1* intron 3 and  $\beta$ -galactosidase. Mice were maintained in our pathogen-free Biological Services Unit at the Barts Cancer Institute, London. Mice were used according to the established institutional welfare guidelines under the authority of a UK Home Office project licence (PL 70/5541) (Guidance on Operation of Animals Scientific Procedures Act 1986). Experimental protocols and procedures were also approved by the UK Home Office and performed under the following personal licence number: PIL 70/22431.

## 2.2 TISSUE CULTURE

### 2.2.1 GENERATION OF BONE MARROW-DERIVED MACROPHAGES

Mice were culled by cervical dislocation and the tibiae and femurs of WT and HVCN1<sup>-/-</sup> mice were collected and the bone marrow progenitor cells were flushed out with 20 ml of Dulbecco's Modified Eagle's Medium (DMEM; PAA – E15-S10) supplemented with 10 % v/v heat-inactivated (HI) foetal bovine serum (FBS; PAA – A15-102) and 1 % v/v penicillin/streptomycin (PAA – P11-010) using a 27G needle under sterile conditions. The cell suspensions were centrifuged at 1500 rpm for 5 minutes. The cells were resuspended in 10 ml of medium and passed through a 70 µm-wide cut-off strainer.  $7 \times 10^6$  cells were seeded in 100 x 20 mm non-treated cell culture plates in 25 ml of medium. A final concentration of 20 ng/ml macrophage colony stimulating factor (eBioscience 14-8983-80) was added to each plate, which were then allowed to incubate at 37 °C and 5 % CO<sub>2</sub>. After 3 days, the medium was supplemented with a final concentration of 20 ng/ml M-CSF. On day 6/7 of culture, non-adherent cells were removed by washing with phosphate buffered saline (PBS; PAA – H15-002). Adherent cells were collected by adding 15 ml cell-dissociation buffer (Life Tech – 13151-014), incubating at 37 °C and 5 % CO<sub>2</sub> for 30 minutes and then displacing the cells with cell scrapers.

## 2.3 PROTEIN ANALYSIS

### 2.3.1 PROTEIN EXTRACTION

BMDMs were seeded into 6-well plates at  $1 \times 10^6$  cells/well and incubated overnight at 37 °C and 5 % CO<sub>2</sub>. Cells were then either untreated or given 100ng/ml LPS (invivogen – tlr-eklps) for 0 to 60 min and were allowed to incubate at 37 °C and 5 % CO<sub>2</sub>. In some experiments, cells were pre-treated with 100 µM Mito-TEMPO (Santa Cruz – sc-221945) or 10 µM Apocynin (Sigma – W508454) for 1 hour.

Once the given time point had been reached, the wells were washed once with PBS, placed on ice and given 50 µl supplemented radioimmunoprecipitation (RIPA) buffer (Sigma - R0278). This buffer had been supplemented with Complete Protease Inhibitor Cocktail (Roche - 11836153001) and phosphatase inhibitor cocktail 2 and 3 (Sigma - P5726 and P004). Plates were incubated on ice for at least 15 minutes whereupon the cell lysates were harvested by scrapping with a rubber policeman. Lysates were collected into 1.5 ml Eppendorf tubes and were centrifuged at 1320 rpm for 30 min at 4 °C to pellet the cell debris. Lysates were then transferred into new 1.5 ml Eppendorf tubes and stored at -20 °C until use.

### 2.3.2 PROTEIN QUANTIFICATION

The concentration of protein was determined using the bicinchoninic acid (BCA) protein assay. The first step is the biuret reaction, which involves the reduction of Cu<sup>2+</sup> to Cu<sup>+</sup> by proteins in an alkaline environment. This produces a light blue complex. In the second step, the chelation of two molecules of BCA with one cuprous ion results in a purple-coloured reaction product. The water-soluble

BCA/copper complex exhibits a strong linear absorbance at 595 nm with increasing protein concentrations.

A stock solution of bovine serum albumin (BSA; Sigma – A9418) was diluted in PBS to generate a standard curve ranging from 0 to 1 mg/ml. 10  $\mu$ L BSA standard, sample or control were pipetted into a 96-well plate. Working reagent was prepared by combining one part of Copper (II) sulfate solution (Sigma - C2284;) with 50 parts BCA solution (Sigma - B9643). 200  $\mu$ L of working reagent was dispensed into each well and the plate was incubated at 37 °C for 30 minutes. The optical density (OD) was read at 595nm using a spectrophotometer and the protein concentrations of the samples were calculated using the known concentrations of the BSA standard curve.

### **2.3.3 WESTERN BLOT**

In order to identify proteins within a sample they need to be chemically and physically denatured followed by separation, according to their molecular weight, in a Bis-Tris buffered sodium dodecyl sulfate (SDS) polyacrylamide gel. Once the proteins have been separated they can then be transferred onto a polyvinylidene fluoride (PVDF) membrane to allow detection with antibodies.

Samples (20  $\mu$ g) were mixed with NuPAGE LDS Sample Buffer (Life Tech - NP0007) and NuPAGE Sample Reducing Agent (Life Tech - NP0004). They were then heated to 75 °C for 10 minutes followed by brief centrifugation to collect any condensation. Samples remained at room temperature until they were loaded onto the gel. Novex Sharp Pre-stained protein standard (Life Tech - LC5800) was run on all gels. Prestained molecular weight standards allow monitoring of electrophoresis, determination of the apparent mass (kDA) of proteins of interest and, to some

extent, confirmation of protein transfer onto PVDF. Novex Bis-Tris gels were run by electrophoresis in NuPAGE MOPS SDS Running Buffer (Life Tech - NP0001). NuPAGE Antioxidant (Life Tech - NP0005) was added to the upper (cathode) buffer chamber. The antioxidant prevents the reoxidation of sensitive amino acids by migrating with the reduced proteins to maintain reducing conditions. Gels were run at a constant voltage of 150 V for 1 hour and 30 minutes.

Resolved proteins were transferred to PVDF membranes by XCell II Blot Module tank transfer (Life Tech - LC2005 and EI9051, respectively). PVDF membranes are hydrophobic and were therefore hydrated in methanol for one minute prior to use. The gel and PVDF membrane were sandwiched between Whatmann paper and sponge pads (Life Tech - LC2005 and EI9052, respectively). The transfer module was immersed in NuPAGE Transfer Buffer (Life Tech - NP0006-1) and electrotransfer was performed at a constant voltage of 30 V for 1 hour.

Membranes were blocked with 5 % milk powder in tris buffered saline (TBS) with 0.1 % v/v Tween-20 (TBS-T) for 1 hour at room temperature on a rocking platform to prevent non-specific antibody binding. Primary antibodies were diluted in the 5 % milk solution and allowed to incubate with the membranes over night at 4 °C. Membranes were washed 3 x 5 minutes in TBS-T and were then incubated in 5 % milk solution containing horseradish peroxidises (HRP)-conjugated secondary antibodies for 1 hour. Following a further three washes, a substrate for HRP (Amersham ECL Western Blotting Detection Reagents, GE Healthcare - RPN2106) was added to the membranes and this was followed by exposure onto Super RX autoradiography films (Fujifilm - P10M000266A) to detect the emitted light. HRP can

catalyse the oxidation of luminol to 3-aminophthalate, which causes emission of low intensity light. Certain chemicals, such as p-indophenol, can enhance this reaction in order to increase light emission. This is referred to as enhanced chemiluminescence (ECL). The amount of protein is thus semi-quantitatively determined because the intensity of light emitted is a measure of the number of enzyme molecules reacting.

Membranes could be incubated with a different primary antibody by stripping of previous antibodies. This was achieved by incubation in Re-blot solution (Millipore - 2504) for 5 minutes at room temperature, followed by a 5 minute incubation in 5 % milk solution. At this point, membranes were blocked in 5 % milk solution for 1 hour and treated as described above.

All primary and secondary antibodies used are listed below in Table 2 -1 and 2 - 2, respectively.

Antibody	Supplier	Cat. Ref.	Isotype	Dilution
B-actin	Sigma Aldrich	A1978	Mouse IgG1	1:5000
HVCN1	Abcam	105344	Rabbit IgG	1:500
SOD2	Abcam	68155	Rabbit IgG	1:1000
p-p44/p42	Cell Signalling	4370	Rabbit IgG	1:1000
p44/p42	Cell Signalling	4695	Rabbit IgG	1:1000
p-SAPK/JNK	Cell Signalling	4668	Rabbit IgG	1:1000
SAPK/JNK	Cell Signalling	9258	Rabbit IgG	1:1000
p-p38 MAPK	Cell Signalling	4511	Rabbit IgG	1:1000
P38 MAPK	Cell Signalling	8690	Rabbit IgG	1:1000
p-I $\kappa$ B $\alpha$	Cell Signalling	2859	Rabbit IgG	1:1000
I $\kappa$ B $\alpha$	Cell Signalling	4812	Rabbit IgG	1:1000
p-IKK $\alpha$ / $\beta$	Cell Signalling	2078	Rabbit IgG	1:1000
IKK $\beta$	Cell Signalling	2370	Rabbit IgG	1:1000

**Table 2 - 1 Primary antibodies used for Western Blot.**

Table describes the primary antibodies used for Western Blot and lists the relevant details of each antibody.

Antibody	Supplier	Cat. Ref.	Dilution
Anti-mouse IgG HRP	GE Healthcare	NXA931	1:5000
Anti-rabbit IgG HRP	GE Healthcare	NA934	1:2000

**Table 2 - 2 Secondary antibodies used for Western Blot.**

Table describes the secondary antibodies for Western Blot and lists the relevant details of each antibody.

### 2.3.4 ENZYME-LINKED IMMUNOSORBENT ASSAY (ELISA)

BMDMs were seeded into 96-well plates at  $5 \times 10^4$  cells/well and incubated overnight at 37 °C and 5 % CO<sub>2</sub>. Cells were then either untreated or given 100 ng/ml LPS for 3 to 48 hours. In some experiments, cells were pre-treated with 100 μM Mito-TEMPO or 10 μM Apocynin for 1 hour.

The supernatant was collected by centrifugation of the microplates at 1200 rpm for 5 minutes to remove any dead cells or debris and then the supernatant was transferred into new microplates and stored at -80 °C. The supernatant was subjected to no more than two freeze/thaw cycles.

ELISA kits were used to measure the levels of IL-10 (555252), IL-6 (555240), IL12p70 (555256) and TNFα (558534) protein according to the manufacturer's guidelines (all BD Biosciences).

Briefly, 96-well ELISA microplates were coated with 50μl capture antibody (anti-mouse monoclonal Ab) in PBS and incubated over night at 4 °C. ELISA microplates were washed three times with PBS supplemented with 0.05 % Tween-20 (PBS/T) and then unspecific binding was blocked with the addition of 100 μl blocking solution (PBS with 10 % FBS) to each well and incubated for 1 hour at room temperature. ELISA microplates were washed three times with PBS/T and 50 μl of standards, samples, and control supernatants were added to the wells and the microplates were incubated for 2 hours at room temperature. Plates were washed for a total of five times after which 50 μl of working detector solution was added to each well and plates were incubated for 1h at room temperature. The solution consisted of detection antibody (biotinylated anti-mouse monoclonal Ab) and streptavidin-

horseradish peroxidase conjugate (SAv-HRP). Plates were washed for a total of seven times followed by addition of 50  $\mu$ l substrate solution (tetramethylbenzidine and hydrogen peroxide; BioLegend - 421101) and were then allowed to incubate at room temperature in the dark for 5-15 minutes. The enzyme reaction was quenched by adding 25  $\mu$ l stop solution (1 M  $H_3PO_4$ ) to each well. The absorbance was read at 450 nm with 570 nm within 30 minutes of stopping the reaction on a spectrophotometer. Protein concentrations (pg/ml) were calculated using the known concentrations of the cytokine standard curve.

## 2.4 NUCEIC ACIDS

### 2.4.1 TOTAL RNA ISOLATION

BMDMs were seeded into 24-well plates at  $2 \times 10^5$  cells/well and incubated overnight at 37 °C and 5 % CO<sub>2</sub>. Cells were then either untreated or given 100 ng/ml LPS for 6 hours and were allowed to incubate at 37 °C and 5 % CO<sub>2</sub>. In some experiments, cells were pre-treated with 100 µM Mito-TEMPO or 10 µM Apocynin for 1 hour.

RNeasy technology (Qiagen – 74104) was used to purify RNA from adherent BMDMs according to the manufacturer's guidelines.

Cells were lysed directly by the addition of 350 µl of RLT buffer to each well. The lysate was pipetted onto a QIAshredder spin column (Qiagen – 79656) and centrifuged for 2 minutes at 1300 rpm. An equal volume of 70 % ethanol was added to the homogenized lysate and mixed well by pipetting in order to provide adequate binding conditions. The lysate was transferred onto an RNeasy spin column to allow the total RNA to bind to the membrane of the column and centrifuged for 15 seconds at 1300 rpm to wash off contaminants (flow-through was discarded). 350 µl of buffer RW1 was used to wash the membrane-bound RNA by centrifugation at 1300 rpm for 15 seconds (flow-through discarded). On-column DNase digestion was achieved using the RNase-free DNase Set to digest potentially contaminating DNA. A solution of 10 µl DNase I and 70 µl of buffer RDD was applied directly onto the spin column membrane and then incubated for 15 minutes at room temperature. This was followed by another wash with 350 µl of buffer RW1 at 1300 rpm for 15 seconds

(flow-through discarded), after which the spin column membrane was washed twice with 500  $\mu$ l of buffer RPE at 1300 rpm for 30 seconds each. A small volume (30-50  $\mu$ l) of RNase-free water was used to elute the high-quality RNA at 1300 rpm for one minute. The resultant RNA was stored at -80 °C.

#### **2.4.2 RNA QUANTIFICATION AND QUALITY CONTROL**

RNA concentrations were determined using the ND-100 spectrophotometer (Nanodrop Technologies). Two ratios of absorbance were considered when assessing the purity of RNA:

- The ratio of sample absorbance at 260 and 280 nm (260/280). RNA is absorbed at 260 nm and contaminants are absorbed at 280 nm. A sample ratio with a value of 2.0 is considered to be 'pure'. A lower ratio would indicate the presence of protein or other contaminants.
- A ratio of sample absorbance at 260 and 230 nm (260/230). Similarly as described above, a sample ratio of 2.0 is considered to be 'pure'. Lower ratios may indicate the presence of contaminants that absorb at 230nm.

#### **2.4.3 cDNA SYNTHESIS**

M-MLV Reverse Transcriptase (Promega – M1705) was used according to the manufacturer's guidelines to perform cDNA synthesis. 1  $\mu$ g of random primers (Invitrogen – 48190-011) was added to 1  $\mu$ g of DNase-treated RNA in a final volume of 14  $\mu$ l. Primer annealing and breakdown of secondary structures was achieved by incubating samples at 75 °C for 5 minutes and then snap-cooled on ice for a further 5

minutes to prevent the structures from reforming. The following reagents were added to each sample:

- 200 units M-MLV Reverse Transcriptase
- 5  $\mu$ l M-MLV buffer (Promega – M5313)
- 5 nM dNTPs (Applied Biosystems – N8080007)
- 0.6  $\mu$ l RNasin Ribonuclease inhibitor (Promega – N2111)

The samples were allowed to incubate for 10 minutes at room temperature followed by 60 minutes at 40 °C for the cDNA synthesis. The final sample volume was adjusted to 100  $\mu$ l with deionised water and stored at -80 °C.

#### **2.4.4 QUANTITATIVE REAL TIME POLYMERASE CHAIN REACTION (qRT-PCR)**

Taqman Gene Expression Assays contain forward/reverse primers and a fluorogenic probe coupled to a reporter fluorescent dye at the 5' end (FAM/VIC) and an MGB-nonfluorescent quencher on the 3' end (TAMRA). At the beginning of the reaction the fluorescence from the dye is quenched by the quencher, as the probe is still intact. Once the primers and probe anneal to their specific target sequences, the probe is cleaved by the enzymatic activity of DNA polymerase (5' end) and thus separating the dye from the quencher. Each cycle of PCR increases the amount of free dye molecules; therefore, the fluorescent intensity is proportional to the amount of amplicon produced.

Each qRT-PCR reaction consisted of 500 ng of cDNA, 10  $\mu$ l Master Mix (Applied Biosystems – 4364340), 1  $\mu$ l Taqman assay for the gene of interest (Table 2 - 3), 1  $\mu$ l

Taqman assay for the eukaryote 18S gene (Applied Biosystems – 4310893E) and DNase-free water to a final volume of 25  $\mu$ l. The reaction mixture was transferred to MicroAmp optical 96-well reaction plates (Applied Biosystems – 4306737) and amplified using a StepOne Real-Time PCR system (Applied Biosystems).

The thermal cycler conditions were as follows:

Step 1: 50°C for 2min

Step 2: 95°C for 10min

Step 3: 95°C for 15s

Step 4: 60°C for 1min

Step 5: Repeat steps 3 and 4 for 39 cycles

Gene	Cat. Ref.	Amplicon size (base pairs)
<i>18S</i>	4310893E	187
<i>Hvcn1</i>	Mm01199507	56

**Table 2 - 3 Primers used for qRT-PCR.**

Table describes primers used for qRT-PCR and lists the relevant details of each primer.

Data was collected and analysed using the StepOne Software version 2.1 (Applied Biosystems) to determine the threshold cycle (Ct) values for each sample. Data was further analysed using the Comparative Ct Method ( $2^{-\Delta\Delta Ct}$ ):

$$\Delta Ct = Ct (\text{target gene}) - Ct (18S)$$

$$\Delta\Delta Ct = \Delta Ct (\text{test sample}) - \Delta Ct (\text{control/reference sample})$$

## 2.5 CELLULAR BIOENERGETICS

### 2.5.1 XF CELL TECHNOLOGY

The XF24 Extracellular Flux Analyser is an instrument that measures in real time the uptake and excretion of primary metabolites. It simultaneously monitors the two major energy pathways of a cell, glycolysis and oxidative phosphorylation; thus, it can determine the metabolic phenotype of cells. The instrument achieves this by measuring the oxygen consumption rate (OCR) and extracellular acidification rate (ECAR) in the media surrounding the cells cultured in the XF24 Cell Culture Microplate (Seahorse Biosciences – 100777-004).

Each XF assay kit contains a disposable sensor cartridge that has 24 pairs of embedded fluorophores. One fluorophore measures oxygen whilst the other measures protons. The measurement is accomplished by the sensor cartridge being lowered to 200  $\mu\text{m}$  above the cells, thus creating a transient microchamber. The microchamber allows the detection of changes in oxygen and protons as well as repetitive measurements of the same cell population. When the instrument detects a 10 % drop in oxygen/proton concentration, the sensor cartridge rises allowing the medium to restore the cells to baseline. Each sensor cartridge has four reagent injection ports that enable the sequential addition of compounds during an experiment.

### 2.5.2 XF CELL ASSAY

XF Calibrant Solution (Seahorse Biosciences – 102353-004) was added to the wells of the Extracellular Flux Assay plate (Seahorse Biosciences – 100850-001), which was then incubated over night at 37 °C in a non-CO<sub>2</sub> incubator.

BMDMs were seeded into 24-well XF Cell Culture plates at  $2 \times 10^5$  cells/well and incubated overnight at 37 °C and 5 % CO<sub>2</sub>. Cells were then either untreated or given 100 ng/ml LPS for 24 hours. In some experiments, cells were pre-treated with 100 µM Mito-TEMPO for 1 hour.

Oligomycin A, Carbonyl cyanide-4-(trifluoromethoxy)phenylhydrazone (FCCP), Rotenone and Antimycin A were added to the reagent injection ports of the plate at a 10x working concentration (Table 2 - 4). At the start of the XF assay, the instrument calibrated all 24 pairs of fluorophores to the known pH and oxygen concentration in the XF Calibrant solution. In the meantime, the prepared XF Cell Culture Microplate was washed twice with XF Assay medium and incubated for 20 minutes at 37 °C in a non-CO<sub>2</sub> incubator. Once the calibration had finished, the XF Cell Culture Microplate was inserted into the instrument. The assay conditions were as follows:

Step 1: Equilibrate (12min)

Step 2: 4x Baseline measurements (24min)

Step 3: Inject Port A

Step 4: 3x Post-injection measurements (18min)

Step 5: Repeat steps 3 and 4 for injection ports B and C.

Compound	Company	Cat. Ref.	Concentration
Oligomycin A	Sigma	75351	1 $\mu$ M
FCCP	Sigma	C2920	1 $\mu$ M
Rotenone	Sigma	R8875	1 $\mu$ M
Antimycin A	Sigma	A8674	1 $\mu$ M

**Table 2 - 4 Compounds used for the XF assay.**

Table describes the compounds used for the XF assay and lists the relevant details of each compound.

## 2.6 FLOW CYTOMETRY

Flow cytometry was performed using an LSRFortessa cell analyser (BD Biosciences) and FACSDiva software version 6.2. The fluorescence of at least 10,000 events was acquired for each sample. Data were analysed with the FlowJo software (Tree Star Inc).

The basic concept of flow cytometry is that individual cells are passed through a light beam and this causes the ray of light to be scattered. The fluorophores used to label the cells are excited by the light beam and thus emit a light at a longer wavelength than the light source. This emitted light is detected and converted into electric signals. Each individual cell is shown as an event on a graphical scale.

The excitation/emission for 4',6-diamidino-2-phenylindole (DAPI; Life Tech – D1306) is 358/461 nm.

### 2.6.1 MITOCHONDRIAL BIOMASS

MitoTracker Green FM (Life Tech - M7514) is a green-fluorescent mitochondrial stain that localises to mitochondria regardless of mitochondrial potential. Once this cell-permeant probe enters a cell it is sequestered in the mitochondria, where it reacts with thiols on proteins and peptides to form a fluorescent conjugate.

BMDMs were seeded at  $5 \times 10^5$  cells/well into 6-well plates and incubated at 37 °C and 5 % CO<sub>2</sub> over night. Cells were then either untreated or given 100 ng/ml LPS for 24 hours and were allowed to incubate at 37 °C. Supernatant was discarded and cells were washed once in PBS. A 25 nM solution of MitoTracker Green FM was prepared

in PBS and cells were stained with this solution for 15 minutes at 37 °C and 5 % CO<sub>2</sub>. Cells were washed three times in PBS and were then collected into flow cytometry tubes by scrapping gently with a rubber policeman. Tubes were kept on ice until analysis by flow cytometry. Immediately prior to analysis DAPI was added to each tube at a final concentration of 2.5 µg/ml.

The excitation/emission for MitoTracker Green FM is 490/516 nm.

### **2.6.2 INTRACELLULAR ROS LEVELS**

CellROX Deep Red (Life Tech - C10422) is a fluorogenic probe designed to measure ROS in cells. In its reduced state, the probe is nonfluorescent or very weakly fluorescent. Once it is oxidised within the cell it exhibits a strong fluorogenic signal. CellROX Deep Red is localised in the cytoplasm.

BMDMs were seeded as described in sub-section 2.6.1. Cells were then either untreated or given 100 ng/ml LPS for 1 hour and were allowed to incubate at 37 °C. In some experiments, cells were pre-treated with 100 µM Mito-TEMPO or 10 µM Apocynin for 1 hour. Cells were stained with 5 µM CellROX Deep Red 30 minutes at 37 °C and 5 % CO<sub>2</sub>. Cells were then prepared for flow cytometry as described in sub-section 2.6.1.

The excitation/emission for CellROX Deep Red is 640/665 nm.

### **2.6.3 PHAGOCYTOSIS**

Fluoresbrite YO microspheres (Polysciences - 19393-5) are fluorescent polystyrene microspheres that can be used for phagocytosis studies. These polystyrene beads are inert so they do not provide a metabolic load to the phagocytes. This slightly

reductive approach has the benefit of assessing phagocytic ability independent of confounding factors.

BMDMs were seeded as described in sub-section 2.6.1. Cells were then either untreated or given 100 ng/ml LPS for 24 hours and were allowed to incubate at 37 °C. Supernatant was discarded and cells were washed once in PBS. Microspheres (3 μM) were added at a concentration of 5-6 beads per cell and were incubated at 37 °C and 5 % CO<sub>2</sub> to allow bead phagocytosis for 0 to 60 minutes. A control condition where macrophages were given microspheres, but kept on ice for 60 minutes, was used to control for beads that had merely associated with the cells and not been ingested. Cells were then prepared for flow cytometry as described in sub-section 2.6.1.

The excitation/emission for Fluoresbrite YO Microspheres is 529/546 nm.

#### **2.6.4 MITOCHONDRIAL MEMBRANE POTENTIAL**

JC-1 Mitochondrial Potential Sensor (Life Tech - T3168) is a cationic dye that exhibits potential-dependent accumulation in mitochondria. At low concentrations, the dye exists as a monomer and yields green fluorescence. At higher concentrations, the dye forms aggregates that yield red fluorescence.

The use of a ratiometric dye allows for the comparative measurement of mitochondrial membrane potential without confounding factors such as mitochondrial size, shape and density that may influence single-component fluorescent dyes.

BMDMs were seeded as described in sub-section 2.6.1. Cells were then either untreated or given 100 ng/ml LPS for 24 hours and were allowed to incubate at 37 °C. Supernatant was discarded and cells were washed once in PBS. Cells were stained with 2 µM for 15 minutes at 37 °C and 5 % CO<sub>2</sub>. Cells were then prepared for flow cytometry as described in sub-section 2.6.1.

The excitation/emission for JC-1 Mitochondrial Potential Sensor is 485/530 for the green monomer alone and 535/590 for the red aggregate.

## 2.7 CHEMILUMINESCENCE

### 2.7.1 ATP LEVELS

The CellTiter-Glo Luminescent Assay (Promega - G7570) generates a luminescent signal from lysed cells that is proportional to the amount of ATP present. The assay relies on the properties of a thermostable luciferase. The luciferase reaction involves the mono-oxygenation of luciferin in the presence of  $Mg^{2+}$ , ATP and molecular oxygen. The reaction products are oxyluciferin, AMP,  $CO_2$  and light emission. The amounts of ATP were measured according to the manufacturer's guidelines.

BMDMs were seeded at  $1 \times 10^4$  cells/well into white opaque-walled 96-well plates and incubated at 37 °C and 5 %  $CO_2$  over night. White opaque-walled plates are used for luminescent assays as the white colour reflects light and thus maximises light output signal. Cells were then either untreated or given 100 ng/ml LPS for 24 hours and were allowed to incubate at 37 °C. In some experiments, cells were pre-treated with 100  $\mu$ M Mito-TEMPO or 10  $\mu$ M Apocynin for 1 hour.

The plate and its contents were equilibrated at room temperature for 30 minutes. The CellTiter-Glo Reagent was prepared by mixing the CellTiter-Glo Buffer with the CellTiter-Glo Substrate. A volume of CellTiter-Glo equal to the volume of cell culture medium present in each well was added to the cells. The plates were placed on an orbital shaker for 2 minutes to induce cell lysis after which the plates were incubated at room temperature for 10 minutes to stabilise the luminescent signal. The signal was recorded with a luminescent microplate reader (Tecan Infinite 200 PRO).

## 2.8 CONFOCAL MICROSCOPY - IMMUNOFLUORESCENCE

All confocal images were acquired with a laser scanning-microscope LSMA 510 (Zeiss) with a digital signal processor using the LSM software.

Glass cover slips (13 mm  $\emptyset$ ; VWR – 631-0150) were washed in 70 % ethanol, air-dried and then transferred into 24-well plates. WT and HVCN1<sup>-/-</sup> BMDMs were seeded at  $5 \times 10^4$  cells/well and incubated at 37 °C and 5 % CO<sub>2</sub> over night.

Cells were washed twice with ice-cold PBS and fixed with 4 % paraformaldehyde (Ecolab – 416479) at room temperature for 15 minutes. Cells were washed twice with PBS and then permeabilised with 0.1 % Triton X (Sigma – X100) in PBS at room temperature for 5 minutes. Cells were washed again and quenched with 50 mM ammonium chloride in PBS at room temperature for 15 minutes. After another wash with PBS, cells were blocked with 10 % goat serum in PBS at room temperature for 1 hour. Cells were then incubated with primary antibody or isotype control diluted in blocking solution at room temperature for 1 hour (Table 2 - 5). Cells were washed twice with PBS and then incubated with secondary antibody in blocking solution at room temperature for 1 hour in the dark (Table 2 - 6). Cells were washed again with PBS and once with water after which the cover slips were mounted on slides using Prolong Gold antifade reagent with DAPI (Life Tech – P36931).

Antibody	Supplier	Cat. Ref	Isotype	Dilution
HVCN1	Abcam	105344	Rabbit IgG	1:300
LAMP-1	Abcam	25245	Rat IgG2a	1:200
Transferrin receptor	Abcam	60344	Rat IgG2a	1:200
GRP94	Abcam	90458	Rat IgG2a	1:200
MitoTracker Deep Red FM	Life Tech	M22426	N/A	25 nM
Isotype control	BD Biosciences	550875	Rabbit IgG	N/A
Isotype control	eBioscience	14-4321	Rat IgG2a	N/A

**Table 2 - 5 Primary antibodies used for immunofluorescence.**

Table describes the primary antibodies used for immunofluorescence and lists the relevant details of each antibody.

Antibody	Supplier	Cat. Ref.	Dilution
Anti-rabbit Alexa Fluor 488	Invitrogen	A11008	1:1000
Anti-rat Alexa Fluor 546	Invitrogen	A11077	1:1000

**Table 2 - 6 Secondary antibodies used for immunofluorescence.**

Table describes the secondary antibodies used for immunofluorescence and lists the relevant details of each antibody.

## 2.9 STATISTICAL ANALYSIS

All data were presented as the mean of individual experiments with error bars, representing the standard error of the mean (SEM); unless otherwise stated in the figure legend.

The unpaired and paired Student's t test was used as the statistical methods to determine significant differences between two groups.

All p values of 0.05 or less were considered statistically significant. The level of statistical significance was indicated by asterisks as follows: \*  $p < 0.05$ , \*\*  $p < 0.01$  and \*\*\*  $p < 0.001$ ; unless otherwise stated in the figure legend.

**CHAPTER THREE: ELEVATED BASAL ROS AND  
ATTENUATED RESPIRATORY BURST IN *Hvcn1*<sup>-/-</sup>  
MACROPHAGES**

### 3.1 INTRODUCTION

As described in Chapter 1, voltage-gated proton channels are expressed in both epithelial and immune cells. Investigations into the role of HVCN1 in a number of immune cell types have found it to be involved in diverse functions, such as nicotinamide adenine dinucleotide phosphate (NADPH) oxidase-mediated respiratory burst (DeCoursey et al., 2003, Ramsey et al., 2006) and histamine release (Musset et al., 2008).

The majority of published studies have focused on the particular role that HVCN1 plays at the plasma membrane in the NADPH oxidase-mediated respiratory burst. This acute production of reactive oxygen species (ROS) is crucial for pathogen elimination by phagocytes such as macrophages and neutrophils (Dale et al., 2008, Segal, 2005). The process of respiratory burst relies heavily on the recruitment and assembly of the NADPH oxidase complex subunits at the plasma membrane (Sumimoto, 2008). Defects in the assembly or activity of the complex leads to impaired pathogen elimination (Geiszt et al., 2001). In humans, mutations in the NADPH oxidase components cause chronic granulomatous disease (CGD), a disease characterised by the phagocytes of the individual having an impaired respiratory burst and thus unable to eliminate pathogens. Patients are susceptible to recurrent infections due to the decreased capacity of the immune system (Segal, 1987).

Previous studies in several immune cell types found that ROS production was significantly impaired in HVCN1<sup>-/-</sup> eosinophils, B cells, T cells and neutrophils (Zhu et al., 2013, Capasso et al., 2010, Sasaki et al., 2013, Ramsey et al., 2006, DeCoursey et al., 2003). However, it is unclear how HVCN1 is involved in other functional aspects

of immune cells and very little is known about downstream signalling upon HVCN1 activation.

The finding of Musset et al. indicated proton channels to regulate histamine release, via a possible intracellular acidification mechanism in basophils, but this was not further investigated (Musset et al., 2008). In addition, the Demaurex group suggested HVCN1 to be involved in regulating neutrophil migration, at least *in vitro* (El Chemaly et al., 2010). Although the study suggested a defect in calcium (Ca<sup>2+</sup>) entry in *Hvcn1*<sup>-/-</sup> neutrophils, no further downstream signalling defects were analysed. A comprehensive study of signalling events regulated by HVCN1 was conducted in B cells, with HVCN1-deficient B cells, showing impaired B cell receptor (BCR) signalling (Capasso et al., 2010).

Not many studies have investigated where HVCN1 is localised in immune cells. In addition to being expressed on the plasma membrane, proton channels were also detected in the cytosol in resting B cells (Capasso et al., 2010). HVCN1 partially co-localised with the BCR on the plasma membrane and the proportion detected in the cytosol did not co-localise with endosomes, endoplasmic reticulum (ER), Golgi, mitochondria, or peroxisomes (Capasso, unpublished observations).

The existence of proton channels in both murine (Kapus et al., 1993) and human macrophages (Holevinsky et al., 1994) has previously been shown through patch clamp recordings, however little else is known about the role of HVCN1 in macrophages.

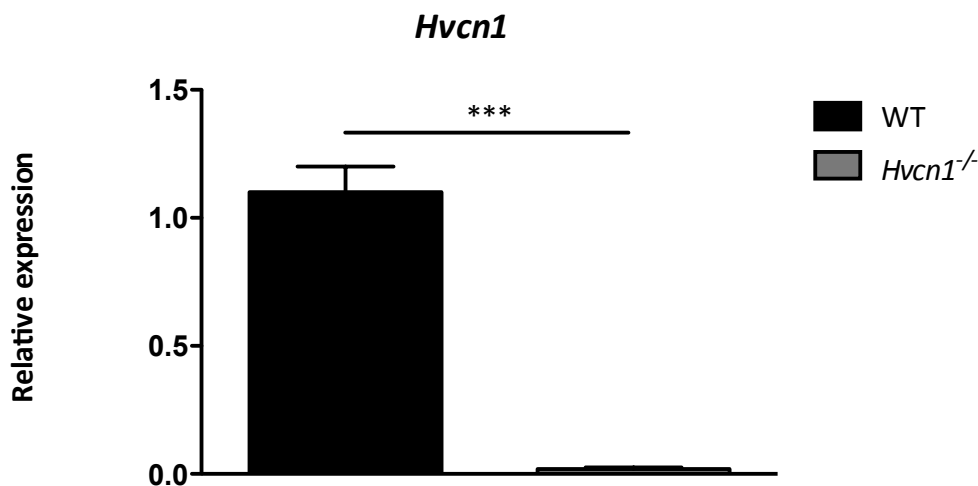
### 3.2 AIMS

This chapter describes my initial investigations into the expression of HVCN1 in macrophages and its potential involvement in their classical functions. My aims were to address the following questions:

- Is HVCN1 expressed in macrophages? Is the proton channel knocked out in *Hvcn1*<sup>-/-</sup> macrophages?
- What are the basal ROS levels of WT and *Hvcn1*<sup>-/-</sup> macrophages? What is/are the source(s) of this basal ROS production?
- Is the respiratory burst impaired in *Hvcn1*<sup>-/-</sup> macrophages?
- Is the phagocytic capacity of *Hvcn1*<sup>-/-</sup> macrophages impaired?
- What is the subcellular localisation of HVCN1 in macrophages?

### 3.2.1 EXPRESSION OF HVCN1 IN MACROPHAGES

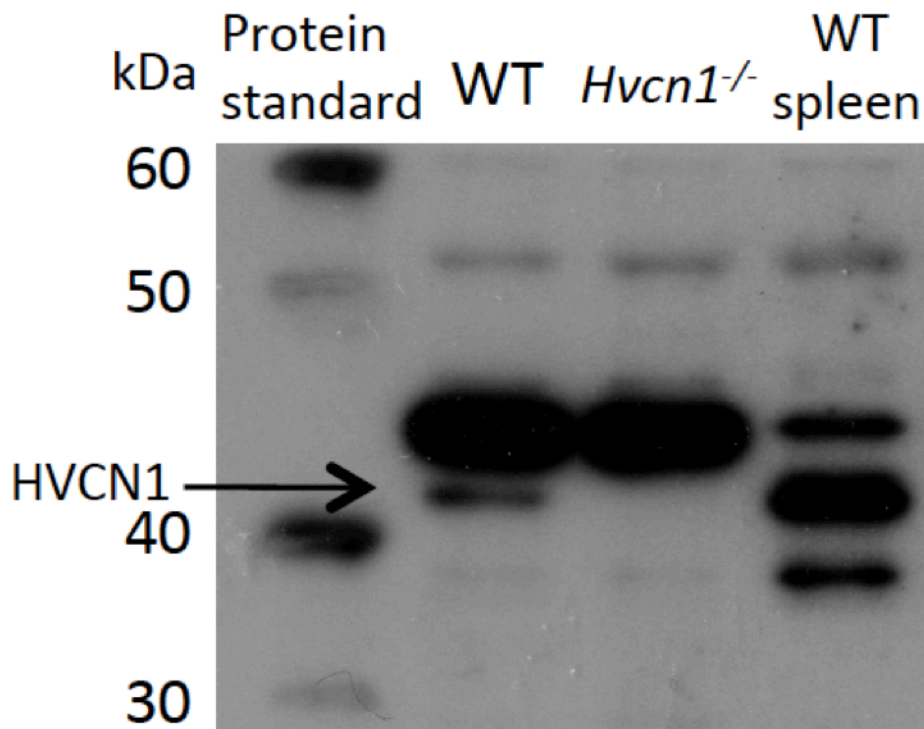
In order to study the role of voltage-gated proton channels in macrophages, we used mice with a genetrap insertion within the HVCN1 gene (Okochi et al., 2009, Ramsey et al., 2009). These genetically altered mice have been widely used in the HVCN1 field of study. Quantitative real-time polymerase chain reaction (qRT-PCR) of macrophages for *Hvcn1* messenger ribonucleic acid (mRNA) confirmed that proton channel mRNA was produced in WT macrophages whilst it was absent in *Hvcn1*<sup>-/-</sup> macrophages (Figure 3 -1).



**Figure 3 -1 *Hvcn1* is not expressed in *Hvcn1*<sup>-/-</sup> macrophages.**

*Hvcn1* mRNA levels in untreated WT and *Hvcn1*<sup>-/-</sup> BMDMs relative to untreated WT BMDMs, as measured by QRT-PCR. *18s* mRNA was used as a control. Data represents means  $\pm$  SEM of three independent experiments. \*\*\*,  $p < 0.001$ .

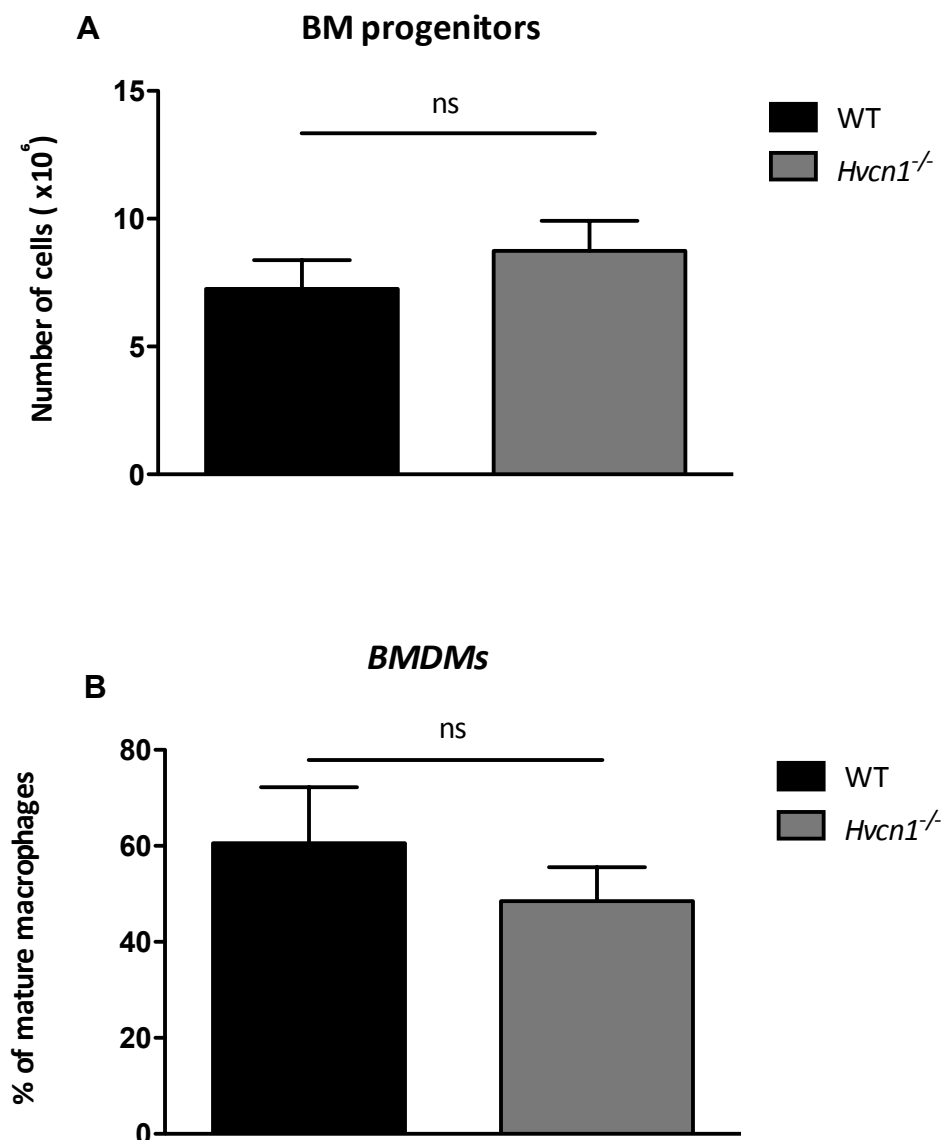
In accordance with the mRNA data, I found HVCN1 protein to be expressed in WT macrophages, whereas no expression was detectable by Western Blot in *Hvcn1*<sup>-/-</sup> macrophages. WT spleen was used as a positive control. (Figure 3 - 2). These data confirm the findings of Kapus et al. at both mRNA and protein level (Kapus et al., 1993).



**Figure 3 - 2 HVCN1 expressed in WT macrophages and knocked out in *Hvcn1*<sup>-/-</sup> macrophages.**

HVCN1 protein levels in untreated BMDMs were measured by Western Blot analysis. Actin was used as a loading control. Data are representative of two independent experiments.

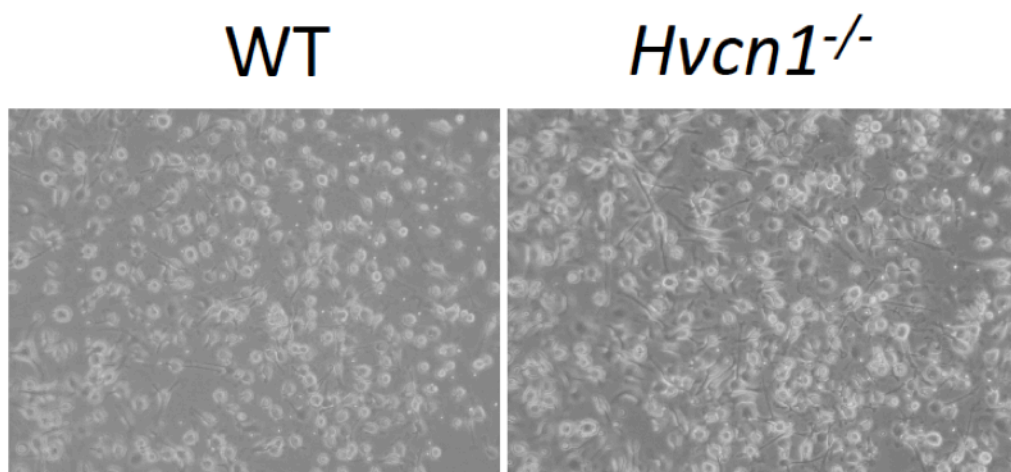
As the *Hvcn1*<sup>-/-</sup> mice have the protein globally knocked out, I wanted to investigate any potential differences in numbers of progenitors found in the bone marrow as well as the ability of those progenitors to produce mature macrophages. Cell counts of the bone marrow flushes showed that there were no differences between the two groups (Figure 3 -3 A). Likewise, both WT and *Hvcn1*<sup>-/-</sup> BM progenitors produced similar numbers of macrophages (Figure 3 -3 B).



**Figure 3 - 3 Bone marrow progenitor and macrophage yield.**

Numbers of (A) BM progenitors and (B) BMDMs were counted from WT and *Hvcn1*<sup>-/-</sup> mice. Data represents means ± SEM of three independent experiments.

In addition, there were no differences microscopically between the WT and the *Hvcn1*<sup>-/-</sup> macrophages (Figure 3 – 4).

**Figure 3 - 4 Microscopic images of WT and *Hvcn1*<sup>-/-</sup> macrophages.**

Numbers of BM progenitors and BMDMs were counted from WT and *Hvcn1*<sup>-/-</sup> mice. Data are representative of three independent experiments.

### 3.2.2 ELEVATED BASAL ROS LEVELS IN *Hvcn1*<sup>-/-</sup> MACROPHAGES

Having confirmed that HVCN1 is indeed expressed in macrophages, I wanted to investigate phagocyte functions that the proton channel had been previously implicated to be involved in. Even though decreased production of ROS in bone marrow cells (which contain a small population of macrophages) from *Hvcn1*<sup>-/-</sup> mice had been reported previously (Ramsey et al., 2009), the specific functional impact of proton channel absence in mature macrophages had not been investigated. I therefore assessed basal ROS levels and respiratory burst in macrophages lacking HVCN1. Interestingly, with the use of a novel fluorogenic probe (CellROX) I observed significantly elevated basal ROS in *Hvcn1*<sup>-/-</sup> macrophages compared to their WT counterparts (Figure 3 - 5). This would suggest either dysregulated ROS production or impaired scavenging of ROS.

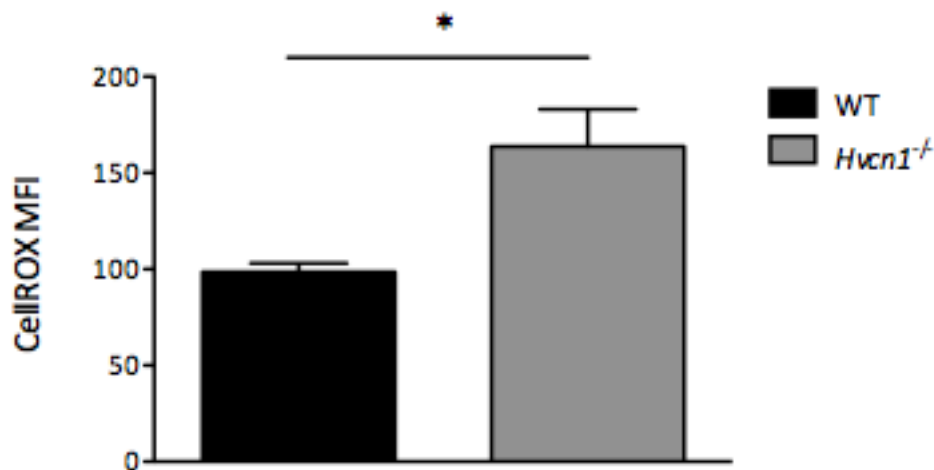


**Figure 1 - 5 Increased basal ROS levels in *Hvcn1*<sup>-/-</sup> macrophages.**

ROS levels were measured in untreated BMDMs generated from WT and *Hvcn1*<sup>-/-</sup> mice, shown as relative to untreated WT BMDMs. Data represents means ± SEM of three independent experiments. \*, p < 0.05.

It was therefore important to determine the source of the increased basal levels of ROS observed in the *Hvcn1*<sup>-/-</sup> macrophages in order to understand whether this was due to dysregulated ROS production at a discrete subcellular site. The two main sites of ROS production are the NADPH oxidase complex and the mitochondria. Therefore, I used a mitochondrial-targeted antioxidant, Mito-TEMPO, and a highly selective NADPH oxidase inhibitor, Apocynin.

Mito-TEMPO is a fusion of the antioxidant piperidine nitroxide (TEMPO) with the lipophilic cation triphenylphosphonium, allowing Mito-TEMPO to easily pass through lipid bilayers and thus accumulate several hundred-fold in the mitochondria where it scavenges ROS ((Murphy and Smith, 2007)). Apocynin is a naturally occurring methoxy-substituted catechol that is oxidised by myeloperoxidases within the cell to give Apocynin dimers (Ximenes et al., 2007). Its mechanism of action is not well defined, but it has been found to prevent the translocation of the cytosolic component of the NADPH oxidase complex, p47phox, to the plasma membrane (Stefanska and Pawliczak, 2008).

The two compounds were firstly titrated to determine the optimum concentration to use in experiments (Figure 3 – 6). They were next assessed for potential cytotoxicity at the given concentrations. Neither Mito-TEMPO nor Apocynin treatment affected cell viability (Figure 3 - 7) as assessed by the ability to reduce a water-soluble tetrazolium salt into formazan. Other NADPH oxidase inhibitors, such as diphenyleneiodonium (DPI), have recently been found to also inhibit complex I of the electron transport chain and as such are not specific inhibitors of the NADPH oxidase complex (Lambert et al., 2008). I therefore wanted to assess the specificity of

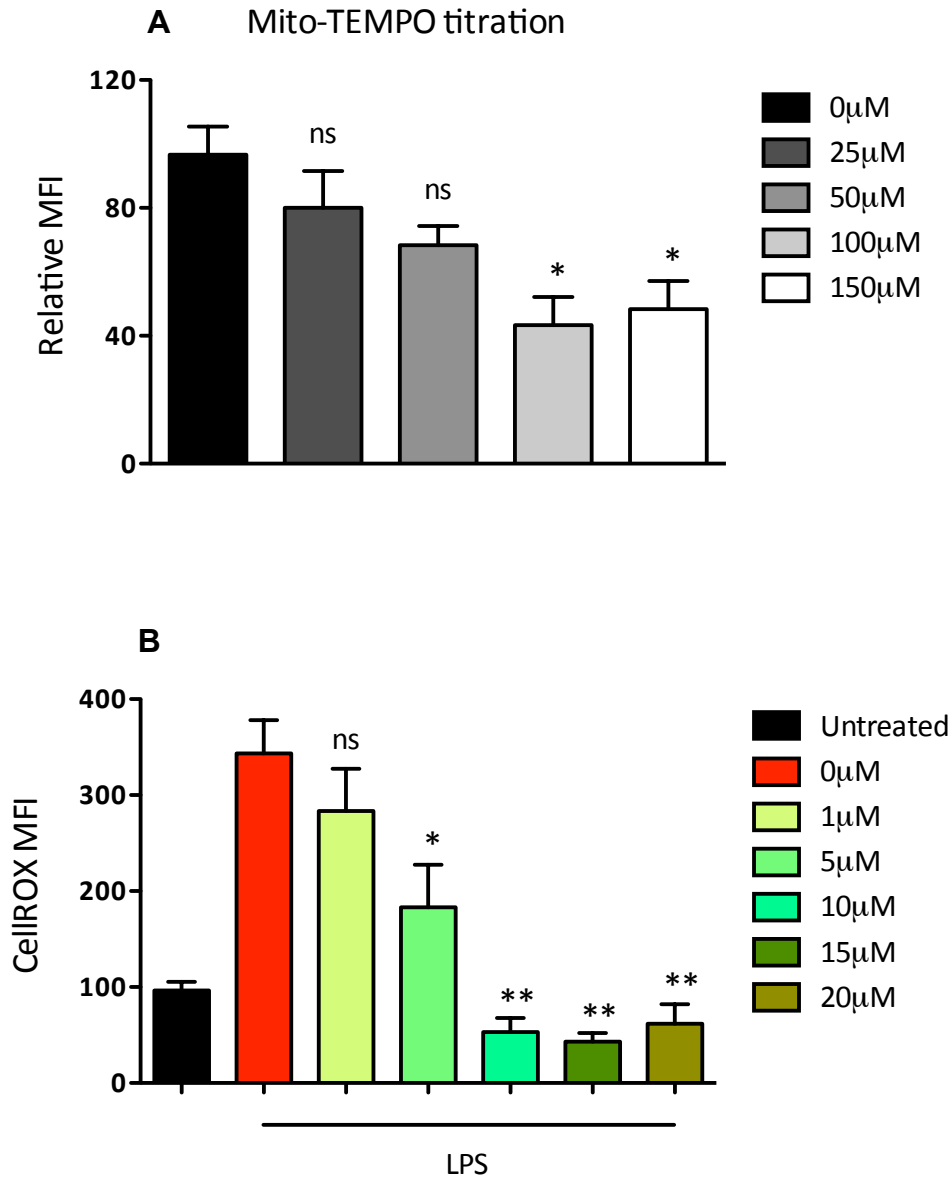


**Figure 3 - 6 Mito-TEMPO and Apocynin titration.**

ROS levels were measured in BMDMs untreated or pre-treated for 1 hour with varying concentrations of either (A) Mito-TEMPO or (B) Apocynin, shown as relative to untreated WT BMDMs. Data represents means  $\pm$  SEM of three independent experiments. \*,  $p < 0.05$ ; \*\*,  $p < 0.01$ ; ns, no significance.

Apocynin and similarly the specificity of Mito-TEMPO, to ensure that its effects were due to mitochondrial ROS scavenging and not inhibition of the electron transport chain (ETC). Oxygen consumption, a measure of ETC activity, was not affected by either compound (Figure 3 - 8). Rotenone and Antimycin A, which block complex I and complex III respectively, were used as positive controls in the assay.

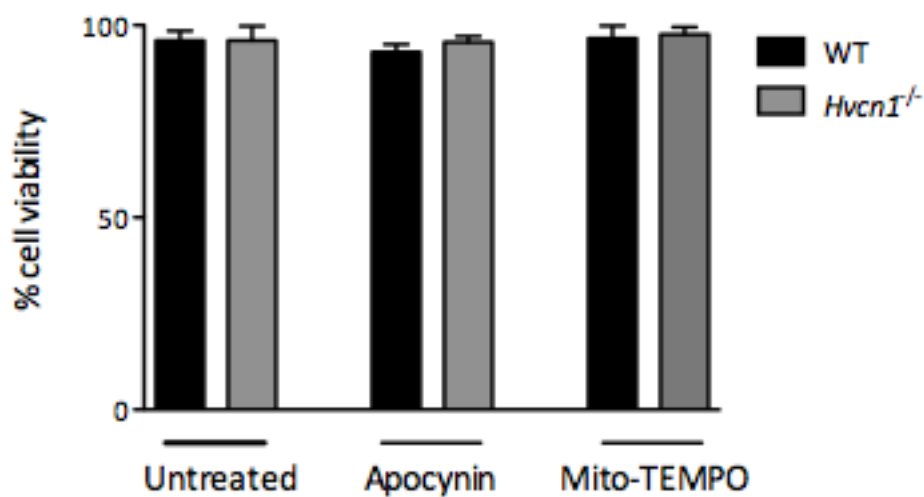


**Figure 3 - 7 Mito-TEMPO and Apocynin do not affect cell viability.**

Percentage of viable BMDMs (expressed as percentage over vehicle) untreated or pre-treated for 1 hour with either 10  $\mu$ M Apocynin or 100  $\mu$ M Mito-TEMPO. Data represents means  $\pm$  SEM of three independent experiments.

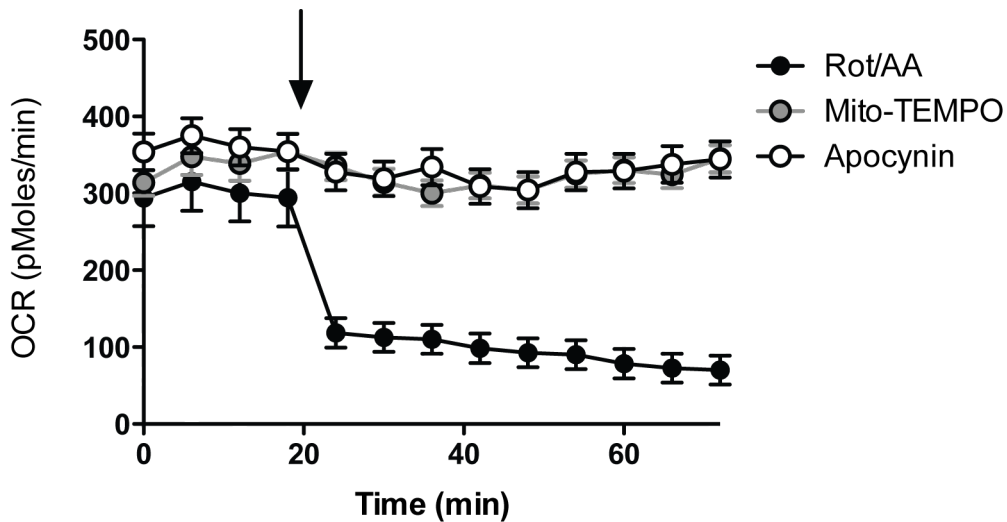


**Figure 3 - 8 Mito-TEMPO and Apocynin do not affect mitochondrial respiration.**

Measurement of mitochondrial respiration (OCR) in BMDMs. The arrow indicates time of addition of the inhibitors. Addition of Rotenone (Rot) and Antimycin A (AA), which block mitochondrial respiration, was used as a control. Data represents means  $\pm$  SEM of three independent experiments.

The addition of Mito-TEMPO reduced the basal ROS levels of *Hvcn1*<sup>-/-</sup> macrophages to similar levels seen in their WT counterpart (Figure 3 - 9); indicating their mitochondrial origin. In contrast, Apocynin did not reduce basal ROS levels and thus confirming that the NADPH oxidase is not activated in quiescent macrophages (Figure ); therefore, the increase in ROS observed in *Hvcn1*<sup>-/-</sup> macrophages is indeed of mitochondrial origin.

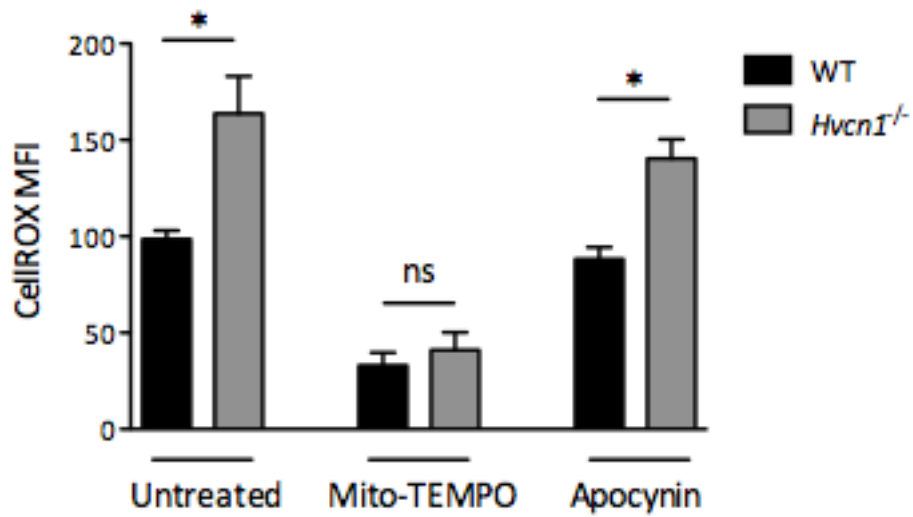


**Figure 3 - 9 Mito-TEMPO reduces basal ROS levels in WT and *Hvcn1*<sup>-/-</sup> macrophages.**

ROS levels were measured in BMDMs untreated or pre-treated for 1 hour with either 10  $\mu$ M Apocynin or 100  $\mu$ M Mito-TEMPO, shown as relative to untreated WT BMDMs. Data represents means  $\pm$  SEM of three independent experiments. \*,  $p < 0.05$ ; ns, no significance.

### 3.2.3 ATTENUATED REGULATION OF MITOCHONDRIAL ROS

#### PRODUCTION

I had ascertained that the increase in ROS observed in *Hvcn1*<sup>-/-</sup> macrophages was of mitochondrial origin. However, the data was not conclusive of whether this was due to an overproduction of ROS in the mitochondria or impairment in ROS scavenging by antioxidant enzymes. It was important to investigate this further as mitochondrial ROS play a significant role in signalling pathways in a number of cell types (Collins et al., 2012). The current data suggest that mitochondrial ROS act as signalling molecules to maintain homeostasis as well as adapt to stress (Rhee et al., 2000). Tight regulation of mitochondrial ROS is therefore crucial in order to allow it to participate in cell signalling pathways without causing redox stress. This is achieved in several ways. Antioxidant enzymes, both in the cytosol and within the mitochondria themselves, exist in order to eliminate ROS (Murphy, 2009). The superoxide dismutase (SOD) family of antioxidant enzymes can be found within the mitochondria. The enzymatic activity of SODs generates hydrogen peroxide (H<sub>2</sub>O<sub>2</sub>) from superoxide anion (O<sub>2</sub><sup>-</sup>), which is highly unstable and has a strong oxidative potential. SOD2 is found within the mitochondrial matrix and is one of the primary enzyme that deals with ROS produced from the ETC (Sena and Chandel, 2012).

Elevated levels of ROS can induce increased expression of SOD2 in order to prevent potential injury from oxidative damage (Miao and St Clair, 2009). I therefore sought to determine if the observed elevated basal ROS in *Hvcn1*<sup>-/-</sup> BMDMs might result in this biological response by assessing the levels of SOD2 protein expression. At steady state, SOD2 protein levels were similar in both cell types (Figure 3 - 10).

Mitochondrial ROS have been indicated to act as signalling molecules to trigger inflammatory cytokine production (Bulua et al., 2011, Nakahira et al., 2011, Zhou et al., 2011), therefore LPS might regulate SOD2 activity. LPS activation of macrophages did not increase the expression of SOD2 compared to untreated macrophages (Figure 3 -10). No difference in SOD2 expression was observed between LPS activated WT and *Hvcn1*<sup>-/-</sup> macrophages (Figure 3 -10). This was further confirmed by densitometry analysis of the blots (Figure 3 – 11). This would indicate that the increase in basal ROS observed in *Hvcn1*<sup>-/-</sup> macrophages is due to an overproduction of ROS by the mitochondria.

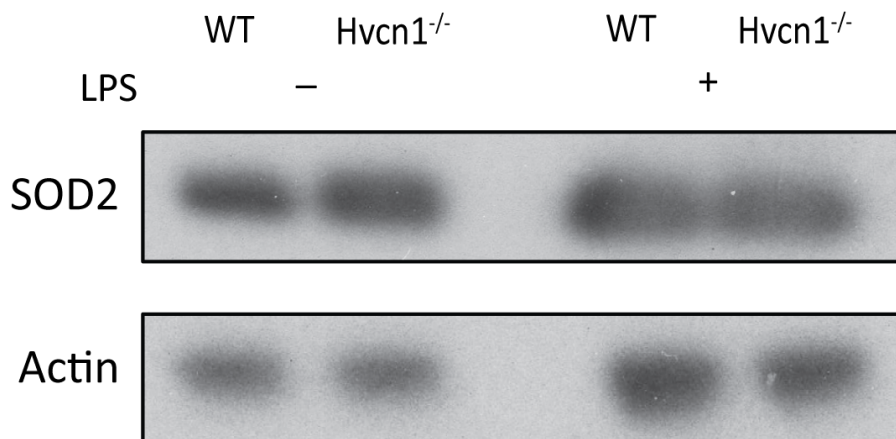


**Figure 3 - 10 Comparable SOD2 protein levels in untreated and activated macrophages.**

SOD2 protein levels in BMDMs untreated or activated with 100 ng/ml LPS for 24 hours were analysed by Western Blot. Actin was used as a loading control. Data is representative of two independent experiments.

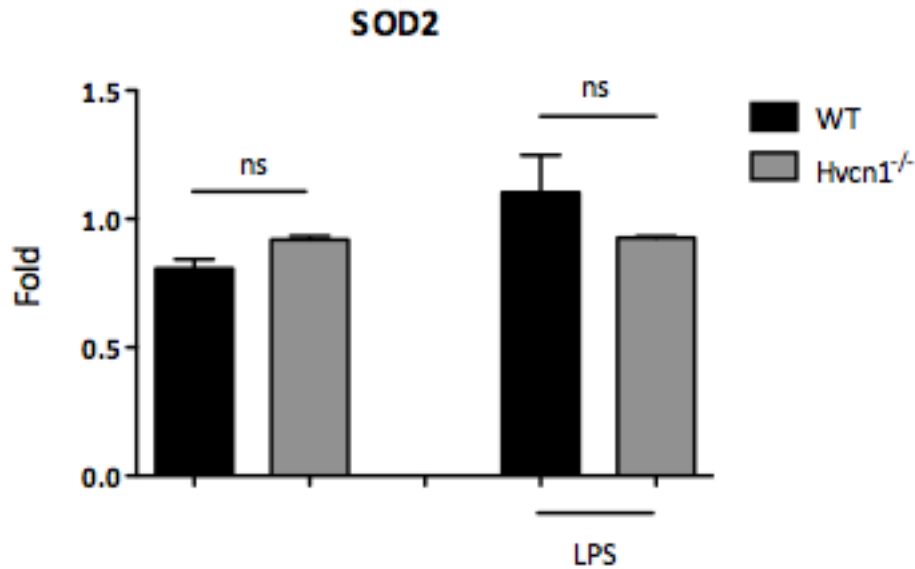


**Figure 3 - 11 Comparable SOD2 fold change in untreated and activated macrophages.**

Densitometry analysis of SOD2 Western blots. Data represents means  $\pm$  SEM of two independent experiments. ns, no significance.

Another important determinant of mitochondrial ROS production is the electrochemical gradient that is generated across the inner mitochondrial membrane. This gradient is highly dependent on the mitochondrial membrane potential. As the electrochemical gradient and thus the mitochondrial membrane potential increases, a parallel increase is observed in mitochondrial ROS production (Handy and Loscalzo, 2012). However, it has been proposed that an increase in ROS production can occur at both extremes of high and low mitochondrial membrane potential (Aon et al., 2010). In addition, these processes are closely linked to ETC activity and as such mitochondrial respiration. A high mitochondrial membrane

potential is observed with a high rate of ETC activity and mitochondrial respiration (Echtay et al., 2002).

It was thus important to assess the state of the mitochondrial membrane potential in WT and *Hvcn1*<sup>-/-</sup> macrophages. The single fluorescent dyes available to measure mitochondrial membrane potential are limited by confounding factors such as mitochondrial size, shape and density (Perry et al., 2011). With this in mind, I used a novel ratiometric dye that uses the ratio of two fluorescent probes to accurately only depend on the mitochondrial membrane potential and not the confounding factors described above (Tucsek et al., 2011). A decreased mitochondrial membrane potential was observed in the *Hvcn1*<sup>-/-</sup> macrophages compared to their WT counterparts (Figure 3 - 12). Activation with LPS significantly lowered the mitochondrial membrane potential to a similar extent in both cell types (Figure 3 - 12), as previously reported (Everts et al., 2012). FCCP was used as a positive control of very low mitochondrial membrane potential in this assay. FCCP is a lipid soluble ionophore, which inserts itself into the inner mitochondrial membrane and transports H<sup>+</sup> across to the intermembrane space. This leads to an uncoupling of the ETC with the ATP synthase, thus dissipating the mitochondrial membrane potential (Joshi and Bakowska, 2011).

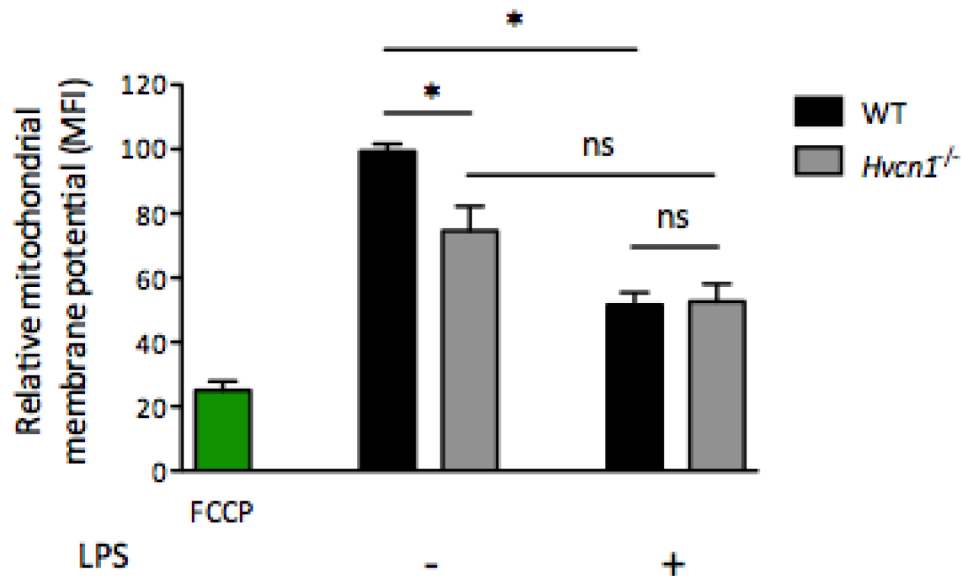


**Figure 3 - 12 Lowered mitochondrial membrane potential in *Hvcn1*<sup>-/-</sup> macrophages.**

Mitochondrial membrane potential was measured in BMDMs untreated or activated with 100 ng/ml LPS for 24 hours, shown as relative to untreated WT BMDMs. Data represents means  $\pm$  SEM of three independent experiments.

### 3.2.4 IMPAIRED RESPIRATORY BURST IN *Hvcn1*<sup>-/-</sup> MACROPHAGES

Previous work in neutrophils has shown the essential role of HVCN1 in facilitating the NADPH oxidase-mediated respiratory burst (Ramsey et al., 2009). This strong ROS production is an important defence mechanism against pathogens as it produces large amounts of ROS to eliminate pathogens (Dale et al., 2008) and I thus wanted to assess the capacity of *Hvcn1*<sup>-/-</sup> macrophages to mount this response using the classical immune stimulus LPS, a bacterial derived lipopolysaccharide.

After LPS stimulation, ROS production from *Hvcn1*<sup>-/-</sup> macrophages was significantly lower compared to that of WT macrophages (Figure 3 - 13). Diminished ROS production was observed in the presence of Apocynin in both cells types, which confirmed that the majority of the LPS-induced ROS were generated by the NADPH oxidase (Figure 3 - 13). This is shown more clearly when the data are represented as fold induction over the respective untreated macrophages (Figure 3 - 14). In addition, Apocynin treatment did not affect cell viability after LPS treatment (Figure 3 - 15).

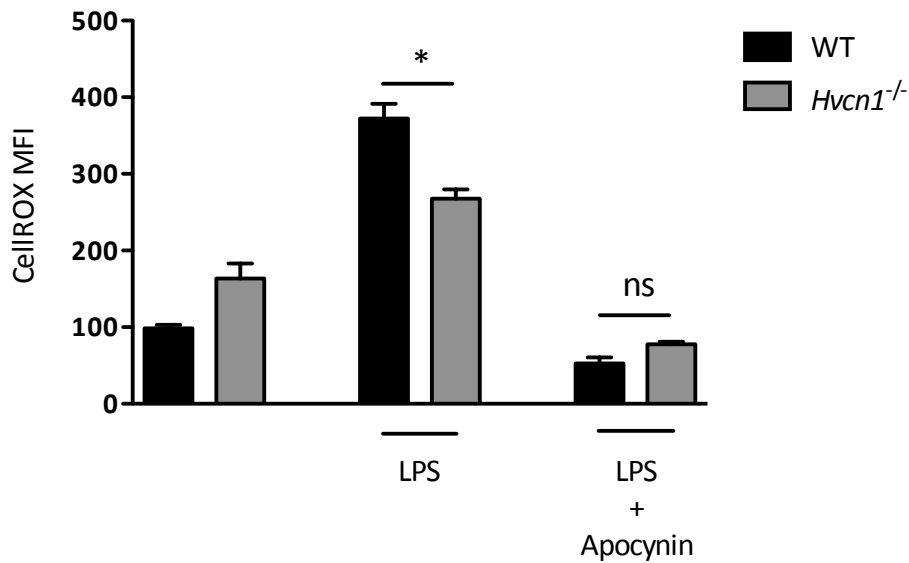


**Figure 3 - 13 Impaired respiratory burst in *Hvcn1*<sup>-/-</sup> macrophages.**

ROS levels of WT and *Hvcn1*<sup>-/-</sup> BMDMs in response to 1 hour stimulation with 100 ng/ml LPS. Data are represented as relative to untreated WT BMDMs. Data represents means  $\pm$  SEM of three independent experiments. \*,  $p < 0.05$ ; ns, no significance.

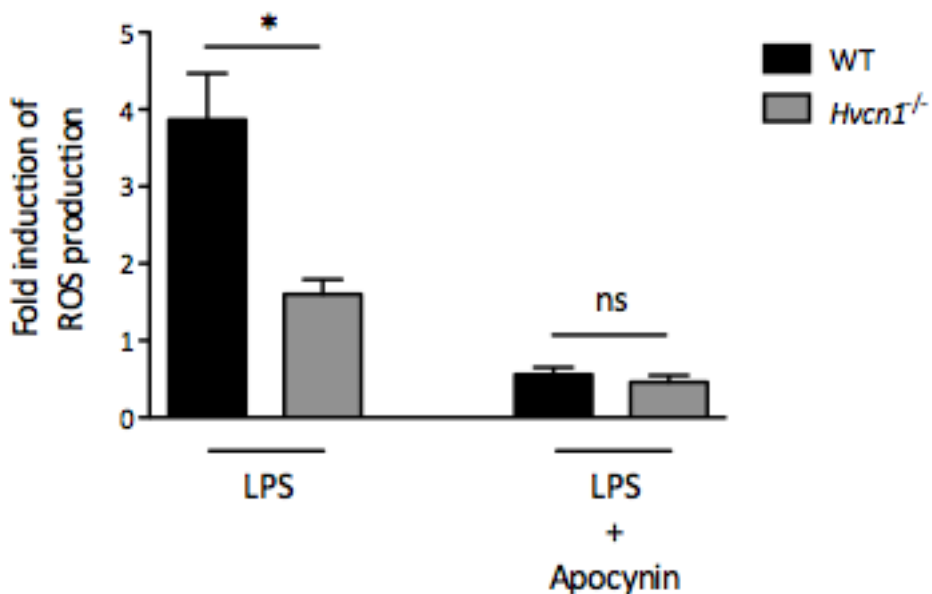


**Figure 3 - 14 Impaired respiratory burst in *Hvcn1*<sup>-/-</sup> macrophages (relative levels).**

ROS levels of WT and *Hvcn1*<sup>-/-</sup> BMDMs in response to 1 hour stimulation with 100 ng/ml LPS. Data are represented as fold induction over the respective untreated macrophages. Data represents means  $\pm$  SEM of three independent experiments. \*,  $p < 0.05$ ; ns, no significance.

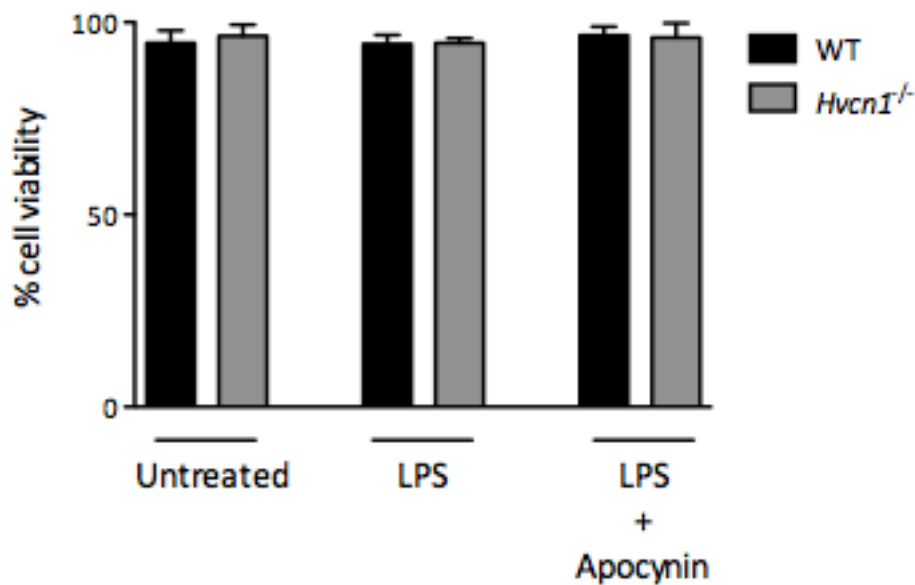


**Figure 3 - 15 Apocynin does not affect the viability of LPS-stimulated macrophages.**

Percentage of viable BMDMs (expressed as percentage over vehicle) untreated or pre-treated for 1 hour with either 10  $\mu$ M Apocynin or 100  $\mu$ M Mito-TEMPO. Data represents means  $\pm$  SEM of three independent experiments.

Despite the observed significant reduction in superoxide production in *Hvcn1*<sup>-/-</sup> neutrophils, no data were available on their phagocytic capacity (Ramsey et al., 2009). I therefore assessed whether HVCN1-deficiency affected phagocytic capacity

in macrophages. No differences in phagocytic capacity were observed between WT and *Hvcn1*<sup>-/-</sup> macrophages at steady state (Figure 3 - 16). LPS activation of macrophages increased the phagocytic capacity of both cell types, however no differences were observed (Figure 3 - 16). These data would suggest that neither the ability to mount a respiratory burst nor the presence of proton channels has any involvement in the phagocytic capacity of macrophages.

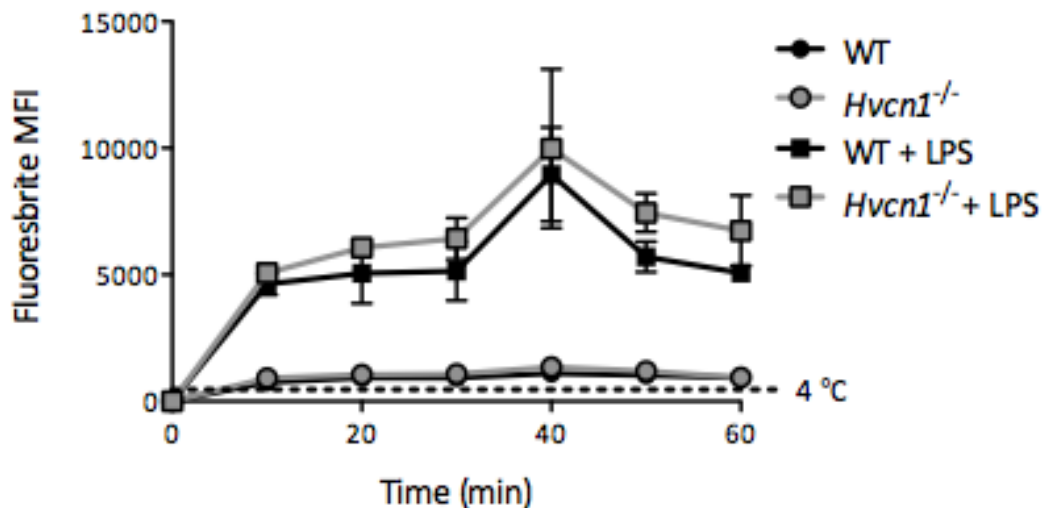


**Figure 3 - 16 Phagocytic capacity of steady state and activated *Hvcn1*<sup>-/-</sup> macrophages is not impaired.**

Fluorescent-labelled latex beads were given to untreated BMDMs or those activated with 100 ng/ml LPS for 24 hours. Bead uptake was measured over a period of time. BMDMs incubated at 4 °C during phagocytosis were used as control. Data represents means  $\pm$  SEM of three independent experiments.

### 3.2.5 HVCN1 IS LOCALISED ON THE PLASMA MEMBRANE IN MACROPHAGES

As discussed previously, there is little data on the localisation of HVCN1 in immune cells. Electrophysiological investigations in immune cells, such as macrophages, have shown that proton currents are mediated at the plasma membrane (Holevinsky et al., 1994, Kapus et al., 1993). Other studies in epithelial cells have shown evidence for proton channel expression on intracellular organelles (Schapiro and Grinstein, 2000, Li et al., 2010). In B cells, HVCN1 was present at the plasma membrane as well as in the cytoplasm (Capasso et al., 2010).

Given the observations made about the mitochondrial ROS production and membrane potential in *Hvcn1*<sup>-/-</sup> macrophages, I next wanted to determine if the proton channel were expressed in the mitochondria. Immunofluorescence imaging showed that HVCN1 was expressed on the plasma membrane of macrophages, however it did not co-localise with MitoTracker Deep Red FM, a mitochondrial marker (Figure 3 - 17). In addition, there was no co-localisation of HVCN1 with the ER (GRP94) (Figure 3 - 17). These results indicate that the role of HVCN1 on mitochondrial ROS and membrane potential is not due to direct function mediated in the mitochondria.

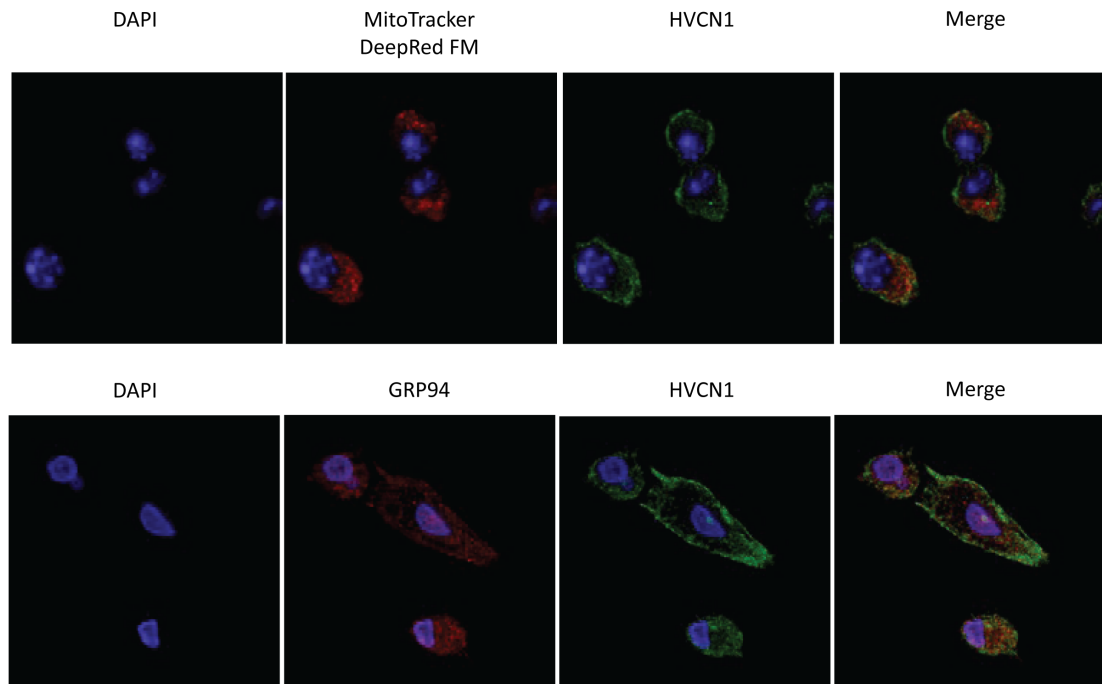


**Figure 3 - 17 HVCN1 does not co-localise with the mitochondria or the endoplasmic reticulum.**

WT macrophages were stained with MitoTracker DeepRed FM and GRP94 that are markers for the mitochondria and endoplasmic reticulum, respectively. Data are representative figures of two independent experiments.

### 3.3 CHAPTER DISCUSSION

Only two studies to date have investigated proton channels in macrophages (Kapus et al., 1993, Holevinsky et al., 1994) and therefore little is known about the role of HVCN1 in these immune cells. These earlier studies have confirmed the existence of proton channels in macrophages through patch clamp recordings. The field of proton channel research has been hampered to a certain extent by the lack of commercially available antibodies against HVCN1 and it is only in recent years that such antibodies have become available. The present work demonstrates for the first time the expression of HVCN1 at the protein level in macrophages. Furthermore, it confirms the absence of HVCN1 protein in macrophages from *Hvcn1*<sup>-/-</sup> mice.

Interestingly, I observed elevated basal ROS in *Hvcn1*<sup>-/-</sup> macrophages. It was determined through pharmacological manipulation that they were of a mitochondrial origin rather than due to the activity of the NADPH oxidase complex. As discussed previously, this has been observed in *Hvcn1*<sup>-/-</sup> B cells and neutrophils (Capasso et al., 2010, Decleva et al., 2013); an effect that was reversed by treatment of neutrophils with gramicidin, a molecule that generates pores permeable to protons and other monovalent cations. However, the observation in these two cell types was not further investigated.

Assessment of expression levels of the mitochondrial antioxidant enzyme SOD2 showed similar expression at steady state in both WT and *Hvcn1*<sup>-/-</sup> macrophages. This was also true after LPS activation, indicating that increased ROS are not inducing a feedback upregulation of SOD2 in macrophages. Whilst there might not be any differences in the amount of SOD2 enzyme, its rate of activity might be different.

Investigating the specific activity of SOD2 would provide a better insight into the state of this antioxidant system in the mitochondria. In addition, it would be important to assess other antioxidant enzymes, such as glutathione peroxidase (GPx) and peroxiredoxins, and also cofactors, such as glutathione levels (Li et al., 2013).

Mitochondrial ROS production is tightly regulated by a number of factors, one of those being the mitochondrial membrane potential. It is well described that a higher mitochondrial membrane potential is associated with greater production of mitochondrial ROS, which is associated with increased electron transport (Handy and Loscalzo, 2012). However, a range of agents that lower mitochondrial membrane potential (LPS, ETC inhibitors, etc.) paradoxically increase mitochondrial ROS production. The exact mechanism for this disparity is not well defined (West et al., 2011, Everts et al., 2012). This appears to be the case in the *Hvcn1*<sup>-/-</sup> macrophages, where a reduced mitochondrial membrane potential was observed compared to their WT counterparts. A “redox-optimised ROS balance hypothesis” has been proposed to explain this paradox and it states that oxidative stress can occur at either extremes of high or low mitochondrial potential (Aon et al., 2010).

In accordance with the literature, *Hvcn1*<sup>-/-</sup> macrophages displayed an impaired respiratory burst. In neutrophils, the lack of proton channels resulted in an intracellular acidification, due to the activity of NADPH oxidase in the absence of charge and intracellular pH (pH<sub>i</sub>) compensation (El Chemaly et al., 2010, Morgan et al., 2009). HVCN1 extrudes protons (H<sup>+</sup>) that rapidly accumulate in the cytosol and delivers them into the phagosome, where they are used in crucial chemical reactions to produce ROS (Morgan et al., 2009). This mechanism is most likely the same in

macrophages, but investigations into intracellular acidification during activation or phagocytosis would need to be undertaken to confirm this.

Ramsey et al. showed no differences in the capacity of *Hvcn1*<sup>-/-</sup> neutrophils to phagocytose opsonised bacteria compared to WT cells (Ramsey et al., 2009). In accordance, my own investigations showed no differences in the phagocytic capacity of WT and *Hvcn1*<sup>-/-</sup> macrophages. It needs to be noted that fluorescently-labelled latex beads that are classically used in phagocytic assays, and were also used in the present study, do not provide the cells with a metabolic load, as the latex beads cannot be degraded by the cells. On the other hand, opsonised bacteria or apoptotic cells are more physiologically relevant to the phagocytic process as they do provide a metabolic load. Nonetheless, given that no impairment was observed in *Hvcn1*<sup>-/-</sup> neutrophil phagocytosing bacteria (Ramsey et al., 2009), it is likely that this process is not linked to HVCN1 regulation of ROS production and therefore not regulated by proton channels.

Regarding HVCN1 subcellular localisation, I observed it on the plasma membrane of macrophages and could not detect any co-localisation with mitochondrial markers. Therefore, the steady state increase in mitochondrial ROS is not due to a direct role of HVCN1 in macrophages. It might be due to the effect of cytosolic charge and pH balance, which might affect mitochondrial function.

I have presented here for the first time the functional expression of HVCN1 in macrophages and have found overproduction of mitochondrial ROS in *Hvcn1*<sup>-/-</sup> macrophages. Cellular metabolism is closely linked to ROS production and thus I next wanted to investigate the metabolism of *Hvcn1*<sup>-/-</sup> macrophages.

**CHAPTER FOUR: ATTENUATED MITOCHONDRIAL  
RESPIRATION AND DIMINISHED SPARE  
RESPIRATORY CAPACITY IN *Hvca1*<sup>-/-</sup>  
MACROPHAGES**

## 4.1 INTRODUCTION

Previous studies discussed in Chapter 1 and my own investigations in Chapter 3 have demonstrated a link between HVCN1 and ROS production. Most of these studies have focused on the role the proton channel plays in NADPH oxidase-dependent ROS production. Whilst observations of elevated basal mitochondrial ROS have been made previously in HVCN1<sup>-/-</sup> B cells (Capasso et al., 2010) and, more recently, in zinc (Zn<sup>2+</sup>)-treated neutrophils (Decleva et al., 2013), no further investigations have been undertaken into how the lack of proton channels may modulate mitochondrial ROS or how elevated basal ROS levels may affect cellular processes such as metabolism.

To date, only one study has assessed the effects of HVCN1-deficiency on metabolic processes (Capasso et al., 2010). The study demonstrated that *Hvcn1*<sup>-/-</sup> B cells used the same amount of oxidative phosphorylation and glycolysis as their WT counterparts. However after BCR stimulation, B cells lacking HVCN1 used less oxidative phosphorylation and glycolysis than WT cells. This difference was not apparent when B cells were stimulated with LPS or anti-CD40.

It has been known for some time that metabolic profiles are closely linked to macrophage polarisation and function. In recent years, emerging evidence has suggested that the functional phenotype acquired by macrophages in response to environmental cues is heavily dependent on metabolic processes (Biswas and Mantovani, 2012).

Classically activated macrophages, which are characterised by their pro-inflammatory phenotype, shift their metabolism towards the anaerobic glycolytic

pathway. This shift is absent in alternatively activated macrophages, which are characterised by an anti-inflammatory phenotype (Rodriguez-Prados et al., 2010). The rapid rate of adenosine triphosphate (ATP) production by glycolysis allows classically activated macrophages to cope with their increased energy demands in order to trigger microbicidal functions. In contrast, oxidative metabolism is the metabolic pathway favoured by alternatively activated macrophages. It generates large amounts of ATP and thus provides sustained energy for the wound healing and tissue remodelling functions of these macrophages (Odegaard and Chawla, 2011).

## 4.2 AIMS

This chapter describes my investigation to define the role of HVCN1 in macrophage metabolism. My aims were to address the following questions:

- Is mitochondrial respiration and/or glycolysis altered in *Hvcn1*<sup>-/-</sup> macrophages?
- Are *Hvcn1*<sup>-/-</sup> macrophages able to produce comparable amounts of ATP, as their WT counterparts, despite their intracellular ROS overproduction?
- Is the mitochondrial biomass similar in WT and *Hvcn1*<sup>-/-</sup> macrophages?
- Does HVCN1-deficiency affect the spare respiratory capacity?

### 4.2.1 ATTENUATED MITOCHONDRIAL RESPIRATION IN *Hvcn1*<sup>-/-</sup>

#### MACROPHAGES

Since HVCN1 appears to play a role in mitochondrial ROS production in *Hvcn1*<sup>-/-</sup> macrophages, I next explored the impact of HVCN1 deficiency in macrophage metabolism. I assessed mitochondrial respiration and glycolysis in macrophages by measuring oxygen consumption rate (OCR) and extracellular acidification rate (ECAR).

Real-time measurements of the OCR of WT and *Hvcn1*<sup>-/-</sup> macrophages found significantly lower rates at steady state in cells lacking the proton channel (Figure 4-1). However, activation with LPS decreased the OCR in both cell types to a similar extent (Figure 4-1). This is in accordance with the decreased mitochondrial membrane potential observed in *Hvcn1*<sup>-/-</sup> macrophages (Figure ), suggesting a mitochondrial defect in these cells.

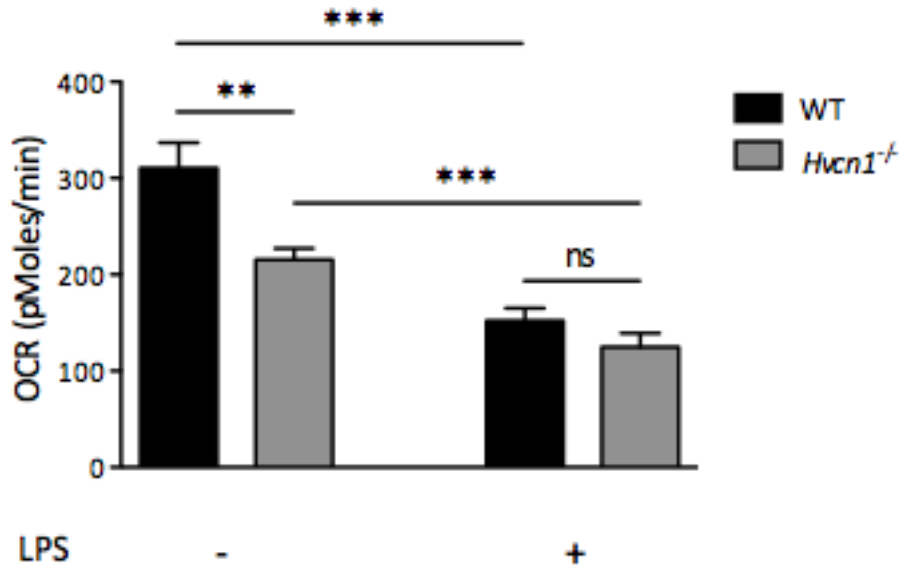


**Figure 4-1 Attenuated mitochondrial respiration in *Hvcn1*<sup>-/-</sup> macrophages.**

Measurement of mitochondrial respiration (OCR) in BMDMs untreated or activated with 100 ng/ml LPS for 24 hours. Data represents means  $\pm$  SEM of three independent experiments. \*\*,  $p < 0.01$ ; \*\*\*,  $p < 0.001$ ; ns, no significance.

No differences were observed in the real-time steady state ECAR of either cell type (Figure 4-2). Activation with LPS led to an increase in the ECAR of both WT and *Hvcn1*<sup>-/-</sup> macrophages, however the latter showed a significantly greater increase in glycolytic flux (Figure 4-2).

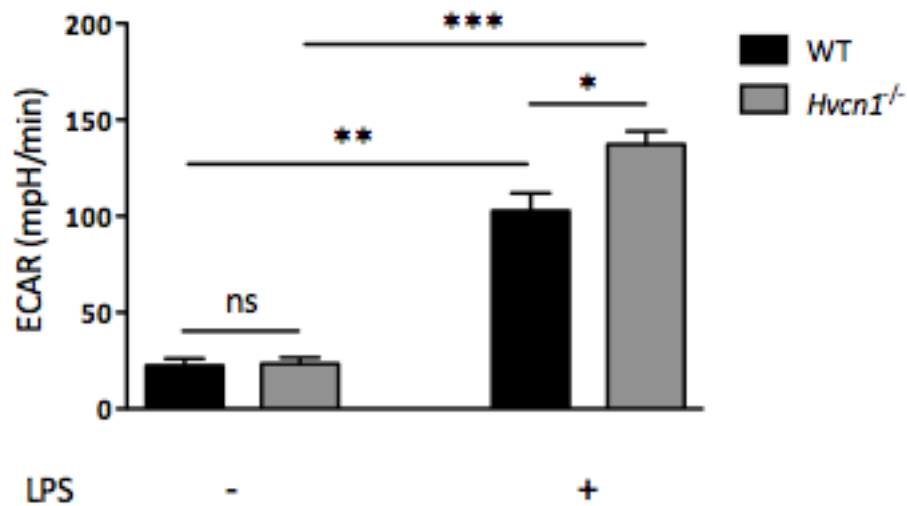


**Figure 4-2 Increased glycolysis in activated *Hvcn1*<sup>-/-</sup> macrophages.**

Measurement of glycolytic flux (ECAR) in BMDMs untreated or activated with 100 ng/ml LPS for 24 hours. Data represents means  $\pm$  SEM of three independent experiments. \*,  $p < 0.05$ ; \*\*,  $p < 0.01$ ; \*\*\*,  $p < 0.001$ .

Both WT and *Hvcn1*<sup>-/-</sup> macrophages responded in a similar manner to LPS stimulation by switching from oxidative metabolism to anaerobic glycolysis, which is a hallmark of classical activation (Rodriguez-Prados et al., 2010). This suggests that *Hvcn1*<sup>-/-</sup> macrophages have no defects in inducing an increase in their glycolytic flux and thus suggesting that the defect in the metabolism of these cells is mitochondria specific.

### 4.2.2 DECREASED ATP LEVELS IN *Hvcn1*<sup>-/-</sup> MACROPHAGES

The observations of the metabolism of *Hvcn1*<sup>-/-</sup> macrophages in the previous section would suggest mitochondrial impairment because glycolysis occurs in the cytoplasm whereas oxidative phosphorylation occurs inside the mitochondria. I thus wanted to investigate the potential impact this would have on cellular energy levels. In addition, I wanted to ascertain that these observations were not due to differences in mitochondrial biomass.

In support of altered mitochondrial respiration, steady state ATP levels in *Hvcn1*<sup>-/-</sup> macrophages were significantly lower compared to their WT counterparts (Figure 4-3). Activation with LPS decreased the ATP levels in both cell types. Interestingly, *Hvcn1*<sup>-/-</sup> macrophages had lower ATP levels after LPS stimulation (Figure 4-3) despite having a greater induction of glycolytic flux (Figure 4-2).

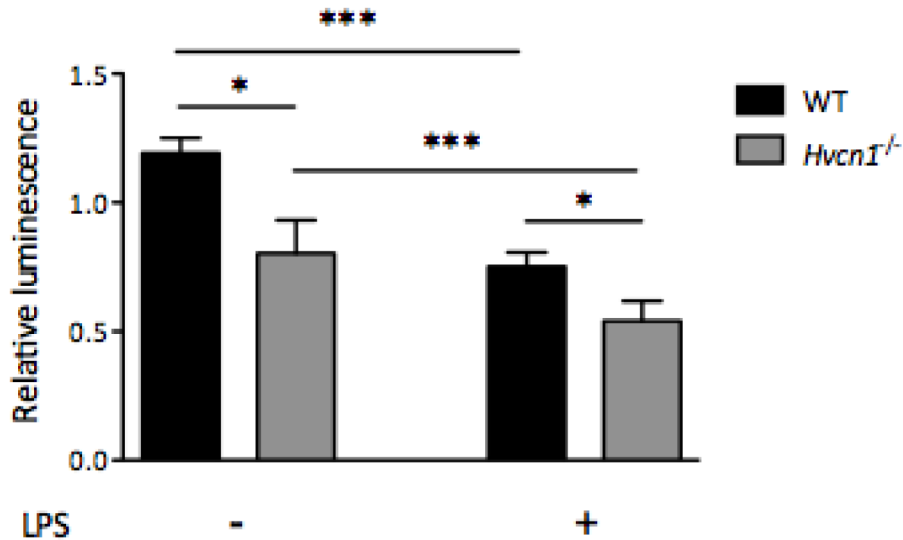


**Figure 4-3 Attenuated ATP levels in untreated and activated *Hvcn1*<sup>-/-</sup> macrophages.**

Measurement of ATP levels in BMDMs untreated or activated with 100 ng/ml LPS for 24 hours, shown as relative to untreated WT BMDMs. Data represents means  $\pm$  SEM of three independent experiments. \*,  $p < 0.05$ ; \*\*\*,  $p < 0.001$ .

I next assessed mitochondrial biomass in order to confirm that these observations were not due to differences in numbers of mitochondria present in the macrophages. I used a mitochondrial dye (MitoTracker Green FM) that localises to mitochondria regardless of their membrane potential. I found similar levels of mitochondrial biomass in the two cell types at the steady state and this was also true after activation with LPS (Figure 4-4). Mitochondrial biogenesis was induced in response to LPS activation to comparable levels in WT and *Hvcn1*<sup>-/-</sup> macrophages (Figure 4-4), however this did not reach statistical significance.

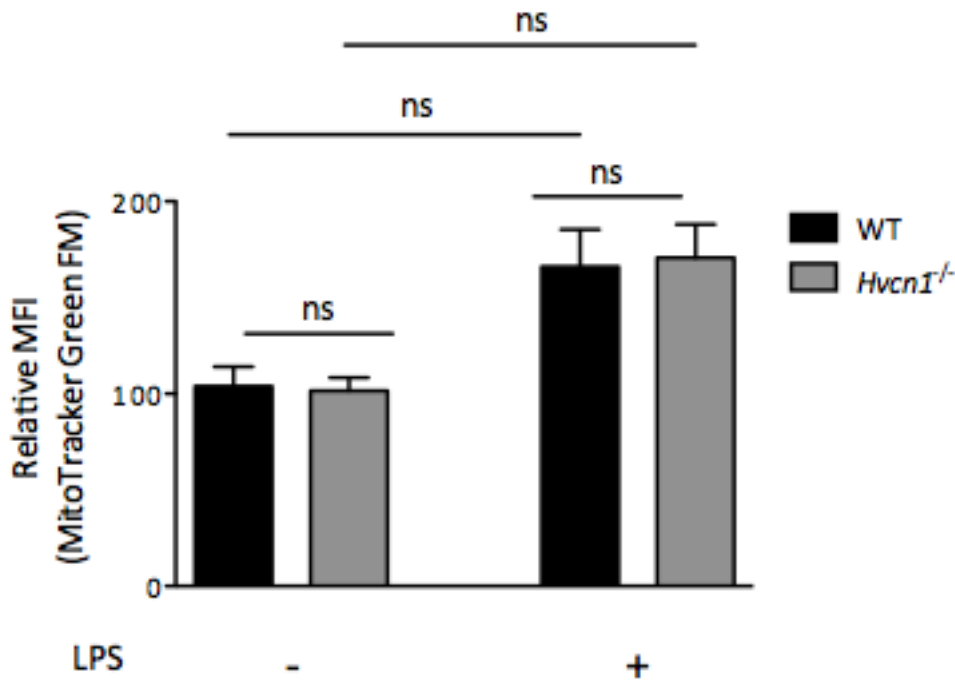


**Figure 4-4 Comparable mitochondrial biomass in WT and *Hvcn1*<sup>-/-</sup> macrophages.**

Mitochondrial biomass in BMDMs untreated or activated with 100 ng/ml LPS for 24 hours, shown as relative to untreated WT BMDMs. Data represents means  $\pm$  SEM of three independent experiments.

Whilst I observed no differences in mitochondrial biomass, *Hvcn1*<sup>-/-</sup> macrophages may have acquired mutations in their mitochondrial DNA due to their elevated basal mitochondrial ROS (Shokolenko et al., 2009). The complexes of the ETC are essential to mitochondrial function; I therefore assessed their protein expression levels. Genes found in the mitochondrial DNA encode all of the complex proteins; except for complex II, which is encoded by nuclear DNA (Bai et al., 2004). Western blot analysis of all five complexes of the ETC showed comparable levels in WT and *Hvcn1*<sup>-/-</sup>

macrophages, at steady state and after LPS activation (Figure 4 – 5). This was further confirmed by densitometry analysis of the blots (Figure 4 - 6).

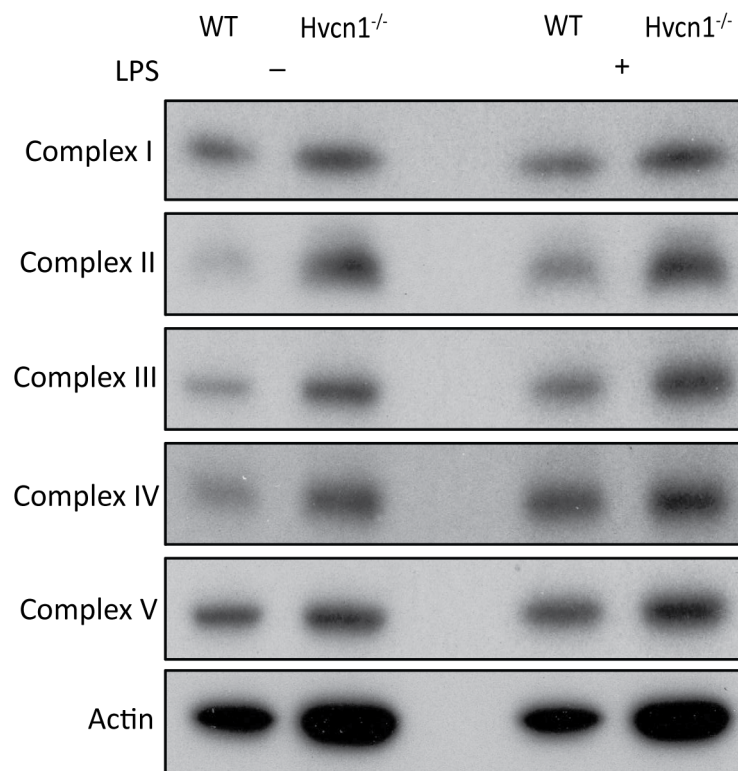


**Figure 4-5 HVCN1 loss does not affect protein expression of ETC complexes.**

Protein levels of ETC complexes in untreated and LPS activated BMDMs were measured by Western Blot analysis. Actin was used as a loading control. Data are representative of two independent experiments.

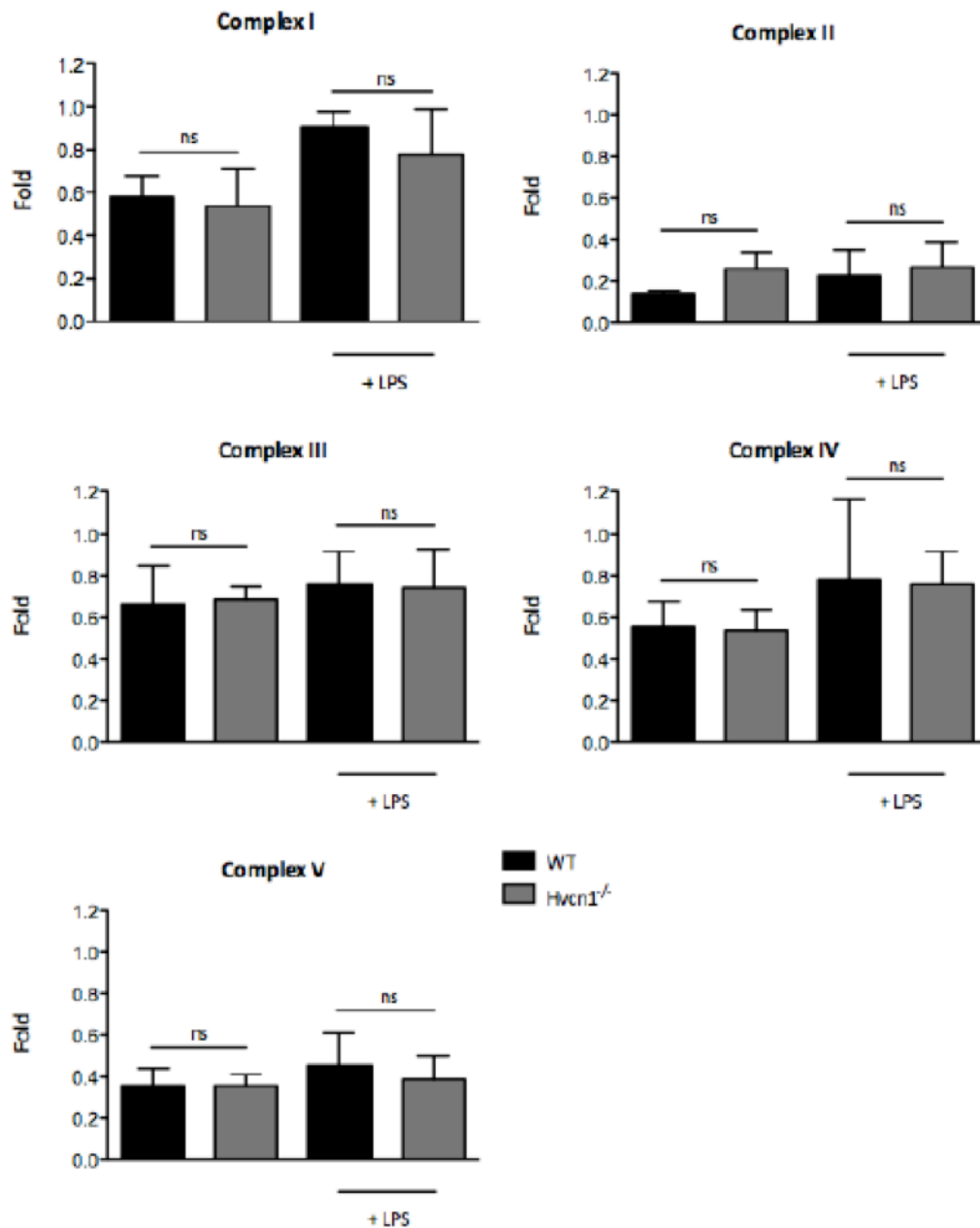


**Figure 4 - 6 HVCN1 loss does not affect protein expression of ETC complexes.**

Protein levels of ETC complexes in untreated and LPS activated BMDMs measured by Western Blot analysis followed by densitometry analysis. Data represents means  $\pm$  SEM of two independent experiments.

### 4.2.3 DIMINISHED SPARE RESPIRATORY CAPACITY IN *Hvcn1*<sup>-/-</sup>

#### MACROPHAGES

In the event of a sudden increase in energy demand or stress, cells can engage their spare respiratory capacity (SRC). This extra mitochondrial capacity allows the cells to effectively manage cellular stress such as hypoxia and low levels of nutrients. It is believed to be crucial for both cellular survival and function (van der Windt et al., 2012, Nicholls, 2009).

Figure shows the real-time OCR measurements made pre- and post sequential injections of Oligomycin A, FCCP, and Rotenone and Antimycin A. Oligomycin A inhibits ATP synthase (complex V), which decreases the basal OCR of cells to a certain extent. FCCP allows increased H<sup>+</sup> movement across the inner mitochondrial membrane. This effect on the electrochemical gradient greatly increases the ETC activity and thus the OCR (Joshi and Bakowska, 2011). Rotenone and Antimycin A inhibit complexes I and III, respectively. This leads to a complete inhibition of the ETC and is followed by a sharp decline in OCR (Liu et al., 2002). The difference between the maximum OCR, seen after FCCP addition, and the basal OCR is calculated as the SRC (van der Windt et al., 2012).

I investigated this capacity in steady state and LPS activated macrophages. A significantly lower SRC was observed in the *Hvcn1*<sup>-/-</sup> macrophages at steady state (Figure 4 - 7), which agrees with my previous observations of mitochondrial respiration (Figure 4-1). This result confirms further that mitochondria in *Hvcn1*<sup>-/-</sup> macrophages are defective. Activation with LPS greatly reduced the SRC in both WT

and *Hvcn1*<sup>-/-</sup> macrophages to comparable levels (Figure 4 - 7). Despite this, no negative effect on cell survival was observed in response to LPS (Figure 3 - 7).

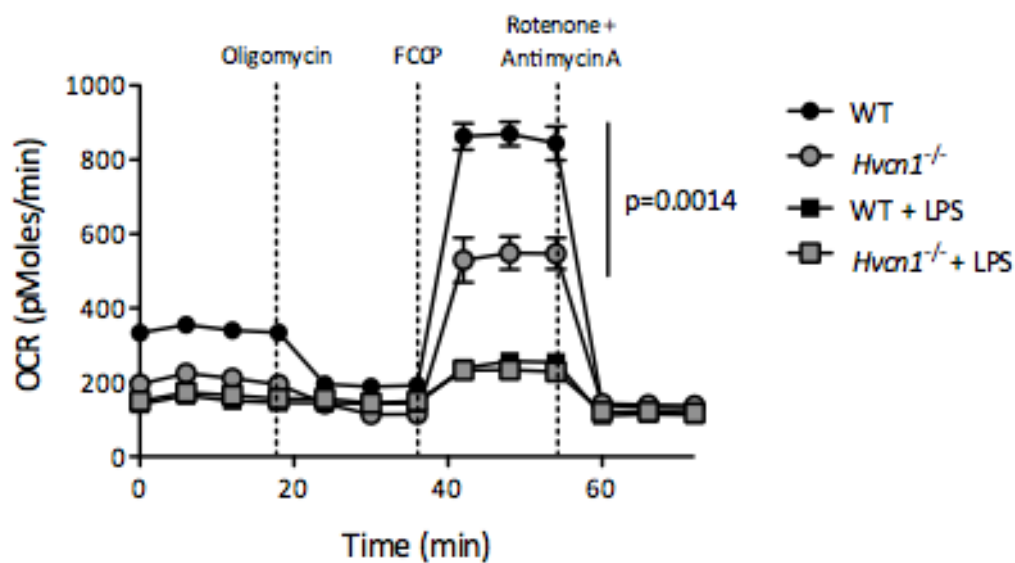


**Figure 4 - 7 Diminished spare respiratory capacity in *Hvcn1*<sup>-/-</sup> macrophages.**

Real-time mitochondrial respiration (OCR) measurements during sequential treatments of BMDMs (untreated or activated with 100 ng/ml LPS for 24 hours) with Oligomycin A, FCCP, and Rotenone and Antimycin A. Data represent means  $\pm$  SEM of three independent experiments.

### 4.3 CHAPTER DISCUSSION

The findings described in Chapter 3 lead me to focus on the mitochondria and as such, macrophage metabolism. HVCN1-deficiency has previously been shown to impair metabolism in activated B cells (Capasso et al., 2010). I sought to investigate the impact of elevated basal ROS and attenuated mitochondrial membrane potential on macrophage metabolism.

In agreement with the mitochondrial membrane potential data, *Hvcn1*<sup>-/-</sup> macrophages in the steady state used significantly lower mitochondrial respiration in comparison to WT macrophages. No differences were observed in regards to glycolytic flux in the steady state. Both WT and *Hvcn1*<sup>-/-</sup> macrophages switched from oxidative metabolism to anaerobic glycolysis upon LPS stimulation, however the cells lacking the channel were able to increase their rate of glycolysis to a further extent. This may indicate that the *Hvcn1*<sup>-/-</sup> macrophages are in a state of hyper reactivity, due to a greater volume of ROS signalling molecules, and can thus induce a greater rate of glycolysis (Bulua et al., 2011). This highlights the fact that there might be mitochondrial impairment in *Hvcn1*<sup>-/-</sup> macrophages as glycolysis occurs in the cytosol whilst oxidative phosphorylation occurs within the mitochondrial matrix (Papa et al., 2012).

Significantly lower levels of ATP were detected in *Hvcn1*<sup>-/-</sup> macrophages, which supports the findings of attenuated mitochondrial respiration. Interestingly, *Hvcn1*<sup>-/-</sup> cells had lower ATP levels even after LPS stimulation despite having a greater induction of glycolytic flux. It is possible that the lower ATP levels are due to an increased ATP consumption.

I hypothesised that differences in mitochondrial biomass may give rise to the observations I had made previously. A greater quantity of mitochondria could account for the greater ROS production that is observed in *Hvcn1*<sup>-/-</sup> macrophages whilst lower quantities of mitochondria could correlate with reduced levels of mitochondrial respiration. However, we found similar levels of mitochondrial biomass in WT and *Hvcn1*<sup>-/-</sup> macrophages at steady state and after LPS activation. It has been shown that mitochondrial biogenesis factors, such as proliferator-activated receptor- $\gamma$  coactivator 1 $\alpha$  (PGC1 $\alpha$ ), regulate both mitochondrial biomass and the expression of several antioxidant enzymes in macrophages (Vats et al., 2006). It is therefore thought that mitochondrial biomass is not an important factor in terms of regulating mitochondrial ROS.

The elevated basal mitochondrial ROS levels observed in *Hvcn1*<sup>-/-</sup> macrophages may be present during their maturation process from monocytes. Mitochondrial DNA is in close proximity to the ETC and can potentially acquire mutations in response to damaging ROS (Shokolenko et al., 2009). Mitochondrial DNA encodes all of the complex proteins; except for complex II, which is encoded by nuclear DNA (Bai et al., 2004). It was therefore imperative to assess the protein expression levels of the ETC complexes. No differences in expression levels of the ETC complexes were observed between WT and *Hvcn1*<sup>-/-</sup> macrophages. This suggests that the mitochondrial defects observed in the latter are not due to changes in complex proteins. It could be argued that the activity of individual complex proteins might be affected and as such this could be addressed by investigating isolated mitochondria from both types of macrophages.

It is important for immune cells to rapidly respond to environmental stimuli to perform their functions and as such they need to be able to manage increased levels of stress or energy demand. In those instances, the SRC is believed to be involved in both cellular survival and function (van der Windt et al., 2012, Nicholls, 2009). *Hvcn1*<sup>-/-</sup> macrophages were found to have a diminished SRC, which provides further confirmation that their mitochondria may be defective. Despite this, I observed no effects on cell survival in response to LPS. It has been shown in other myeloid populations that the loss of SRC following LPS stimulation was found to be due to inhibition of oxidative phosphorylation by nitric oxide (NO), which constitutes part of the glycolytic shift observed in myeloid cells after activation (Everts et al., 2012).

My investigations into the metabolism of *Hvcn1*<sup>-/-</sup> macrophages found a mitochondrial defect in these cells. Both cellular metabolism and ATP production was affected. With an observed overproduction of mitochondrial ROS and attenuated cellular metabolism in *Hvcn1*<sup>-/-</sup> macrophages, I next wanted to investigate redox signalling and cytokine production in these cells.

**CHAPTER FIVE: ENHANCED REDOX SIGNALLING  
AND INFLAMMATORY CYTOKINE PRODUCTION IN  
*Hvcn1*<sup>-/-</sup> MACROPHAGES**

## 5.1 INTRODUCTION

Until recently, ROS were thought to exclusively cause damaging effects on cellular proteins and lack a physiological function. However, ROS are now appreciated to function as signalling molecules that can modulate cellular processes through redox-dependent signalling (Sena and Chandel, 2012).

A great deal of evidence indicates that ROS can regulate signalling pathways by causing reversible protein modifications. Hydrogen peroxide oxidation of cysteine groups can alter the DNA binding activity of transcription factors, protein-protein interactions and affect the catalytic activity of enzymes (Brandes et al., 2009). Phosphatases are particularly susceptible to regulation by ROS as they possess a reactive cysteine in their catalytic domains. These enzymes inhibit protein kinases through the processes of dephosphorylation, thus oxidation of their cysteine residue inhibits the enzymatic activity of phosphatases (Janssen-Heininger et al., 2008). Some notable examples of susceptible phosphatases are protein tyrosine phosphatase 1b (PTP1b) (Lee et al., 1998), PTEN (Kwon et al., 2004) and MAPK phosphatases (Levinthal and Defranco, 2005).

MAPKs are crucial for relaying extracellular signals to the nucleus and accomplish this through a number of phosphorylation events, which are negatively regulated by MAPK phosphatases (Cargnello and Roux, 2011). Three subgroups of MAPKs exist: the extracellular signal regulated kinases (ERKs), the JNKs, and the p38 MAPKs. MAPKs are involved in several cellular functions such as cell survival, differentiation and inflammatory responses (Boutros et al., 2008). A number of studies have demonstrated ROS-induced MAPK activation and this is further evident as

antioxidants have been shown to inhibit MAPK activation after cell stimulation (Ding et al., 2010). ROS have also been indicated in the pro-inflammatory cytokine production of macrophages through their activation of MAPKs (Kasahara et al., 2011, Emre et al., 2007).

The NF- $\kappa$ B signalling pathway plays a highly important role in the immune system as it regulates the expression of a number of genes involved in inflammation such as those for cytokines and growth factors (Li and Verma, 2002). The members of the NF- $\kappa$ B family are found in the cytoplasm of cells bound to I $\kappa$ B family proteins. This prevents the NF- $\kappa$ B proteins to translocate to the nucleus, thus inhibiting activation of the pathway (Hayden and Ghosh, 2004). NF- $\kappa$ B signalling can occur through a classical or alternative pathway. In the classical pathway of NF- $\kappa$ B activation, stimulation of the TLR4, for example, activates the I $\kappa$ B kinase (IKK)  $\beta$  complex. This in turn phosphorylates I $\kappa$ B proteins, which are targeted for degradation by the ubiquitin ligases (Figure 5 – 0). In the case of the alternative activation, IKK $\alpha$  phosphorylates the p100 NF- $\kappa$ B protein, which is processed by the proteasome (Bonizzi and Karin, 2004). Several novel mechanisms have been reported for ROS-induced NF- $\kappa$ B activation such as tyrosine phosphorylation of I $\kappa$ B, activation of IKK and serine phosphorylation of p65 (Takada et al., 2003). Studies have shown that ROS can regulate the production of cytokines, such as TNF, in macrophages through its actions on the NF- $\kappa$ B signalling pathway (Rose et al., 2000) (Bulua et al., 2011).

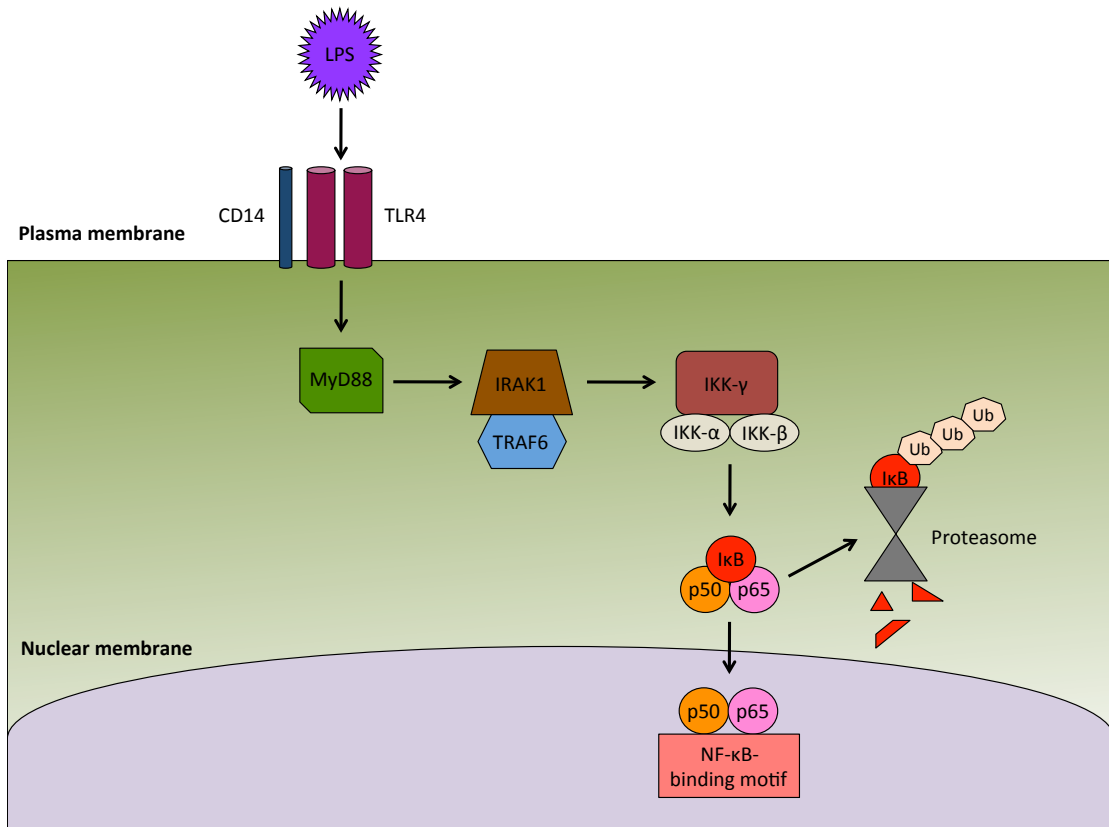


**Figure 5 - 0 LPS activation of the NF- $\kappa$ B signalling pathway.**

LPS activates TLR4 on the plasma membrane of macrophages and this leads to a downstream signalling cascade. Eventually the IKK complex is phosphorylated and it in turn phosphorylates the NF- $\kappa$ B complex. Phosphorylation of I $\kappa$ B results in its ubiquitination and degradation by proteasomes. This releases the p50/p65 complex and allows it to enter the nucleus where it binds to the NF- $\kappa$ B binding motif, which leads to gene activation. Adapted from (Oeckinghaus et al., 2011).

## 5.2 AIMS

This chapter describes my investigations into the impact of HVCN1-deficiency in macrophages on redox signalling pathways and potential effects on cytokine production. My aims were to address the following questions:

- Does the overproduction of mitochondrial ROS observed in *Hvcn1*<sup>-/-</sup> macrophages affect the redox signalling of the MAP Kinase and NF-κB pathways?
- What role does NADPH oxidase-dependent ROS and mitochondrial ROS play in macrophage redox signalling?
- Does the overproduction of mitochondrial ROS and attenuated metabolism observed in *Hvcn1*<sup>-/-</sup> macrophages affect cytokine production?
- What role does NADPH oxidase-dependent ROS and mitochondrial ROS play in cytokine production in macrophages?

### 5.2.1 ENHANCED REDOX SIGNALLING IN *Hvcn1*<sup>-/-</sup> MACROPHAGES

Given the findings of Chapters 3 and 4, I wanted to investigate if elevated mitochondrial ROS levels and impaired mitochondrial respiration would affect cellular signalling pathways and a crucial macrophage function, cytokine production.

LPS activation of macrophages triggers a cascade of signalling that involves the MAPKs (ERK, JNK, and p38) as well as the NF- $\kappa$ B pathway (Emre et al., 2007). These signalling pathways have been shown in macrophages to be redox-sensitive and as such would be susceptible to the increased mitochondrial ROS production observed in the *Hvcn1*<sup>-/-</sup> macrophages. I therefore decided to investigate the activation and kinetics of these two pathways.

Stimulation of WT macrophages with LPS resulted in the phosphorylation of p44/p42 MAPK within 15 minutes after addition of the stimulus. Phosphorylation of the protein was sustained for at least 15 minutes, and was followed by a pronounced decline in phosphorylation at 60 minutes post stimulation (Figure 5-1A). In contrast, *Hvcn1*<sup>-/-</sup> macrophages showed a faster kinetic that was evident by phosphorylation of p44/p42 MAPK at 5 minutes after LPS stimulation. Peak activation was reached at 15 minutes, similar to WT macrophages, but the phosphorylation was sustained even at 60 minutes (Figure 5-1A).

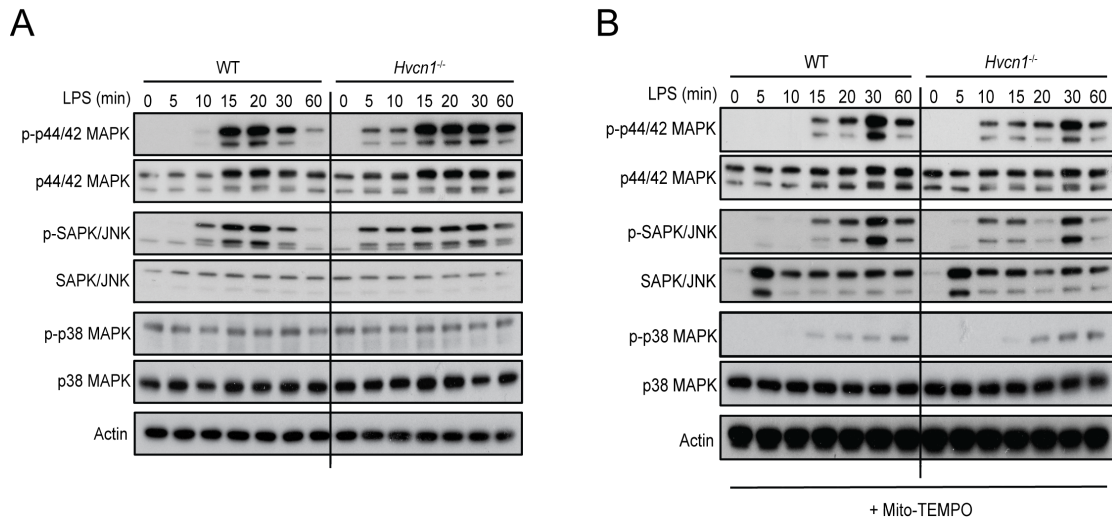


**Figure 5-1 Enhanced MAPK signalling in *Hvcn1*<sup>-/-</sup> macrophages in response to LPS.**

WT and *Hvcn1*<sup>-/-</sup> BMDMs were treated with (A) 100 ng/ml LPS or (B) pre-treated with 100  $\mu$ M Mito-TEMPO for 1 hour before stimulation with 100 ng/ml LPS for the indicated time points after which ERK, SAPK/JNK and p38 MAPK phosphorylation was measured by Western Blot. Data are representative of two independent experiments.

A similar activation pattern was observed for the SAPK/JNK pathway. For WT macrophages phosphorylation of SAPK/JNK occurred at the 10 minutes mark, reached peak activation at 15 minutes, and rapidly declined after reaching peak activation. Almost complete de-phosphorylation of SAPK/JNK was observed at 60 minutes after LPS stimulation (Figure 5-1A). In macrophages lacking the proton channel activation of the pathway occurred after 5 minutes and only reached peak activation at the 30 minutes mark. Whilst there was decline from that time point onwards, a great deal of phosphorylated protein was still observed after 60 minutes (Figure 5-1A).

No apparent differences in phosphorylation kinetics between WT and *HVCN1*<sup>-/-</sup> macrophages were evident for the p38 MAPK pathway.

As discussed previously, NF- $\kappa$ B is a transcription factor that is sequestered in the cytoplasm by I $\kappa$ B $\alpha$ , which is targeted for proteosomal degradation after it is phosphorylated. In WT macrophages I $\kappa$ B $\alpha$  was phosphorylated after 5 minutes and the total protein was completely degraded by 10 minutes (Figure 5-2A). However, in *Hvcn1*<sup>-/-</sup> macrophages a basal phosphorylated state of I $\kappa$ B $\alpha$  was evident. This also meant that the protein was completely degraded after 5 minutes (Figure 5-2A). In both cell types, a phosphorylation/degradation 'loop' was observed, but this occurred at a later time point in the *Hvcn1*<sup>-/-</sup> macrophages compared to their WT counterpart.

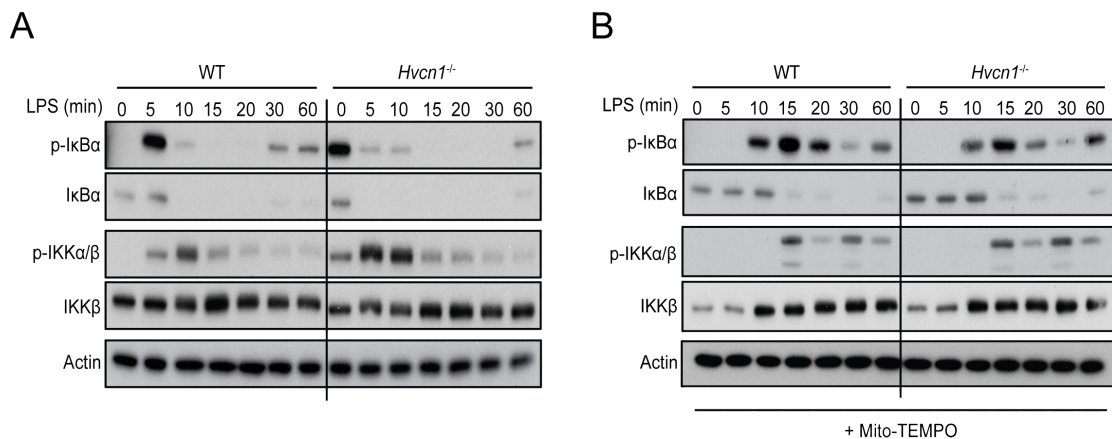


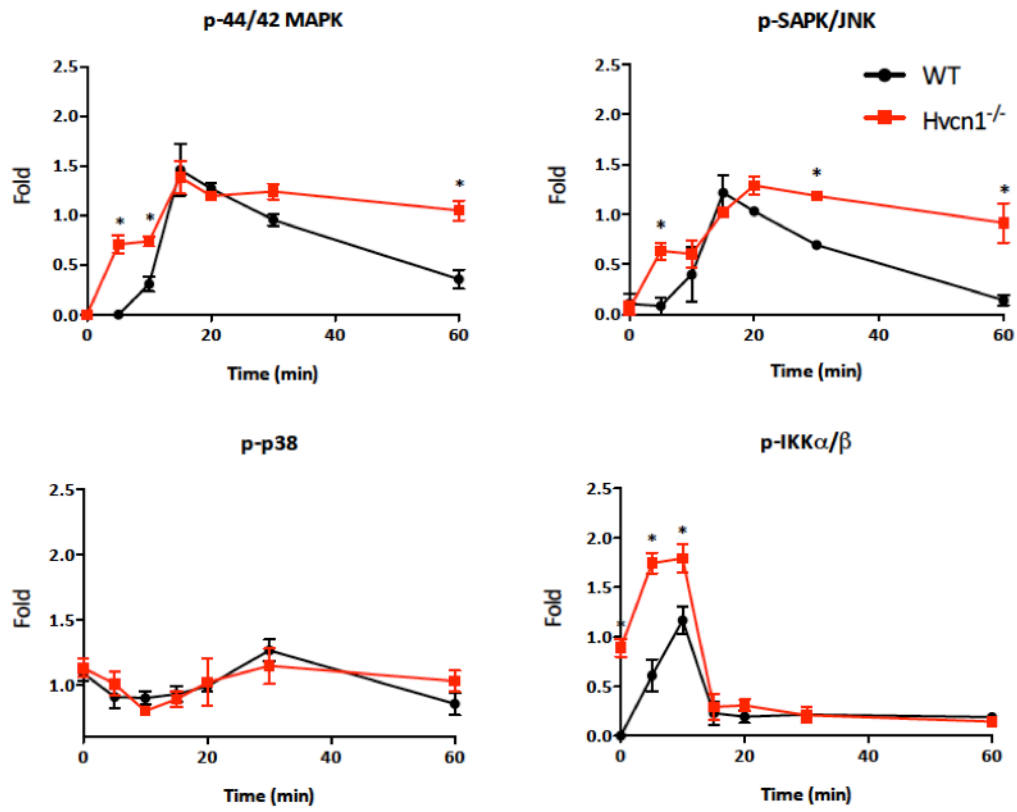
**Figure 5-2 Enhanced NF- $\kappa$ B signalling in *Hvcn1*<sup>-/-</sup> macrophages in response to LPS.**

WT and *Hvcn1*<sup>-/-</sup> BMDMs were treated with (A) 100 ng/ml LPS or (B) pre-treated with 100  $\mu$ M Mito-TEMPO for 1 hour before stimulation with 100 ng/ml LPS for the indicated time points after which I $\kappa$ B $\alpha$  and IKK $\alpha$ / $\beta$  phosphorylation was measured by Western Blot. Data are representative of two independent experiments.

A basal phosphorylation of IKK $\alpha/\beta$  was also observed in the *Hvcn1*<sup>-/-</sup> macrophages (Figure 5-2). Considerable phosphorylation was sustained over the 5 minutes and 10 minutes time points. In contrast, activation occurred at 5 minutes in WT macrophages, but a great amount of phosphorylated protein could only be detected at the 10 minutes mark after which there was a decline (Figure 5-2A).

Mitochondrial ROS have previously been reported to affect redox-sensitive signalling pathways by inhibiting phosphatases (Kamata et al., 2005, Murphy et al., 2011). We therefore wanted to determine if Mito-TEMPO could 'rescue' the enhanced signalling observed in *HVCN1*<sup>-/-</sup> BMDMs. Indeed, this antioxidant was able to attenuate the aberrant signalling in these cells (Figure 5-1B and Figure 5-2B). Antioxidant treatment also affected normal cell signalling by slowing the activation kinetics of the proteins in the MAPK and NF- $\kappa$ B pathways.

These results were further confirmed by densitometry analysis of the blots, which showed significantly faster phosphorylation kinetics in the *Hvcn1*<sup>-/-</sup> macrophages compared to their WT counterparts (Figure 5 – 3A). This enhanced signalling was abrogated in the presence of Mito-TEMPO (Figure 5 – 3B).



- Mito-TEMPO

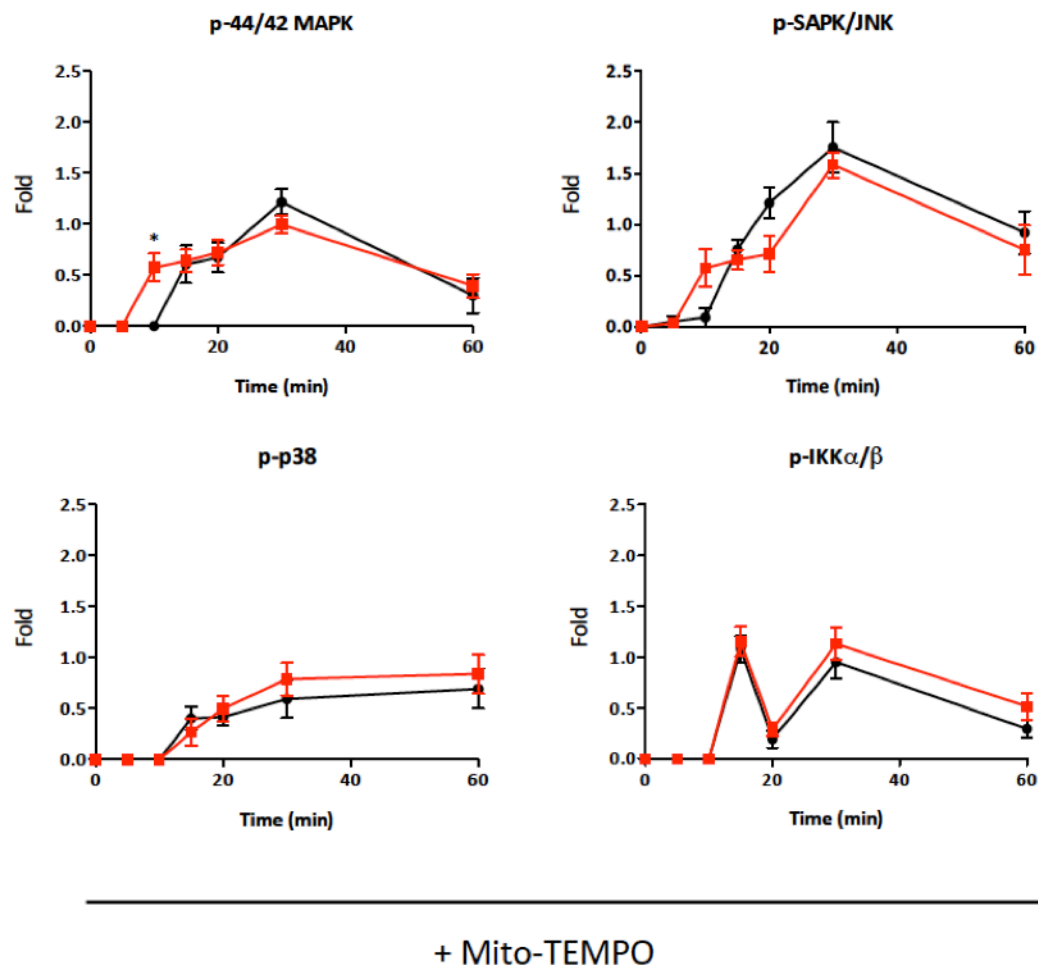


**Figure 5 - 3 Densitometry analysis of phosphorylation events in WT and *Hvcn1*<sup>-/-</sup> macrophages.**

Densitometry results of phosphorylation events in the (A) absence and (B) presence of Mito-TEMPO. Data represent means  $\pm$  SEM of two independent experiments. \*,  $p < 0.05$ .

In contrast, treatment with the NADPH oxidase inhibitor Apocynin did not significantly affect signalling (Figure 5 - 4A and B). These results were further confirmed by densitometry analysis of the blots,

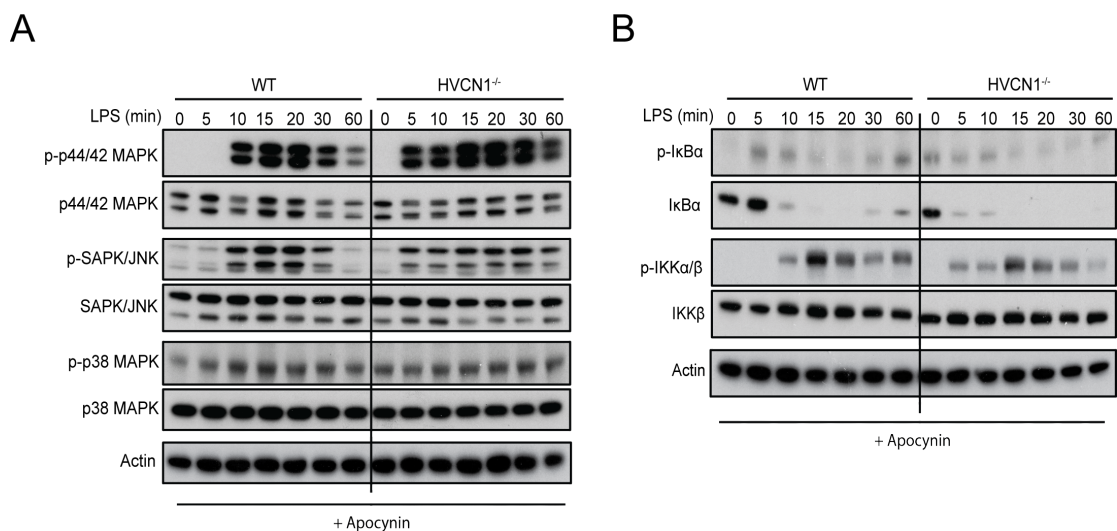


**Figure 5 - 4 Apocynin does not significantly affect cell signalling in macrophages in response to LPS>**

WT and *Hvcn1*<sup>-/-</sup> BMDMs were pre-treated with 100 μM Mito-TEMPO for 1 hour before stimulation with 100 ng/ml LPS for the indicated time points after which (A) ERK, SAPK/JNK and p38 MAPK and (B) IκBα and IKKα/β phosphorylation was measured by Western Blot. Data are representative of two independent experiments.

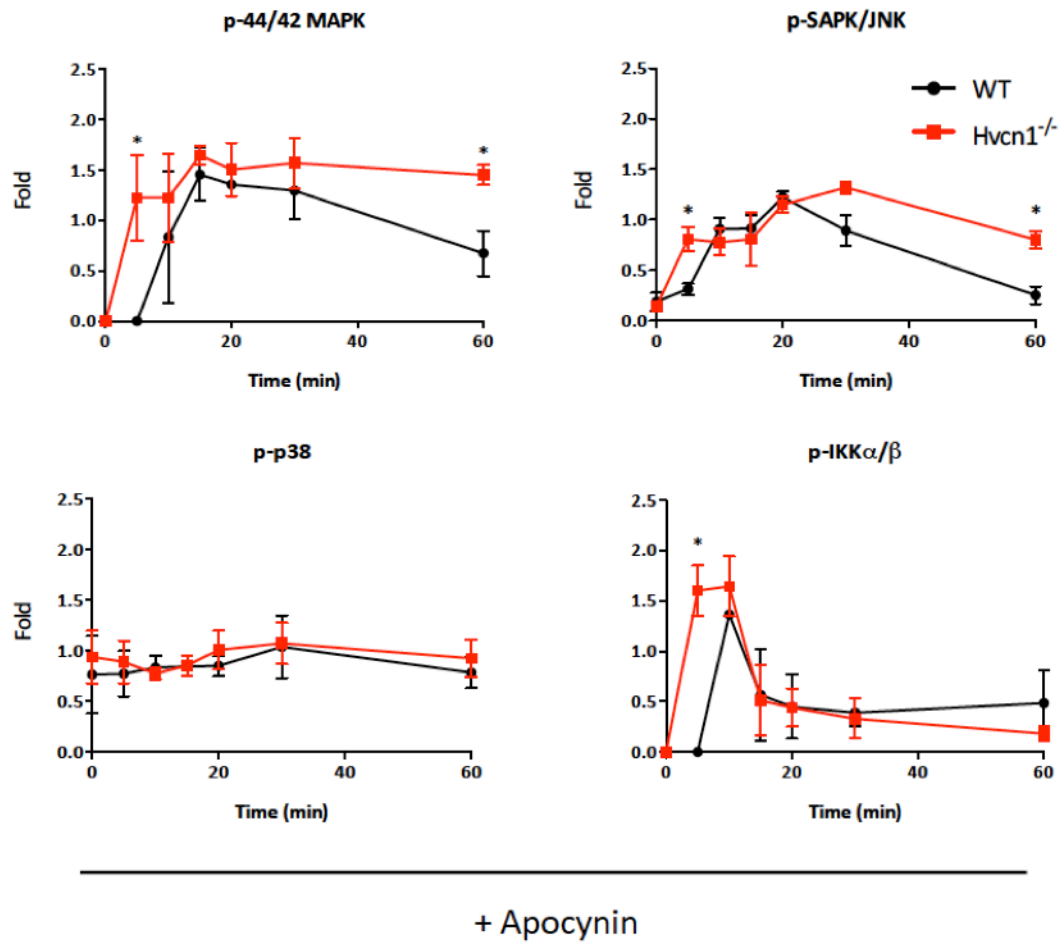


**Figure 5 - 5 Densitometry analysis of phosphorylation events in WT and *Hvcn1*<sup>-/-</sup> macrophages.**

Densitometry results of phosphorylation events in the presence of Apocynin. Data represent means  $\pm$  SEM of two independent experiments. \*, p < 0.05.

## 5.2.2 INCREASED INFLAMMATORY CYTOKINE PRODUCTION IN *Hvcn1*<sup>-/-</sup> MACROPHAGES

MAPKs are involved in several cellular functions such as cell survival, differentiation and inflammatory responses (Boutros et al., 2008). The NF- $\kappa$ B signalling pathway is also very important in macrophages as it regulates the expression of a number of genes involved in inflammation such as those for cytokines and growth factors (Li and Verma, 2002). To further assess the impact of the enhanced redox signalling that was observed in *Hvcn1*<sup>-/-</sup> macrophages, I measured cytokine production in macrophages stimulated with LPS.

I found that there was an overproduction of the cytokines IL-6, IL-10, IL-12p40 and TNF $\alpha$  by the *Hvcn1*<sup>-/-</sup> macrophages compared to WT cells. Mito-TEMPO significantly blocked cytokine production in both cell types, decreasing production to similar levels (Figure 5 – 6). This is consistent with the ‘rescued’ cell signalling observed in the *Hvcn1*<sup>-/-</sup> macrophages in the presence of Mito-TEMPO. In accordance with the delayed signalling activation kinetics observed, there was decreased cytokine production in WT macrophages. ROS have been previously implicated to play a role in the normal inflammatory response to LPS stimulation (Finkel, 2012).

Apocynin treatment did not affect IL-6, TNF $\alpha$  or IL-12p40 production, whereas it significantly attenuated IL-10 production in both WT and *Hvcn1*<sup>-/-</sup> macrophages (Figure 5 – 5). This is consistent with previous observations showing little contribution by NADPH oxidase-dependent ROS on inflammatory cytokine production (Bulua et al., 2011). These results suggest a role for HVCN1 in modulating the intensity of the inflammatory response to LPS in macrophages.

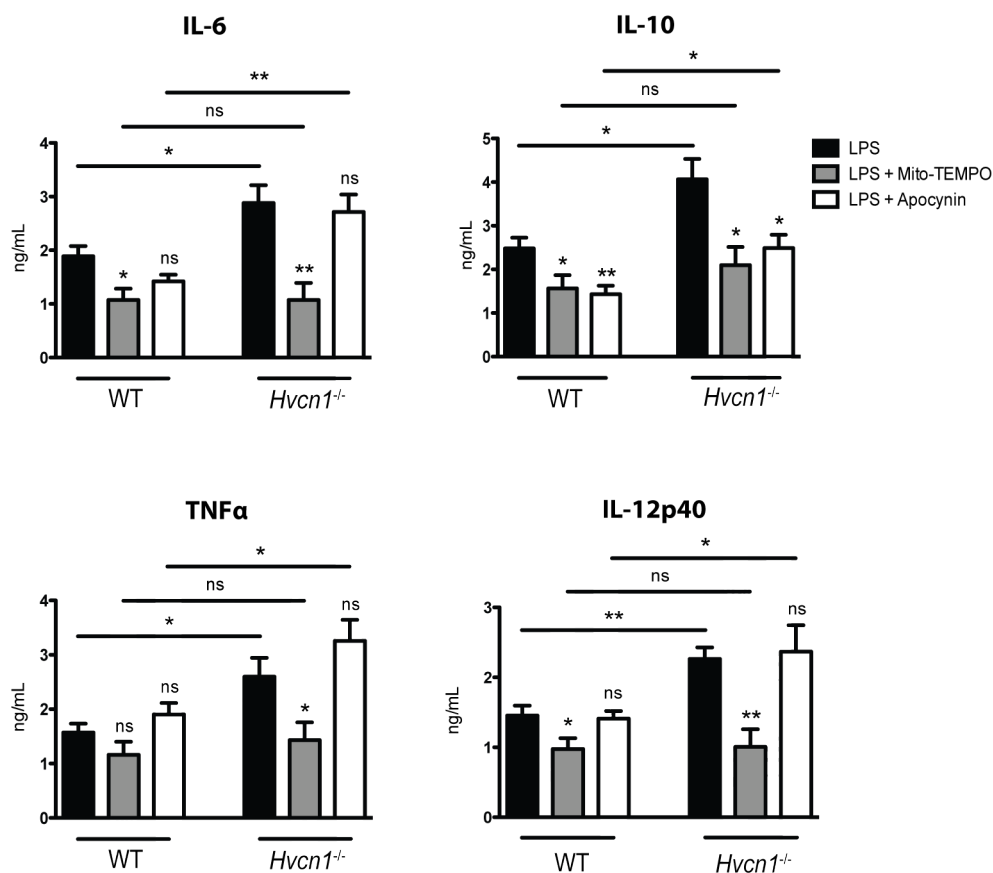


**Figure 5 - 6 Mitochondrial ROS are involved in LPS-induced cytokine production in macrophages.**

WT and *Hvcn1*<sup>-/-</sup> BMDMs were untreated or pre-treated with the indicated compounds for 1 hour before activation with 100 ng/ml LPS for 6 hours. IL-6, IL-10, TNFα and IL-12p40 levels were measured in culture supernatants. Statistical analysis was performed between groups (indicated by lines) and also to untreated WT and *Hvcn1*<sup>-/-</sup> BMDMs, respectively (indicated by \*/NS above bars) Data represent means ± SEM of three independent experiments. \*, p < 0.05; \*\*, p < 0.01; ns, no significance.

### 5.3 CHAPTER DISCUSSION

Redox signalling can occur when there is a change in the levels of ROS in a biological system (Hamanaka and Chandel, 2010). For years ROS were simply viewed as damaging agents in pathology, but more recent studies have found that some ROS can act as intracellular signalling molecules (Reth, 2002). Mitochondria are therefore acknowledged as important redox signalling nodes partly because of their production of ROS, but also because of their central role in cellular metabolism (Finkel, 2012).

The MAPK and NF- $\kappa$ B pathways are known to be redox-sensitive signalling pathways (Son et al., 2011, Forman and Torres, 2002). Hydrogen peroxide oxidation of cysteine groups can alter the DNA binding activity of transcription factors, protein-protein interactions and affect the catalytic activity of enzymes (Brandes et al., 2009). Phosphatases are particularly susceptible to regulation by ROS as they possess a reactive cysteine in their catalytic domains. These enzymes inhibit protein kinases through the processes of dephosphorylation, thus oxidation of their cysteine residue inhibits the enzymatic activity of phosphatases (Janssen-Heininger et al., 2008). Some notable examples of susceptible phosphatases are protein tyrosine phosphatase 1b (PTP1b) (Lee et al., 1998), PTEN (Kwon et al., 2004) and MAPK phosphatases (Levinthal and Defranco, 2005).

Cell signalling studies of WT and *Hvcn1*<sup>-/-</sup> macrophages showed that the cells lacking proton channels displayed quicker activation kinetics as well as sustained activation compared to their WT counterparts. This was true for both the MAPKs investigated and the NF- $\kappa$ B signalling pathway. I hypothesised that the enhanced signalling seen

in the *Hvcn1*<sup>-/-</sup> macrophages could potentially be abrogated with the use of a mitochondrial ROS scavenger. In the presence of Mito-TEMPO, I was able to 'restore' the signalling in *Hvcn1*<sup>-/-</sup> macrophages. However, as mitochondrial ROS molecules are important redox signalling agents, the addition of Mito-TEMPO slowed the activation kinetics of both the WT and the *Hvcn1*<sup>-/-</sup> macrophages. Previous studies have found similar results with the use of general and mitochondrial-specific ROS scavengers (Bulua et al., 2011). In contrast, treatment with Apocynin did not significantly affect signalling, which is in accordance with the literature (Zhou et al., 2011).

The MAPKs and the NF-κB signalling pathway are important for several macrophage functions, such as cytokine production (Boutros et al., 2008, Li and Verma, 2002). I therefore investigated the levels of IL-6, IL-10, TNF, and IL-12p40. I observed a significant increase in cytokine production in the *Hvcn1*<sup>-/-</sup> macrophages. In accordance with the cell signalling data, the addition of Mito-TEMPO 'restored' cytokine production by reducing the output to similar levels in both cell types. I would expect that this would affect cytokine production in WT cell because of the slowed cell signalling activation kinetics seen in the presence of the mitochondrial ROS scavenger. Inhibition of the NADPH oxidase by Apocynin only decreased the production of IL-10 in both cell type. This is an interesting result as it is generally accepted that NADPH oxidase-dependent ROS contribute little to inflammatory cytokine production (Bulua et al., 2011). Further investigations into this would be necessary to gain more insight into the mechanism.



## **CHAPTER SIX: DISCUSSION**

The importance of macrophages in the innate immune system has been recognised for decades. Macrophages are often the first type of cell to encounter a pathogen or foreign substance. They have the ability to ingest pathogens and particles via phagocytosis, one of their most distinctive properties (Wynn et al., 2013). Macrophages can detect these pathogens using a number of pattern recognition receptors such as the toll-like receptors. In addition, they have an arsenal of antimicrobial effector mechanisms to eliminate pathogens including oxidation, antimicrobial peptides and enzymatic degradation (Rees, 2010). Macrophages are also important in amplifying the adaptive immune response through their antigen-presenting abilities (Bonilla and Oettgen, 2010).

Upon phagocyte activation, ROS are rapidly produced to destroy the engulfed pathogen. The NADPH oxidase enzyme complex is crucial for the production of a number of ROS such as superoxide and hydrogen peroxide (Lambeth, 2004). This process is highly dependent on voltage-gated proton channels to extrude protons in order to maintain  $pH_i$ , as low pH levels can inhibit the activity of the NADPH oxidase (Morgan et al., 2009). In addition, the extrusion of protons into the phagosome allows for a number of chemical reactions to occur and thus produce potent ROS (Ramsey et al., 2009). Voltage-gated proton channels are thus involved in an important mechanism of phagocyte-mediated killing.

The voltage-gated proton channel HVCN1 is expressed in a number of immune cells including granulocytes (Ramsey et al., 2009, Musset et al., 2008, Zhu et al., 2013), B cells (Capasso et al., 2010), T cells (Sasaki et al., 2013), DCs (Sztejn et al., 2012) and macrophages (Kapus et al., 1993, Holevinsky et al., 1994). However, the data on

HVCN1 in macrophages is based on electrophysiological studies that recorded ion channel currents in the presence and absence of  $Zn^{2+}$ , an unspecific inhibitor of proton channels. My own investigations found HVCN1 to be expressed at both the mRNA and protein levels in murine macrophages, which is in accordance with the electrophysiological data on these cells.

Previous published work has emphasised the crucial involvement of HVCN1 in NADPH oxidase-mediated ROS production in phagocytes (Szteyn et al., 2012, Ramsey et al., 2009) as well as in lymphocytes (Sasaki et al., 2013, Capasso et al., 2010). Of note, elevated basal ROS levels were described in murine *Hvcn1*<sup>-/-</sup> B cells and neutrophils (Capasso et al., 2010, Decleva et al., 2013). In the B cell study the ROS were described as being of mitochondrial origin. Neither study investigated this observation further. It may be that HVCN1-deficiency causes a mitochondrial defect, which leads to an overproduction of ROS. Indeed, in the *Hvcn1*<sup>-/-</sup> B cells attenuated metabolism was observed upon BCR activation. However, this was not apparent at steady state (Capasso et al., 2010). In a similar fashion, the  $pH_i$  of *Hvcn1*<sup>-/-</sup> neutrophils became greatly acidic upon activation (Morgan et al., 2009). It could be suggested that an acidic  $pH_i$  may damage intracellular organelles, such as the mitochondria, leading to defects in their activity. Nonetheless, decreased  $pH_i$  was not observed at steady state. Interestingly, I observed elevated basal ROS levels in murine *Hvcn1*<sup>-/-</sup> macrophages. I found these to be of a mitochondrial origin through the use of specific pharmacological compounds. However, the data was not instructive as to whether this was due to an overproduction of mitochondrial ROS or due to the failure of antioxidant systems to scavenge the ROS.

Elevated levels of ROS can induce increased expression of the mitochondrial antioxidant enzyme SOD2 in order to prevent potential injury from oxidative damage (Miao and St Clair, 2009). In assessing the protein expression levels of SOD2, I observed no differences between WT and *Hvcn1*<sup>-/-</sup> macrophages at steady state. Mitochondrial ROS have been indicated to act as signalling molecules to trigger inflammatory cytokine production (Bulua et al., 2011, Nakahira et al., 2011, Zhou et al., 2011), therefore LPS might regulate SOD2 activity. However, no change in SOD2 protein expression levels were observed after LPS activation, indicating that increased ROS are not inducing a feedback upregulation of SOD2 in macrophages. Whilst there might not be any differences in the amount of SOD2 enzyme, its rate of activity might be different. Investigating the specific activity of SOD2 would provide a better insight into the state of this antioxidant system in the mitochondria. In addition, it would be important to assess other antioxidant enzymes, such as glutathione peroxidase (GPx) and peroxiredoxins, and also cofactors, such as glutathione levels (Li et al., 2013).

Mitochondrial ROS production has been described previously to be tightly regulated by a number of factors, one of those being the mitochondrial membrane potential (Echtay et al., 2002). A higher mitochondrial membrane potential is associated with greater production of mitochondrial ROS, which is associated with increased electron transport (Handy and Loscalzo, 2012). However, a range of agents that lower mitochondrial membrane potential (LPS, ETC inhibitors, etc.) paradoxically increase mitochondrial ROS production. The exact mechanism for this disparity is not well defined (West et al., 2011, Everts et al., 2012), however a “redox-optimised ROS

balance hypothesis” has been proposed to explain this paradox. It states that oxidative stress can occur at either extremes of high or low mitochondrial potential (Aon et al., 2010). This was the case in the *Hvcn1*<sup>-/-</sup> macrophages, where a reduced mitochondrial membrane potential was observed compared to their WT counterparts. These data would suggest that the increased basal ROS in the *Hvcn1*<sup>-/-</sup> macrophages is due to an overproduction in the mitochondria and not due to insufficient ROS scavenging. As mentioned above, SOD2 is only one of a number of antioxidant enzymes in place to scavenge ROS so further investigations into the cellular antioxidant system would be necessary to arrive at a solid conclusion on the matter.

As previously described, an impaired respiratory burst is associated with *Hvcn1*<sup>-/-</sup> phagocytes. HVCN1 is necessary for optimal respiratory burst in phagocytes as it provides the charge compensation that is required during this process (Ramsey et al., 2009). In accordance with the literature, *Hvcn1*<sup>-/-</sup> macrophages displayed an impaired respiratory burst upon LPS activation. In neutrophils, the lack of proton channels also resulted in an intracellular acidification, due to the activity of NADPH oxidase in the absence of charge and  $pH_i$  compensation (El Chemaly et al., 2010, Morgan et al., 2009). HVCN1 extrudes  $H^+$  that rapidly accumulate in the cytosol and delivers them into the phagosome, where they are used in crucial chemical reactions to produce ROS (Morgan et al., 2009). This mechanism might be the same in macrophages, but investigations into intracellular acidification during activation or phagocytosis would need to be undertaken to confirm this. This can be accomplished

through the use of ratiometric fluorescent indicators for intracellular pH, such as carboxy-SNARE, on either confocal microscopy or flow cytometry platforms.

A previous published study showed no differences in the capacity of *Hvcn1*<sup>-/-</sup> neutrophils to phagocytose opsonised bacteria compared to WT cells (Ramsey et al., 2009). In accordance, my own investigations showed no differences between the phagocytic capacity of WT and *Hvcn1*<sup>-/-</sup> macrophages. It needs to be noted that fluorescently-labelled latex beads that are classically used in phagocytic assays, and were also used in the present study, do not provide the cells with a metabolic load, as the latex beads cannot be degraded by the cells. On the other hand, opsonised bacteria or apoptotic cells are more physiologically relevant to the phagocytic process as they do provide a metabolic load (Han and Ravichandran, 2011). Fluorescently-labelled apoptotic thymocytes is another classical phagocytosis assay used to determine phagocytic capacity. Nonetheless, given that no impairment was observed in *Hvcn1*<sup>-/-</sup> neutrophil phagocytosing bacteria (Ramsey et al., 2009), it is likely that this process is not linked to HVCN1 regulation of ROS production and therefore not regulated by proton channels.

Whilst electrophysiological studies of macrophages have indicated the presence of HVCN1 on the plasma membrane, no studies thus far have investigated the subcellular localisation of the proton channel (Kapus et al., 1993, Holevinsky et al., 1994). I observed it on the plasma membrane of macrophages and could not detect any co-localisation with mitochondrial markers. Therefore, the steady state increase in mitochondrial ROS is not due to a direct role of HVCN1 in macrophages. It might

be due to the effect of cytosolic charge and pH balance, which might affect mitochondrial function.

Mitochondrial ROS is generated from the ETC, which is located on the inner mitochondrial membrane, during the process of OXPHOS (Murphy, 2009). Whilst the ETC is highly efficient in transporting electrons through the various complexes, there is some leakage of electrons during the process. This leakage takes place at the sites of complex I (Hirst et al., 2008) and complex III (Zhang et al., 1998), which leads to the reduction of  $O_2$  to form  $O_2^-$ . Approximately 2 % of  $O_2$  consumed by the mitochondria during OXPHOS generates  $O_2^-$ . Complex I leaks  $O_2^-$  into the mitochondrial matrix (Kusmaul and Hirst, 2006) and the  $O_2^-$  leaked from complex III goes into both the mitochondrial matrix and the intermembrane space (Muller et al., 2004). Cellular metabolism is thus closely linked to ROS production and it was imperative to explore the metabolic state of *Hvcn1*<sup>-/-</sup> macrophages. To date, only one study has assessed the effects of HVCN1-deficiency on cellular metabolism (Capasso et al., 2010). The study demonstrated that *Hvcn1*<sup>-/-</sup> B cells used the same amount of mitochondrial respiration and glycolysis as their WT counterparts. However after BCR stimulation, B cells lacking HVCN1 used less mitochondrial respiration and glycolysis than WT cells. This difference was not apparent when B cells were stimulated with LPS or anti-CD40.

My own investigations into the cellular metabolism of *Hvcn1*<sup>-/-</sup> macrophages found decreased mitochondrial respiration in these cells at steady state. This is in agreement with the mitochondrial membrane potential data, where a lower potential was observed in *Hvcn1*<sup>-/-</sup> macrophages in the steady state. As the

electrochemical gradient and thus the mitochondrial membrane potential increases, a parallel increase is observed in mitochondrial ROS production (Handy and Loscalzo, 2012). However, it has been proposed that an increase in ROS production can occur at both extremes of high and low mitochondrial membrane potential (Aon et al., 2010). In addition, these processes are closely linked to ETC activity and as such mitochondrial respiration. A high mitochondrial membrane potential is observed with a high rate of ETC activity and mitochondrial respiration (Echtay et al., 2002).

Similar to WT macrophages, upon LPS activation *Hvcn1*<sup>-/-</sup> macrophages switched their metabolic drive to glycolysis by decreasing their mitochondrial respiration and increasing their glycolytic flux. However, *Hvcn1*<sup>-/-</sup> macrophages were able to reach a significantly higher rate of glycolysis compared to their WT counterparts. This may indicate that the *Hvcn1*<sup>-/-</sup> macrophages are in a state of hyper reactivity, due to a greater volume of ROS signalling molecules, and can thus induce a greater rate of glycolysis (Bulua et al., 2011). This highlights the fact that there might be mitochondrial impairment in *Hvcn1*<sup>-/-</sup> macrophages as glycolysis occurs in the cytosol whilst oxidative phosphorylation occurs within the mitochondrial matrix (Papa et al., 2012).

In support of altered mitochondrial respiration, steady state ATP levels in *Hvcn1*<sup>-/-</sup> macrophages were significantly lower compared to their WT counterparts. Interestingly, *Hvcn1*<sup>-/-</sup> cells had lower ATP levels even after LPS activation despite having a greater rate of glycolytic flux. It is possible that the lower ATP levels are due to an increased ATP consumption.

I hypothesised that differences in mitochondrial biomass may give rise to the observations I had made about ROS production and cellular metabolism. A greater quantity of mitochondria could account for the greater ROS production that is observed in *Hvcn1*<sup>-/-</sup> macrophages whilst lower quantities of mitochondria could correlate with reduced levels of mitochondrial respiration. However, I found similar levels of mitochondrial biomass in WT and *Hvcn1*<sup>-/-</sup> macrophages at steady state and after LPS activation. This data provides further evidence that there is a mitochondrial defect in *Hvcn1*<sup>-/-</sup> macrophages as the same numbers of mitochondria are producing greater quantities of ROS whilst respiring at a lower rate. It has been shown that mitochondrial biogenesis factors, such as proliferator-activated receptor-γ coactivator 1α (PGC1α), regulate both mitochondrial biomass and the expression of several antioxidant enzymes in macrophages (Vats et al., 2006). It is therefore thought that mitochondrial biomass is not an important factor in terms of regulating mitochondrial ROS.

The elevated basal mitochondrial ROS levels observed in *Hvcn1*<sup>-/-</sup> macrophages may be present during their maturation process from monocytes. Mitochondrial DNA is in close proximity to the ETC and can potentially acquire mutations in response to damaging ROS (Shokolenko et al., 2009). Mitochondrial DNA encodes all of the complex proteins; except for complex II, which is encoded by nuclear DNA (Bai et al., 2004). It was therefore imperative to assess the protein expression levels of the ETC complexes. No differences in expression levels of the ETC complexes were observed between WT and *Hvcn1*<sup>-/-</sup> macrophages. This suggests that the mitochondrial defects observed in the latter are not due to changes in complex proteins. It could be argued

that the activity of individual complex proteins might be affected and as such this could be addressed by investigating isolated mitochondria from both types of macrophages.

In the event of a sudden increase in energy demand or stress, cells can engage their SRC. This extra mitochondrial capacity allows the cells to effectively manage cellular stress such as hypoxia and low levels of nutrients. It has been shown to be crucial for both cellular survival and function (van der Windt et al., 2012, Nicholls, 2009). It is important for immune cells to rapidly respond to environmental stimuli to perform their functions and as such they need to be able to manage increased levels of stress or energy demand. *Hvcn1*<sup>-/-</sup> macrophages were found to have a diminished SRC, which provides further confirmation that their mitochondria may be defective. Despite this, I observed no effects on cell survival in response to LPS.

Until recently, ROS were thought to exclusively cause damaging effects on cellular proteins and lack a physiological function (Sena and Chandel, 2012). However, ROS are now appreciated to function as signalling molecules that can modulate cellular processes through redox-dependent signalling. Cellular signalling is important to maintain cell homeostasis and is also crucial for effector functions such as cytokine production in macrophages (Bulua et al., 2011).

It is unclear how HVCN1 is involved in other functional aspects of immune cells other than the respiratory burst and very little is known about downstream signalling upon HVCN1 activation. A comprehensive study of signalling events regulated by HVCN1 was conducted with *Hvcn1*<sup>-/-</sup> B cells, showing impaired B cell receptor (BCR)

signalling (Capasso et al., 2010). No other studies assessing the role of HVCN1 in immune cells has investigated downstream signalling events in *Hvcn1*<sup>-/-</sup> cells.

Cell signalling studies of WT and *Hvcn1*<sup>-/-</sup> macrophages found that the cells lacking proton channels displayed quicker activation kinetics as well as sustained activation compared to their WT counterparts. This was true for both the MAPKs investigated and the NF-κB signalling pathway. This enhanced cell signalling was 'restored' in the presence of a mitochondrial ROS scavenger, thus suggesting that the aberrant signalling was due to the overproduction of mitochondrial ROS. In the same event, scavenging of mitochondrial ROS delayed the activation kinetics of the signalling pathways in both WT and *Hvcn1*<sup>-/-</sup> macrophages. This indicates that mitochondrial ROS can operate as signalling molecules.

The MAPKs and the NF-κB signalling pathway are important for several immune functions, such as cytokine production (Boutros et al., 2008, Li and Verma, 2002). I therefore investigated the levels of IL-6, IL-10, TNF, and IL-12p40. I observed a significant increase in cytokine production in the *Hvcn1*<sup>-/-</sup> macrophages. In accordance with the cell signalling data, scavenging of mitochondrial ROS 'restored' cytokine production by reducing the output to similar levels in both cell types. As this reduction in cytokine production was evident in the WT macrophages, it highlights yet again the involvement of mitochondrial ROS in cell effector functions.

The data in my thesis thus shows the crucial involvement of HVCN1 in the respiratory burst of macrophages. It also highlights a mitochondrial defect in the absence of HVCN1 that leads to aberrant cell signalling and overproduction of inflammatory cytokines.

Given my observations, I would hypothesise that *Hvcn1*<sup>-/-</sup> macrophages would be more efficient at eliminating pathogens, due to their faster signalling and increased production of inflammatory cytokines. However, this phenotype could potentially have a much more damaging effect on the surrounding tissues. It should be noted that faster clearance of pathogens might mean less tissue damage due to pro-inflammatory cytokine production. It would be interesting to assess not only the ability of *Hvcn1*<sup>-/-</sup> macrophages to clear pathogens, but also the rate at which they accomplish it. That being said, it would be important to also assess *Hvcn1*<sup>-/-</sup> macrophages in the presence of IL-4, which induces an M2 phenotype. Drawing from the observations of the metabolic state of steady state *Hvcn1*<sup>-/-</sup> macrophages, one could hypothesise that these cells would not be able to fully polarise to an M2 phenotype, which is characterised by high rates of mitochondrial respiration. The implications of this would mean that *Hvcn1*<sup>-/-</sup> macrophages might fair better in a tumour microenvironment, which is known to polarise macrophages towards the M2 phenotype.

At a cellular level, I would hypothesise that *Hvcn1*<sup>-/-</sup> macrophages would amplify a type 1 response through the recruitment and polarisation of T<sub>H</sub>1 cells. Whilst I have observed a great amount of IL-12 secretion from these cells, it would be necessary to investigate a broader range of cytokines and chemokines, such as CXCL9 and CXCL10, to gain a better understanding of their cytokine profile. In addition, it would be interesting to determine if such polarisation of T cells would indeed occur through the use of *in vitro* co-cultures of *Hvcn1*<sup>-/-</sup> macrophages and T cells.

*In vivo* models of bacterial infection could be used to investigate the number and phenotype of activated T cells. At the present time, there are issues with *in vivo* approaches using *Hvcn1*<sup>-/-</sup> mice. Due to the disrupting mutations within the *Hvcn1* gene, HVCN1 is absent in all cell types that express the channel. This means assessing the impact that *Hvcn1*<sup>-/-</sup> macrophages would have on the outcome of an infection, for example, would be quite difficult. However, this problem could be overcome through the use of Cre-Lox recombinase technology. This technology employs a Cre recombinase enzyme that can recombine target sequences, known as Lox sequences. Cre recombinase technology under the control of a promoter from the *Csfr1* gene would provide a less confounding animal model to use, as CSFR1 is mainly expressed on myeloid cells. This model would allow for the investigation of a number of inflammatory conditions, such as peritonitis and cancer.

## **CHAPTER SEVEN: REFERENCES**

- ADEREM, A. & UNDERHILL, D. M. 1999. Mechanisms of phagocytosis in macrophages. *Annu Rev Immunol*, 17, 593-623.
- AHARINEJAD, S., PAULUS, P., SIOUD, M., HOFMANN, M., ZINS, K., SCHAFER, R., STANLEY, E. R. & ABRAHAM, D. 2004. Colony-stimulating factor-1 blockade by antisense oligonucleotides and small interfering RNAs suppresses growth of human mammary tumor xenografts in mice. *Cancer Res*, 64, 5378-84.
- AJAMI, B., BENNETT, J. L., KRIEGER, C., TETZLAFF, W. & ROSSI, F. M. 2007. Local self-renewal can sustain CNS microglia maintenance and function throughout adult life. *Nat Neurosci*, 10, 1538-43.
- AON, M. A., CORTASSA, S. & O'ROURKE, B. 2010. Redox-optimized ROS balance: a unifying hypothesis. *Biochim Biophys Acta*, 1797, 865-77.
- AUFFRAY, C., SIEWEKE, M. H. & GEISSMANN, F. 2009. Blood monocytes: development, heterogeneity, and relationship with dendritic cells. *Annu Rev Immunol*, 27, 669-92.
- BABIOR, B. M., LAMBETH, J. D. & NAUSEEF, W. 2002. The neutrophil NADPH oxidase. *Arch Biochem Biophys*, 397, 342-4.
- BAI, Y., HU, P., PARK, J. S., DENG, J. H., SONG, X., CHOMYN, A., YAGI, T. & ATTARDI, G. 2004. Genetic and functional analysis of mitochondrial DNA-encoded complex I genes. *Ann N Y Acad Sci*, 1011, 272-83.
- BANCHEREAU, J., BRIERE, F., CAUX, C., DAVOUST, J., LEBECQUE, S., LIU, Y. J., PULENDRAN, B. & PALUCKA, K. 2000. Immunobiology of dendritic cells. *Annu Rev Immunol*, 18, 767-811.
- BARRON, L. & WYNN, T. A. 2011. Macrophage activation governs schistosomiasis-induced inflammation and fibrosis. *Eur J Immunol*, 41, 2509-14.
- BERGER, T. K. & ISACOFF, E. Y. 2011. The pore of the voltage-gated proton channel. *Neuron*, 72, 991-1000.
- BEUTLER, B. 2004. Innate immunity: an overview. *Mol Immunol*, 40, 845-59.
- BILZER, M., ROGGEL, F. & GERBES, A. L. 2006. Role of Kupffer cells in host defense and liver disease. *Liver Int*, 26, 1175-86.
- BISWAS, S. K. & MANTOVANI, A. 2010. Macrophage plasticity and interaction with lymphocyte subsets: cancer as a paradigm. *Nat Immunol*, 11, 889-96.
- BISWAS, S. K. & MANTOVANI, A. 2012. Orchestration of metabolism by macrophages. *Cell Metab*, 15, 432-7.
- BONILLA, F. A. & OETTGEN, H. C. 2010. Adaptive immunity. *J Allergy Clin Immunol*, 125, S33-40.
- BONIZZI, G. & KARIN, M. 2004. The two NF-kappaB activation pathways and their role in innate and adaptive immunity. *Trends Immunol*, 25, 280-8.
- BORREGAARD, N. & HERLIN, T. 1982. Energy metabolism of human neutrophils during phagocytosis. *J Clin Invest*, 70, 550-7.
- BOUTROS, T., CHEVET, E. & METRAKOS, P. 2008. Mitogen-activated protein (MAP) kinase/MAP kinase phosphatase regulation: roles in cell growth, death, and cancer. *Pharmacol Rev*, 60, 261-310.
- BOYD, R. S., JUKES-JONES, R., WALEWSKA, R., BROWN, D., DYER, M. J. & CAIN, K. 2009. Protein profiling of plasma membranes defines aberrant signaling pathways in mantle cell lymphoma. *Mol Cell Proteomics*, 8, 1501-15.

- BRANCATO, S. K. & ALBINA, J. E. 2011. Wound macrophages as key regulators of repair: origin, phenotype, and function. *Am J Pathol*, 178, 19-25.
- BRAND, K. A. & HERMFISSE, U. 1997. Aerobic glycolysis by proliferating cells: a protective strategy against reactive oxygen species. *FASEB J*, 11, 388-95.
- BRANDES, N., SCHMITT, S. & JAKOB, U. 2009. Thiol-based redox switches in eukaryotic proteins. *Antioxid Redox Signal*, 11, 997-1014.
- BRANDT, E., WOERLY, G., YOUNES, A. B., LOISEAU, S. & CAPRON, M. 2000. IL-4 production by human polymorphonuclear neutrophils. *J Leukoc Biol*, 68, 125-30.
- BROEKELMANN, T. J., LIMPER, A. H., COLBY, T. V. & MCDONALD, J. A. 1991. Transforming growth factor beta 1 is present at sites of extracellular matrix gene expression in human pulmonary fibrosis. *Proc Natl Acad Sci U S A*, 88, 6642-6.
- BULUA, A. C., SIMON, A., MADDIPATI, R., PELLETIER, M., PARK, H., KIM, K. Y., SACK, M. N., KASTNER, D. L. & SIEGEL, R. M. 2011. Mitochondrial reactive oxygen species promote production of proinflammatory cytokines and are elevated in TNFR1-associated periodic syndrome (TRAPS). *J Exp Med*, 208, 519-33.
- BYLUND, J., BROWN, K. L., MOVITZ, C., DAHLGREN, C. & KARLSSON, A. 2010. Intracellular generation of superoxide by the phagocyte NADPH oxidase: how, where, and what for? *Free Radic Biol Med*, 49, 1834-45.
- CADENAS, E. & DAVIES, K. J. 2000. Mitochondrial free radical generation, oxidative stress, and aging. *Free Radic Biol Med*, 29, 222-30.
- CAPASSO, M., BHAMRAH, M. K., HENLEY, T., BOYD, R. S., LANGLAIS, C., CAIN, K., DINSDALE, D., PULFORD, K., KHAN, M., MUSSET, B., CHERNY, V. V., MORGAN, D., GASCOYNE, R. D., VIGORITO, E., DECOURSEY, T. E., MACLENNAN, I. C. & DYER, M. J. 2010. HVCN1 modulates BCR signal strength via regulation of BCR-dependent generation of reactive oxygen species. *Nat Immunol*, 11, 265-72.
- CARGNELLO, M. & ROUX, P. P. 2011. Activation and function of the MAPKs and their substrates, the MAPK-activated protein kinases. *Microbiol Mol Biol Rev*, 75, 50-83.
- CHAPLIN, D. D. 2010. Overview of the immune response. *J Allergy Clin Immunol*, 125, S3-23.
- COLLINS, Y., CHOUCANI, E. T., JAMES, A. M., MENGER, K. E., COCHEME, H. M. & MURPHY, M. P. 2012. Mitochondrial redox signalling at a glance. *J Cell Sci*, 125, 801-6.
- COOPER, M. D. & ALDER, M. N. 2006. The evolution of adaptive immune systems. *Cell*, 124, 815-22.
- CRIMEEN-IRWIN, B., SCALZO, K., GLOSTER, S., MOTTRAM, P. L. & PLEBANSKI, M. 2005. Failure of immune homeostasis -- the consequences of under and over reactivity. *Curr Drug Targets Immune Endocr Metabol Disord*, 5, 413-22.
- DALE, D. C., BOXER, L. & LILES, W. C. 2008. The phagocytes: neutrophils and monocytes. *Blood*, 112, 935-45.
- DAVIES, L. C., JENKINS, S. J., ALLEN, J. E. & TAYLOR, P. R. 2013. Tissue-resident macrophages. *Nat Immunol*, 14, 986-95.
- DECLEVA, E., MENEGAZZI, R., FASOLO, A., DEFENDI, F., SEBASTIANUTTO, M. & DRI, P. 2013. Intracellular shunting of O<sub>2</sub>(-) contributes to charge

- compensation and preservation of neutrophil respiratory burst in the absence of voltage-gated proton channel activity. *Exp Cell Res*, 319, 1875-88.
- DECOURSEY, T. E. 2010. Voltage-gated proton channels find their dream job managing the respiratory burst in phagocytes. *Physiology (Bethesda)*, 25, 27-40.
- DECOURSEY, T. E., MORGAN, D. & CHERNY, V. V. 2003. The voltage dependence of NADPH oxidase reveals why phagocytes need proton channels. *Nature*, 422, 531-4.
- DEMPSEY, P. W., VAIDYA, S. A. & CHENG, G. 2003. The art of war: Innate and adaptive immune responses. *Cell Mol Life Sci*, 60, 2604-21.
- DING, M., ZHAO, J., BOWMAN, L., LU, Y. & SHI, X. 2010. Inhibition of AP-1 and MAPK signaling and activation of Nrf2/ARE pathway by quercitrin. *Int J Oncol*, 36, 59-67.
- DOUGALL, W. C., GLACCUM, M., CHARRIER, K., ROHRBACH, K., BRASEL, K., DE SMEDT, T., DARO, E., SMITH, J., TOMETSKO, M. E., MALISZEWSKI, C. R., ARMSTRONG, A., SHEN, V., BAIN, S., COSMAN, D., ANDERSON, D., MORRISSEY, P. J., PESCHON, J. J. & SCHUH, J. 1999. RANK is essential for osteoclast and lymph node development. *Genes Dev*, 13, 2412-24.
- DOUGHTY, C. A., BLEIMAN, B. F., WAGNER, D. J., DUFORT, F. J., MATARAZA, J. M., ROBERTS, M. F. & CHILES, T. C. 2006. Antigen receptor-mediated changes in glucose metabolism in B lymphocytes: role of phosphatidylinositol 3-kinase signaling in the glycolytic control of growth. *Blood*, 107, 4458-65.
- DUFORT, F. J., BLEIMAN, B. F., GUMINA, M. R., BLAIR, D., WAGNER, D. J., ROBERTS, M. F., ABU-AMER, Y. & CHILES, T. C. 2007. Cutting edge: IL-4-mediated protection of primary B lymphocytes from apoptosis via Stat6-dependent regulation of glycolytic metabolism. *J Immunol*, 179, 4953-7.
- ECHTAY, K. S., MURPHY, M. P., SMITH, R. A., TALBOT, D. A. & BRAND, M. D. 2002. Superoxide activates mitochondrial uncoupling protein 2 from the matrix side. Studies using targeted antioxidants. *J Biol Chem*, 277, 47129-35.
- EDWARDS, J. P., ZHANG, X., FRAUWIRTH, K. A. & MOSSER, D. M. 2006. Biochemical and functional characterization of three activated macrophage populations. *J Leukoc Biol*, 80, 1298-307.
- EL CHEMALY, A., OKOCHI, Y., SASAKI, M., ARNAUDEAU, S., OKAMURA, Y. & DEMAUREX, N. 2010. VSOP/Hv1 proton channels sustain calcium entry, neutrophil migration, and superoxide production by limiting cell depolarization and acidification. *J Exp Med*, 207, 129-39.
- ELLIOTT, M. R. & RAVICHANDRAN, K. S. 2010. Clearance of apoptotic cells: implications in health and disease. *J Cell Biol*, 189, 1059-70.
- EMRE, Y., HURTAUD, C., NUBEL, T., CRISCUOLO, F., RICQUIER, D. & CASSARD-DOULCIER, A. M. 2007. Mitochondria contribute to LPS-induced MAPK activation via uncoupling protein UCP2 in macrophages. *Biochem J*, 402, 271-8.
- ERWIG, L. P. & HENSON, P. M. 2007. Immunological consequences of apoptotic cell phagocytosis. *Am J Pathol*, 171, 2-8.
- EVERTS, B., AMIEL, E., VAN DER WINDT, G. J., FREITAS, T. C., CHOTT, R., YARASHESKI, K. E., PEARCE, E. L. & PEARCE, E. J. 2012. Commitment to glycolysis sustains survival of NO-producing inflammatory dendritic cells. *Blood*, 120, 1422-31.

- FERNIE, A. R., CARRARI, F. & SWEETLOVE, L. J. 2004. Respiratory metabolism: glycolysis, the TCA cycle and mitochondrial electron transport. *Curr Opin Plant Biol*, 7, 254-61.
- FINKEL, T. 1998. Oxygen radicals and signaling. *Curr Opin Cell Biol*, 10, 248-53.
- FINKEL, T. 2012. Signal transduction by mitochondrial oxidants. *J Biol Chem*, 287, 4434-40.
- FOGG, D. K., SIBON, C., MILED, C., JUNG, S., AUCOUTURIER, P., LITTMAN, D. R., CUMANO, A. & GEISSMANN, F. 2006. A clonogenic bone marrow progenitor specific for macrophages and dendritic cells. *Science*, 311, 83-7.
- FORMAN, H. J. & TORRES, M. 2002. Reactive oxygen species and cell signaling: respiratory burst in macrophage signaling. *Am J Respir Crit Care Med*, 166, S4-8.
- FOX, C. J., HAMMERMAN, P. S. & THOMPSON, C. B. 2005. Fuel feeds function: energy metabolism and the T-cell response. *Nat Rev Immunol*, 5, 844-52.
- FUJIWARA, N. & KOBAYASHI, K. 2005. Macrophages in inflammation. *Curr Drug Targets Inflamm Allergy*, 4, 281-6.
- GALLI, S. J., BORREGAARD, N. & WYNN, T. A. 2011. Phenotypic and functional plasticity of cells of innate immunity: macrophages, mast cells and neutrophils. *Nat Immunol*, 12, 1035-44.
- GAUTIER, E. L., SHAY, T., MILLER, J., GRETER, M., JAKUBZICK, C., IVANOV, S., HELFT, J., CHOW, A., ELPEK, K. G., GORDONOV, S., MAZLOOM, A. R., MA'AYAN, A., CHUA, W. J., HANSEN, T. H., TURLEY, S. J., MERAD, M. & RANDOLPH, G. J. 2012. Gene-expression profiles and transcriptional regulatory pathways that underlie the identity and diversity of mouse tissue macrophages. *Nat Immunol*, 13, 1118-28.
- GEISSMANN, F., MANZ, M. G., JUNG, S., SIEWEKE, M. H., MERAD, M. & LEY, K. 2010. Development of monocytes, macrophages, and dendritic cells. *Science*, 327, 656-61.
- GEISZT, M., KAPUS, A. & LIGETI, E. 2001. Chronic granulomatous disease: more than the lack of superoxide? *J Leukoc Biol*, 69, 191-6.
- GERBER, J. S. & MOSSER, D. M. 2001. Reversing lipopolysaccharide toxicity by ligating the macrophage Fc gamma receptors. *J Immunol*, 166, 6861-8.
- GINHOUX, F., GRETER, M., LEBOEUF, M., NANDI, S., SEE, P., GOKHAN, S., MEHLER, M. F., CONWAY, S. J., NG, L. G., STANLEY, E. R., SAMOKHVALOV, I. M. & MERAD, M. 2010. Fate mapping analysis reveals that adult microglia derive from primitive macrophages. *Science*, 330, 841-5.
- GORDIENKO, D. V., TARE, M., PARVEEN, S., FENECH, C. J., ROBINSON, C. & BOLTON, T. B. 1996. Voltage-activated proton current in eosinophils from human blood. *J Physiol*, 496 ( Pt 2), 299-316.
- GORDON, S. & TAYLOR, P. R. 2005. Monocyte and macrophage heterogeneity. *Nat Rev Immunol*, 5, 953-64.
- GREINER, E. F., GUPPY, M. & BRAND, K. 1994. Glucose is essential for proliferation and the glycolytic enzyme induction that provokes a transition to glycolytic energy production. *J Biol Chem*, 269, 31484-90.
- HAMANAKA, R. B. & CHANDEL, N. S. 2010. Mitochondrial reactive oxygen species regulate cellular signaling and dictate biological outcomes. *Trends Biochem Sci*, 35, 505-13.

- HAMILTON, J. A. 2008. Colony-stimulating factors in inflammation and autoimmunity. *Nat Rev Immunol*, 8, 533-44.
- HAN, C. Z. & RAVICHANDRAN, K. S. 2011. Metabolic connections during apoptotic cell engulfment. *Cell*, 147, 1442-5.
- HANDY, D. E. & LOSCALZO, J. 2012. Redox regulation of mitochondrial function. *Antioxid Redox Signal*, 16, 1323-67.
- HASHIMOTO, D., CHOW, A., NOIZAT, C., TEO, P., BEASLEY, M. B., LEBOEUF, M., BECKER, C. D., SEE, P., PRICE, J., LUCAS, D., GRETER, M., MORTHA, A., BOYER, S. W., FORSBERG, E. C., TANAKA, M., VAN ROOIJEN, N., GARCIA-SASTRE, A., STANLEY, E. R., GINHOUX, F., FRENETTE, P. S. & MERAD, M. 2013. Tissue-resident macrophages self-maintain locally throughout adult life with minimal contribution from circulating monocytes. *Immunity*, 38, 792-804.
- HASHIMOTO, D., MILLER, J. & MERAD, M. 2011. Dendritic cell and macrophage heterogeneity in vivo. *Immunity*, 35, 323-35.
- HAYDEN, M. S. & GHOSH, S. 2004. Signaling to NF-kappaB. *Genes Dev*, 18, 2195-224.
- HENSON, P. M. & HUME, D. A. 2006. Apoptotic cell removal in development and tissue homeostasis. *Trends Immunol*, 27, 244-50.
- HESSE, M., MODOLELL, M., LA FLAMME, A. C., SCHITO, M., FUENTES, J. M., CHEEVER, A. W., PEARCE, E. J. & WYNN, T. A. 2001. Differential regulation of nitric oxide synthase-2 and arginase-1 by type 1/type 2 cytokines in vivo: granulomatous pathology is shaped by the pattern of L-arginine metabolism. *J Immunol*, 167, 6533-44.
- HIRST, J., KING, M. S. & PRYDE, K. R. 2008. The production of reactive oxygen species by complex I. *Biochem Soc Trans*, 36, 976-80.
- HOLEVINSKY, K. O., JOW, F. & NELSON, D. J. 1994. Elevation in intracellular calcium activates both chloride and proton currents in human macrophages. *J Membr Biol*, 140, 13-30.
- HONG, L., PATHAK, M. M., KIM, I. H., TA, D. & TOMBOLA, F. 2013. Voltage-sensing domain of voltage-gated proton channel Hv1 shares mechanism of block with pore domains. *Neuron*, 77, 274-87.
- HONTECILLAS, R., HORNE, W. T., CLIMENT, M., GURI, A. J., EVANS, C., ZHANG, Y., SOBRAL, B. W. & BASSAGANYA-RIERA, J. 2011. Immunoregulatory mechanisms of macrophage PPAR-gamma in mice with experimental inflammatory bowel disease. *Mucosal Immunol*, 4, 304-13.
- HUSSELL, T. & BELL, T. J. 2014. Alveolar macrophages: plasticity in a tissue-specific context. *Nat Rev Immunol*, 14, 81-93.
- IWASAKI, H. & AKASHI, K. 2007. Myeloid lineage commitment from the hematopoietic stem cell. *Immunity*, 26, 726-40.
- JACKSON, S. H., DEVADAS, S., KWON, J., PINTO, L. A. & WILLIAMS, M. S. 2004. T cells express a phagocyte-type NADPH oxidase that is activated after T cell receptor stimulation. *Nat Immunol*, 5, 818-27.
- JAKUBZICK, C., GAUTIER, E. L., GIBBINGS, S. L., SOJKA, D. K., SCHLITZER, A., JOHNSON, T. E., IVANOV, S., DUAN, Q., BALA, S., CONDON, T., VAN ROOIJEN, N., GRAINGER, J. R., BELKAID, Y., MA'AYAN, A., RICHES, D. W., YOKOYAMA, W. M., GINHOUX, F., HENSON, P. M. & RANDOLPH, G. J. 2013. Minimal differentiation of classical monocytes as they survey steady-state tissues and transport antigen to lymph nodes. *Immunity*, 39, 599-610.

- JANSSEN-HEININGER, Y. M., MOSSMAN, B. T., HEINTZ, N. H., FORMAN, H. J., KALYANARAMAN, B., FINKEL, T., STAMLER, J. S., RHEE, S. G. & VAN DER VLIET, A. 2008. Redox-based regulation of signal transduction: principles, pitfalls, and promises. *Free Radic Biol Med*, 45, 1-17.
- JENKINS, S. J., RUCKERL, D., COOK, P. C., JONES, L. H., FINKELMAN, F. D., VAN ROOIJEN, N., MACDONALD, A. S. & ALLEN, J. E. 2011. Local macrophage proliferation, rather than recruitment from the blood, is a signature of TH2 inflammation. *Science*, 332, 1284-8.
- JONES, R. G. & THOMPSON, C. B. 2007. Revving the engine: signal transduction fuels T cell activation. *Immunity*, 27, 173-8.
- JOSHI, D. C. & BAKOWSKA, J. C. 2011. Determination of mitochondrial membrane potential and reactive oxygen species in live rat cortical neurons. *J Vis Exp*.
- KAMATA, H., HONDA, S., MAEDA, S., CHANG, L., HIRATA, H. & KARIN, M. 2005. Reactive oxygen species promote TNF $\alpha$ -induced death and sustained JNK activation by inhibiting MAP kinase phosphatases. *Cell*, 120, 649-61.
- KAPUS, A., ROMANEK, R., QU, A. Y., ROTSTEIN, O. D. & GRINSTEIN, S. 1993. A pH-sensitive and voltage-dependent proton conductance in the plasma membrane of macrophages. *J Gen Physiol*, 102, 729-60.
- KASAHARA, E., SEKIYAMA, A., HORI, M., HARA, K., TAKAHASHI, N., KONISHI, M., SATO, E. F., MATSUMOTO, S., OKAMURA, H. & INOUE, M. 2011. Mitochondrial density contributes to the immune response of macrophages to lipopolysaccharide via the MAPK pathway. *FEBS Lett*, 585, 2263-8.
- KAUFMANN, S. H. 2008. Immunology's foundation: the 100-year anniversary of the Nobel Prize to Paul Ehrlich and Elie Metchnikoff. *Nat Immunol*, 9, 705-12.
- KAWANE, K., OHTANI, M., MIWA, K., KIZAWA, T., KANBARA, Y., YOSHIOKA, Y., YOSHIKAWA, H. & NAGATA, S. 2006. Chronic polyarthritis caused by mammalian DNA that escapes from degradation in macrophages. *Nature*, 443, 998-1002.
- KIM, J. W. & DANG, C. V. 2005. Multifaceted roles of glycolytic enzymes. *Trends Biochem Sci*, 30, 142-50.
- KIRBY, A. C., COLES, M. C. & KAYE, P. M. 2009. Alveolar macrophages transport pathogens to lung draining lymph nodes. *J Immunol*, 183, 1983-9.
- KIRKMAN, H. N., ROLFO, M., FERRARIS, A. M. & GAETANI, G. F. 1999. Mechanisms of protection of catalase by NADPH. Kinetics and stoichiometry. *J Biol Chem*, 274, 13908-14.
- KOCH, H. P., KUROKAWA, T., OKOCHI, Y., SASAKI, M., OKAMURA, Y. & LARSSON, H. P. 2008. Multimeric nature of voltage-gated proton channels. *Proc Natl Acad Sci U S A*, 105, 9111-6.
- KOMINSKY, D. J., CAMPBELL, E. L. & COLGAN, S. P. 2010. Metabolic shifts in immunity and inflammation. *J Immunol*, 184, 4062-8.
- KRAWCZYK, C. M., HOLOWKA, T., SUN, J., BLAGIH, J., AMIEL, E., DEBERARDINIS, R. J., CROSS, J. R., JUNG, E., THOMPSON, C. B., JONES, R. G. & PEARCE, E. J. 2010. Toll-like receptor-induced changes in glycolytic metabolism regulate dendritic cell activation. *Blood*, 115, 4742-9.
- KREIDER, T., ANTHONY, R. M., URBAN, J. F., JR. & GAUSE, W. C. 2007. Alternatively activated macrophages in helminth infections. *Curr Opin Immunol*, 19, 448-53.

- KURODA, E., HO, V., RUSCHMANN, J., ANTIGNANO, F., HAMILTON, M., RAUH, M. J., ANTOV, A., FLAVELL, R. A., SLY, L. M. & KRYSTAL, G. 2009. SHIP represses the generation of IL-3-induced M2 macrophages by inhibiting IL-4 production from basophils. *J Immunol*, 183, 3652-60.
- KUSSMAUL, L. & HIRST, J. 2006. The mechanism of superoxide production by NADH:ubiquinone oxidoreductase (complex I) from bovine heart mitochondria. *Proc Natl Acad Sci U S A*, 103, 7607-12.
- KWON, J., LEE, S. R., YANG, K. S., AHN, Y., KIM, Y. J., STADTMAN, E. R. & RHEE, S. G. 2004. Reversible oxidation and inactivation of the tumor suppressor PTEN in cells stimulated with peptide growth factors. *Proc Natl Acad Sci U S A*, 101, 16419-24.
- LAMBERT, A. J., BUCKINGHAM, J. A., BOYSEN, H. M. & BRAND, M. D. 2008. Diphenyleneiodonium acutely inhibits reactive oxygen species production by mitochondrial complex I during reverse, but not forward electron transport. *Biochim Biophys Acta*, 1777, 397-403.
- LAMBETH, J. D. 2004. NOX enzymes and the biology of reactive oxygen. *Nat Rev Immunol*, 4, 181-9.
- LANGRISH, C. L., CHEN, Y., BLUMENSCHNEIN, W. M., MATTSON, J., BASHAM, B., SEDGWICK, J. D., MCCLANAHAN, T., KASTELEIN, R. A. & CUA, D. J. 2005. IL-23 drives a pathogenic T cell population that induces autoimmune inflammation. *J Exp Med*, 201, 233-40.
- LECH, M., GROBMAYR, R., WEIDENBUSCH, M. & ANDERS, H. J. 2012. Tissues use resident dendritic cells and macrophages to maintain homeostasis and to regain homeostasis upon tissue injury: the immunoregulatory role of changing tissue environments. *Mediators Inflamm*, 2012, 951390.
- LEE, M. S. & KIM, Y. J. 2007. Signaling pathways downstream of pattern-recognition receptors and their cross talk. *Annu Rev Biochem*, 76, 447-80.
- LEE, S. R., KWON, K. S., KIM, S. R. & RHEE, S. G. 1998. Reversible inactivation of protein-tyrosine phosphatase 1B in A431 cells stimulated with epidermal growth factor. *J Biol Chem*, 273, 15366-72.
- LENAZ, G. & GENOVA, M. L. 2009. Structural and functional organization of the mitochondrial respiratory chain: a dynamic super-assembly. *Int J Biochem Cell Biol*, 41, 1750-1772.
- LEVINTHAL, D. J. & DEFRANCO, D. B. 2005. Reversible oxidation of ERK-directed protein phosphatases drives oxidative toxicity in neurons. *J Biol Chem*, 280, 5875-83.
- LI, Q. & VERMA, I. M. 2002. NF-kappaB regulation in the immune system. *Nat Rev Immunol*, 2, 725-34.
- LI, S. J., ZHAO, Q., ZHOU, Q., UNNO, H., ZHAI, Y. & SUN, F. 2010. The role and structure of the carboxyl-terminal domain of the human voltage-gated proton channel Hv1. *J Biol Chem*, 285, 12047-54.
- LI, X., FANG, P., MAI, J., CHOI, E. T., WANG, H. & YANG, X. F. 2013. Targeting mitochondrial reactive oxygen species as novel therapy for inflammatory diseases and cancers. *J Hematol Oncol*, 6, 19.
- LI, Y., HUANG, T. T., CARLSON, E. J., MELOV, S., URSELL, P. C., OLSON, J. L., NOBLE, L. J., YOSHIMURA, M. P., BERGER, C., CHAN, P. H., WALLACE, D. C. & EPSTEIN, C. J. 1995. Dilated cardiomyopathy and neonatal lethality in mutant mice lacking manganese superoxide dismutase. *Nat Genet*, 11, 376-81.

- LIU, Y., FISKUM, G. & SCHUBERT, D. 2002. Generation of reactive oxygen species by the mitochondrial electron transport chain. *J Neurochem*, 80, 780-7.
- LOKE, P., GALLAGHER, I., NAIR, M. G., ZANG, X., BROMBACHER, F., MOHRS, M., ALLISON, J. P. & ALLEN, J. E. 2007. Alternative activation is an innate response to injury that requires CD4+ T cells to be sustained during chronic infection. *J Immunol*, 179, 3926-36.
- LUNT, S. Y. & VANDER HEIDEN, M. G. 2011. Aerobic glycolysis: meeting the metabolic requirements of cell proliferation. *Annu Rev Cell Dev Biol*, 27, 441-64.
- MA, Y. & POPE, R. M. 2005. The role of macrophages in rheumatoid arthritis. *Curr Pharm Des*, 11, 569-80.
- MAHAUT-SMITH, M. P. 1989. The effect of zinc on calcium and hydrogen ion currents in intact snail neurones. *J Exp Biol*, 145, 455-64.
- MARI, M., MORALES, A., COLELL, A., GARCIA-RUIZ, C. & FERNANDEZ-CHECA, J. C. 2009. Mitochondrial glutathione, a key survival antioxidant. *Antioxid Redox Signal*, 11, 2685-700.
- MARI, M., MORALES, A., COLELL, A., GARCIA-RUIZ, C., KAPLOWITZ, N. & FERNANDEZ-CHECA, J. C. 2013. Mitochondrial glutathione: features, regulation and role in disease. *Biochim Biophys Acta*, 1830, 3317-28.
- MARTINEZ, F. O., SICA, A., MANTOVANI, A. & LOCATI, M. 2008. Macrophage activation and polarization. *Front Biosci*, 13, 453-61.
- MASON, S. D. & JOYCE, J. A. 2011. Proteolytic networks in cancer. *Trends Cell Biol*, 21, 228-37.
- MATHIS, D. & SHOELSON, S. E. 2011. Immunometabolism: an emerging frontier. *Nat Rev Immunol*, 11, 81.
- MCINNES, I. B. & SCHETT, G. 2011. The pathogenesis of rheumatoid arthritis. *N Engl J Med*, 365, 2205-19.
- MELNICOFF, M. J., HORAN, P. K., BRESLIN, E. W. & MORAHAN, P. S. 1988. Maintenance of peritoneal macrophages in the steady state. *J Leukoc Biol*, 44, 367-75.
- MIAO, L. & ST CLAIR, D. K. 2009. Regulation of superoxide dismutase genes: implications in disease. *Free Radic Biol Med*, 47, 344-56.
- MICHALEK, R. D., GERRIETS, V. A., JACOBS, S. R., MACINTYRE, A. N., MACIVER, N. J., MASON, E. F., SULLIVAN, S. A., NICHOLS, A. G. & RATHMELL, J. C. 2011. Cutting edge: distinct glycolytic and lipid oxidative metabolic programs are essential for effector and regulatory CD4+ T cell subsets. *J Immunol*, 186, 3299-303.
- MILLS, C. D., KINCAID, K., ALT, J. M., HEILMAN, M. J. & HILL, A. M. 2000. M-1/M-2 macrophages and the Th1/Th2 paradigm. *J Immunol*, 164, 6166-73.
- MORGAN, D., CAPASSO, M., MUSSET, B., CHERNY, V. V., RIOS, E., DYER, M. J. & DECOURSEY, T. E. 2009. Voltage-gated proton channels maintain pH in human neutrophils during phagocytosis. *Proc Natl Acad Sci U S A*, 106, 18022-7.
- MOSSER, D. M. & EDWARDS, J. P. 2008. Exploring the full spectrum of macrophage activation. *Nat Rev Immunol*, 8, 958-69.
- MULLER, F. L., LIU, Y. & VAN REMMEN, H. 2004. Complex III releases superoxide to both sides of the inner mitochondrial membrane. *J Biol Chem*, 279, 49064-73.

- MULLER, F. L., LUSTGARTEN, M. S., JANG, Y., RICHARDSON, A. & VAN REMMEN, H. 2007. Trends in oxidative aging theories. *Free Radic Biol Med*, 43, 477-503.
- MUNITZ, A., BRANDT, E. B., MINGLER, M., FINKELMAN, F. D. & ROTHENBERG, M. E. 2008. Distinct roles for IL-13 and IL-4 via IL-13 receptor alpha1 and the type II IL-4 receptor in asthma pathogenesis. *Proc Natl Acad Sci U S A*, 105, 7240-5.
- MURDOCH, C., MUTHANA, M., COFFELT, S. B. & LEWIS, C. E. 2008. The role of myeloid cells in the promotion of tumour angiogenesis. *Nat Rev Cancer*, 8, 618-31.
- MURPHY, M. P. 2009. How mitochondria produce reactive oxygen species. *Biochem J*, 417, 1-13.
- MURPHY, M. P., HOLMGREN, A., LARSSON, N. G., HALLIWELL, B., CHANG, C. J., KALYANARAMAN, B., RHEE, S. G., THORNALLEY, P. J., PARTRIDGE, L., GEMS, D., NYSTROM, T., BELOUSOV, V., SCHUMACKER, P. T. & WINTERBOURN, C. C. 2011. Unraveling the biological roles of reactive oxygen species. *Cell Metab*, 13, 361-6.
- MURPHY, M. P. & SMITH, R. A. 2007. Targeting antioxidants to mitochondria by conjugation to lipophilic cations. *Annu Rev Pharmacol Toxicol*, 47, 629-56.
- MURPHY, R. & DECOURSEY, T. E. 2006. Charge compensation during the phagocyte respiratory burst. *Biochim Biophys Acta*, 1757, 996-1011.
- MURRAY, P. J. & WYNN, T. A. 2011. Obstacles and opportunities for understanding macrophage polarization. *J Leukoc Biol*, 89, 557-63.
- MUSSET, B., MORGAN, D., CHERNY, V. V., MACGLASHAN, D. W., JR., THOMAS, L. L., RIOS, E. & DECOURSEY, T. E. 2008. A pH-stabilizing role of voltage-gated proton channels in IgE-mediated activation of human basophils. *Proc Natl Acad Sci U S A*, 105, 11020-5.
- MUSSET, B., SMITH, S. M., RAJAN, S., CHERNY, V. V., MORGAN, D. & DECOURSEY, T. E. 2010a. Oligomerization of the voltage-gated proton channel. *Channels (Austin)*, 4, 260-5.
- MUSSET, B., SMITH, S. M., RAJAN, S., CHERNY, V. V., SUJAI, S., MORGAN, D. & DECOURSEY, T. E. 2010b. Zinc inhibition of monomeric and dimeric proton channels suggests cooperative gating. *J Physiol*, 588, 1435-49.
- NAGAOKA, I., TRAPNELL, B. C. & CRYSTAL, R. G. 1990. Upregulation of platelet-derived growth factor-A and -B gene expression in alveolar macrophages of individuals with idiopathic pulmonary fibrosis. *J Clin Invest*, 85, 2023-7.
- NAIK, S. H., SATHE, P., PARK, H. Y., METCALF, D., PROIETTO, A. I., DAKIC, A., CAROTTA, S., O'KEEFFE, M., BAHLO, M., PAPENFUSS, A., KWAK, J. Y., WU, L. & SHORTMAN, K. 2007. Development of plasmacytoid and conventional dendritic cell subtypes from single precursor cells derived in vitro and in vivo. *Nat Immunol*, 8, 1217-26.
- NAITO, M., UMEDA, S., YAMAMOTO, T., MORIYAMA, H., UMEZU, H., HASEGAWA, G., USUDA, H., SHULTZ, L. D. & TAKAHASHI, K. 1996. Development, differentiation, and phenotypic heterogeneity of murine tissue macrophages. *J Leukoc Biol*, 59, 133-8.
- NAKAHIRA, K., HASPEL, J. A., RATHINAM, V. A., LEE, S. J., DOLINAY, T., LAM, H. C., ENGLERT, J. A., RABINOVITCH, M., CERNADAS, M., KIM, H. P., FITZGERALD, K. A., RYTER, S. W. & CHOI, A. M. 2011. Autophagy proteins regulate innate immune responses by inhibiting the release of

- mitochondrial DNA mediated by the NALP3 inflammasome. *Nat Immunol*, 12, 222-30.
- NATHAN, C. & CUNNINGHAM-BUSSEL, A. 2013. Beyond oxidative stress: an immunologist's guide to reactive oxygen species. *Nat Rev Immunol*, 13, 349-61.
- NICHOLLS, D. G. 2009. Spare respiratory capacity, oxidative stress and excitotoxicity. *Biochem Soc Trans*, 37, 1385-8.
- NOVAK, M. L. & KOH, T. J. 2013. Phenotypic transitions of macrophages orchestrate tissue repair. *Am J Pathol*, 183, 1352-63.
- O'SHEA, J. J. & MURRAY, P. J. 2008. Cytokine signaling modules in inflammatory responses. *Immunity*, 28, 477-87.
- ODEGAARD, J. I. & CHAWLA, A. 2011. Alternative macrophage activation and metabolism. *Annu Rev Pathol*, 6, 275-97.
- ODEGAARD, J. I. & CHAWLA, A. 2013. The immune system as a sensor of the metabolic state. *Immunity*, 38, 644-54.
- OECKINGHAUS, A., HAYDEN, M. S. & GHOSH, S. 2011. Crosstalk in NF-kappaB signaling pathways. *Nat Immunol*, 12, 695-708.
- OKADO-MATSUMOTO, A. & FRIDOVICH, I. 2001. Subcellular distribution of superoxide dismutases (SOD) in rat liver: Cu,Zn-SOD in mitochondria. *J Biol Chem*, 276, 38388-93.
- OKOCHI, Y., SASAKI, M., IWASAKI, H. & OKAMURA, Y. 2009. Voltage-gated proton channel is expressed on phagosomes. *Biochem Biophys Res Commun*, 382, 274-9.
- PAPA, S., MARTINO, P. L., CAPITANIO, G., GABALLO, A., DE RASMO, D., SIGNORILE, A. & PETRUZZELLA, V. 2012. The oxidative phosphorylation system in mammalian mitochondria. *Adv Exp Med Biol*, 942, 3-37.
- PARKIN, J. & COHEN, B. 2001. An overview of the immune system. *Lancet*, 357, 1777-89.
- PAULUS, P., STANLEY, E. R., SCHAFER, R., ABRAHAM, D. & AHARINEJAD, S. 2006. Colony-stimulating factor-1 antibody reverses chemoresistance in human MCF-7 breast cancer xenografts. *Cancer Res*, 66, 4349-56.
- PEARCE, E. L. & PEARCE, E. J. 2013. Metabolic pathways in immune cell activation and quiescence. *Immunity*, 38, 633-43.
- PEARCE, E. L., POFFENBERGER, M. C., CHANG, C. H. & JONES, R. G. 2013. Fueling immunity: insights into metabolism and lymphocyte function. *Science*, 342, 1242454.
- PEARCE, E. L., WALSH, M. C., CEJAS, P. J., HARMS, G. M., SHEN, H., WANG, L. S., JONES, R. G. & CHOI, Y. 2009. Enhancing CD8 T-cell memory by modulating fatty acid metabolism. *Nature*, 460, 103-7.
- PERRY, S. W., NORMAN, J. P., BARBIERI, J., BROWN, E. B. & GELBARD, H. A. 2011. Mitochondrial membrane potential probes and the proton gradient: a practical usage guide. *Biotechniques*, 50, 98-115.
- QIAN, B. Z. & POLLARD, J. W. 2010. Macrophage diversity enhances tumor progression and metastasis. *Cell*, 141, 39-51.
- QIU, F., REBOLLEDO, S., GONZALEZ, C. & LARSSON, H. P. 2013. Subunit interactions during cooperative opening of voltage-gated proton channels. *Neuron*, 77, 288-98.

- RAES, G., BESCHIN, A., GHASSABEH, G. H. & DE BAETSELIER, P. 2007. Alternatively activated macrophages in protozoan infections. *Curr Opin Immunol*, 19, 454-9.
- RAMSEY, I. S., MORAN, M. M., CHONG, J. A. & CLAPHAM, D. E. 2006. A voltage-gated proton-selective channel lacking the pore domain. *Nature*, 440, 1213-6.
- RAMSEY, I. S., RUCHTI, E., KACZMAREK, J. S. & CLAPHAM, D. E. 2009. Hv1 proton channels are required for high-level NADPH oxidase-dependent superoxide production during the phagocyte respiratory burst. *Proc Natl Acad Sci U S A*, 106, 7642-7.
- REES, A. J. 2010. Monocyte and macrophage biology: an overview. *Semin Nephrol*, 30, 216-33.
- RETH, M. 2002. Hydrogen peroxide as second messenger in lymphocyte activation. *Nat Immunol*, 3, 1129-34.
- RHEE, S. G., BAE, Y. S., LEE, S. R. & KWON, J. 2000. Hydrogen peroxide: a key messenger that modulates protein phosphorylation through cysteine oxidation. *Sci STKE*, 2000, pe1.
- RODRIGUEZ-PRADOS, J. C., TRAVES, P. G., CUENCA, J., RICO, D., ARAGONES, J., MARTIN-SANZ, P., CASCANTE, M. & BOSCA, L. 2010. Substrate fate in activated macrophages: a comparison between innate, classic, and alternative activation. *J Immunol*, 185, 605-14.
- ROSE, M. L., RUSYN, I., BOJES, H. K., BELYEA, J., CATTLEY, R. C. & THURMAN, R. G. 2000. Role of Kupffer cells and oxidants in signaling peroxisome proliferator-induced hepatocyte proliferation. *Mutat Res*, 448, 179-92.
- ROSENBERGER, C. M. & FINLAY, B. B. 2003. Phagocyte sabotage: disruption of macrophage signalling by bacterial pathogens. *Nat Rev Mol Cell Biol*, 4, 385-96.
- SARASTE, M. 1999. Oxidative phosphorylation at the fin de siecle. *Science*, 283, 1488-93.
- SASAKI, M., TAKAGI, M. & OKAMURA, Y. 2006. A voltage sensor-domain protein is a voltage-gated proton channel. *Science*, 312, 589-92.
- SASAKI, M., TOJO, A., OKOCHI, Y., MIYAWAKI, N., KAMIMURA, D., YAMAGUCHI, A., MURAKAMI, M. & OKAMURA, Y. 2013. Autoimmune disorder phenotypes in *Hvcn1*-deficient mice. *Biochem J*, 450, 295-301.
- SBARRA, A. J. & KARNOVSKY, M. L. 1959. The biochemical basis of phagocytosis. I. Metabolic changes during the ingestion of particles by polymorphonuclear leukocytes. *J Biol Chem*, 234, 1355-62.
- SCHAPIRO, F. B. & GRINSTEIN, S. 2000. Determinants of the pH of the Golgi complex. *J Biol Chem*, 275, 21025-32.
- SCHILLING, T., GRATOPP, A., DECOURSEY, T. E. & EDER, C. 2002. Voltage-activated proton currents in human lymphocytes. *J Physiol*, 545, 93-105.
- SCHULTZ, B. E. & CHAN, S. I. 2001. Structures and proton-pumping strategies of mitochondrial respiratory enzymes. *Annu Rev Biophys Biomol Struct*, 30, 23-65.
- SCHULZ, C., GOMEZ PERDIGUERO, E., CHORRO, L., SZABO-ROGERS, H., CAGNARD, N., KIERDORF, K., PRINZ, M., WU, B., JACOBSEN, S. E., POLLARD, J. W., FRAMPTON, J., LIU, K. J. & GEISSMANN, F. 2012. A lineage of myeloid cells independent of Myb and hematopoietic stem cells. *Science*, 336, 86-90.

- SEGAL, A. W. 1987. Absence of both cytochrome b-245 subunits from neutrophils in X-linked chronic granulomatous disease. *Nature*, 326, 88-91.
- SEGAL, A. W. 2005. How neutrophils kill microbes. *Annu Rev Immunol*, 23, 197-223.
- SENA, L. A. & CHANDEL, N. S. 2012. Physiological roles of mitochondrial reactive oxygen species. *Mol Cell*, 48, 158-67.
- SERBINA, N. V., JIA, T., HOHL, T. M. & PAMER, E. G. 2008. Monocyte-mediated defense against microbial pathogens. *Annu Rev Immunol*, 26, 421-52.
- SHER, R., WADEE, A. & JOFFE, M. 1983. The enhancement of eosinophil function by lymphocyte supernatants. *Clin Exp Immunol*, 51, 525-34.
- SHI, C. & PAMER, E. G. 2011. Monocyte recruitment during infection and inflammation. *Nat Rev Immunol*, 11, 762-74.
- SHI, L. Z., WANG, R., HUANG, G., VOGEL, P., NEALE, G., GREEN, D. R. & CHI, H. 2011. HIF1alpha-dependent glycolytic pathway orchestrates a metabolic checkpoint for the differentiation of TH17 and Treg cells. *J Exp Med*, 208, 1367-76.
- SHOKOLENKO, I., VENEDIKTOVA, N., BOCHKAREVA, A., WILSON, G. L. & ALEXEYEV, M. F. 2009. Oxidative stress induces degradation of mitochondrial DNA. *Nucleic Acids Res*, 37, 2539-48.
- SICA, A. & MANTOVANI, A. 2012. Macrophage plasticity and polarization: in vivo veritas. *J Clin Invest*, 122, 787-95.
- SINDRILARU, A., PETERS, T., WIESCHALKA, S., BAICAN, C., BAICAN, A., PETER, H., HAINZL, A., SCHATZ, S., QI, Y., SCHLECHT, A., WEISS, J. M., WLASCHEK, M., SUNDERKOTTER, C. & SCHARFFETTER-KOCHANER, K. 2011. An unrestrained proinflammatory M1 macrophage population induced by iron impairs wound healing in humans and mice. *J Clin Invest*, 121, 985-97.
- SIRISINHA, S. 2011. Insight into the mechanisms regulating immune homeostasis in health and disease. *Asian Pac J Allergy Immunol*, 29, 1-14.
- SMEITINK, J., VAN DEN HEUVEL, L. & DIMAURO, S. 2001. The genetics and pathology of oxidative phosphorylation. *Nat Rev Genet*, 2, 342-52.
- SON, Y., CHEONG, Y. K., KIM, N. H., CHUNG, H. T., KANG, D. G. & PAE, H. O. 2011. Mitogen-Activated Protein Kinases and Reactive Oxygen Species: How Can ROS Activate MAPK Pathways? *J Signal Transduct*, 2011, 792639.
- STEFANSKA, J. & PAWLICZAK, R. 2008. Apocynin: molecular aptitudes. *Mediators Inflamm*, 2008, 106507.
- STEIN, M., KESHAV, S., HARRIS, N. & GORDON, S. 1992. Interleukin 4 potently enhances murine macrophage mannose receptor activity: a marker of alternative immunologic macrophage activation. *J Exp Med*, 176, 287-92.
- STOUT, R. D., JIANG, C., MATTA, B., TIETZEL, I., WATKINS, S. K. & SUTTLES, J. 2005. Macrophages sequentially change their functional phenotype in response to changes in microenvironmental influences. *J Immunol*, 175, 342-9.
- STRASSMANN, G., PATIL-KOOTA, V., FINKELMAN, F., FONG, M. & KAMBAYASHI, T. 1994. Evidence for the involvement of interleukin 10 in the differential deactivation of murine peritoneal macrophages by prostaglandin E2. *J Exp Med*, 180, 2365-70.
- SUENAGA, T., ARASE, H., YAMASAKI, S., KOHNO, M., YOKOSUKA, T., TAKEUCHI, A., HATTORI, T. & SAITO, T. 2007. Cloning of B cell-specific membrane

- tetraspanning molecule BTS possessing B cell proliferation-inhibitory function. *Eur J Immunol*, 37, 3197-207.
- SUMBAYEV, V. V., NICHOLAS, S. A., STREATFIELD, C. L. & GIBBS, B. F. 2009. Involvement of hypoxia-inducible factor-1 HiF(1alpha) in IgE-mediated primary human basophil responses. *Eur J Immunol*, 39, 3511-9.
- SUMIMOTO, H. 2008. Structure, regulation and evolution of Nox-family NADPH oxidases that produce reactive oxygen species. *FEBS J*, 275, 3249-77.
- SWIRSKI, F. K., NAHRENDORF, M., ETZRODT, M., WILDGRUBER, M., CORTEZ-RETAMOZO, V., PANIZZI, P., FIGUEIREDO, J. L., KOHLER, R. H., CHUDNOVSKIY, A., WATERMAN, P., AIKAWA, E., MEMPEL, T. R., LIBBY, P., WEISSLEDER, R. & PITTET, M. J. 2009. Identification of splenic reservoir monocytes and their deployment to inflammatory sites. *Science*, 325, 612-6.
- SZEKANECZ, Z. & KOCH, A. E. 2007. Macrophages and their products in rheumatoid arthritis. *Curr Opin Rheumatol*, 19, 289-95.
- SZTEYN, K., YANG, W., SCHMID, E., LANG, F. & SHUMILINA, E. 2012. Lipopolysaccharide-sensitive H<sup>+</sup> current in dendritic cells. *Am J Physiol Cell Physiol*, 303, C204-12.
- TAKADA, Y., MUKHOPADHYAY, A., KUNDU, G. C., MAHABELESWAR, G. H., SINGH, S. & AGGARWAL, B. B. 2003. Hydrogen peroxide activates NF-kappa B through tyrosine phosphorylation of I kappa B alpha and serine phosphorylation of p65: evidence for the involvement of I kappa B alpha kinase and Syk protein-tyrosine kinase. *J Biol Chem*, 278, 24233-41.
- THOMAS, R. C. & MEECH, R. W. 1982. Hydrogen ion currents and intracellular pH in depolarized voltage-clamped snail neurones. *Nature*, 299, 826-8.
- TOMBOLA, F., ULBRICH, M. H., KOHOUT, S. C. & ISACOFF, E. Y. 2010. The opening of the two pores of the Hv1 voltage-gated proton channel is tuned by cooperativity. *Nat Struct Mol Biol*, 17, 44-50.
- TROMBETTA, E. S. & MELLMAN, I. 2005. Cell biology of antigen processing in vitro and in vivo. *Annu Rev Immunol*, 23, 975-1028.
- TUCSEK, Z., RADNAI, B., RACZ, B., DEBRECENI, B., PRIBER, J. K., DOLOWSCHIAK, T., PALKOVICS, T., GALLYAS, F., JR., SUMEGI, B. & VERES, B. 2011. Suppressing LPS-induced early signal transduction in macrophages by a polyphenol degradation product: a critical role of MKP-1. *J Leukoc Biol*, 89, 105-11.
- TURVEY, S. E. & BROIDE, D. H. 2010. Innate immunity. *J Allergy Clin Immunol*, 125, S24-32.
- UNDERHILL, D. M. & OZINSKY, A. 2002. Phagocytosis of microbes: complexity in action. *Annu Rev Immunol*, 20, 825-52.
- VALENTINE, W. N. & BECK, W. S. 1951. Biochemical studies on leucocytes. I. Phosphatase activity in health, leucocytosis, and myelocytic leukemia. *J Lab Clin Med*, 38, 39-55.
- VAN DER WINDT, G. J., EVERTS, B., CHANG, C. H., CURTIS, J. D., FREITAS, T. C., AMIEL, E., PEARCE, E. J. & PEARCE, E. L. 2012. Mitochondrial respiratory capacity is a critical regulator of CD8<sup>+</sup> T cell memory development. *Immunity*, 36, 68-78.
- VAN FURTH, R. & COHN, Z. A. 1968. The origin and kinetics of mononuclear phagocytes. *J Exp Med*, 128, 415-35.

- VAN FURTH, R., COHN, Z. A., HIRSCH, J. G., HUMPHREY, J. H., SPECTOR, W. G. & LANGEVOORT, H. L. 1972. The mononuclear phagocyte system: a new classification of macrophages, monocytes, and their precursor cells. *Bull World Health Organ*, 46, 845-52.
- VAN RAAM, B. J., VERHOEVEN, A. J. & KUIJPERS, T. W. 2006. Mitochondria in neutrophil apoptosis. *Int J Hematol*, 84, 199-204.
- VANDER HEIDEN, M. G., CANTLEY, L. C. & THOMPSON, C. B. 2009. Understanding the Warburg effect: the metabolic requirements of cell proliferation. *Science*, 324, 1029-33.
- VANDER HEIDEN, M. G., LUNT, S. Y., DAYTON, T. L., FISKE, B. P., ISRAELSEN, W. J., MATTAINI, K. R., VOKES, N. I., STEPHANOPOULOS, G., CANTLEY, L. C., METALLO, C. M. & LOCASALE, J. W. 2011. Metabolic pathway alterations that support cell proliferation. *Cold Spring Harb Symp Quant Biol*, 76, 325-34.
- VATS, D., MUKUNDAN, L., ODEGAARD, J. I., ZHANG, L., SMITH, K. L., MOREL, C. R., WAGNER, R. A., GREAVES, D. R., MURRAY, P. J. & CHAWLA, A. 2006. Oxidative metabolism and PGC-1beta attenuate macrophage-mediated inflammation. *Cell Metab*, 4, 13-24.
- VELDHOEN, M., HOCKING, R. J., ATKINS, C. J., LOCKSLEY, R. M. & STOCKINGER, B. 2006. TGFbeta in the context of an inflammatory cytokine milieu supports de novo differentiation of IL-17-producing T cells. *Immunity*, 24, 179-89.
- VENGE, P., MOBERG, L., BJORNSSON, E., BERGSTROM, M., LANGSTROM, B. & HAKANSSON, L. 2003. Mechanisms of basal and cytokine-induced uptake of glucose in normal human eosinophils: relation to apoptosis. *Respir Med*, 97, 1109-19.
- WAMELINK, M. M., STRUYS, E. A. & JAKOBS, C. 2008. The biochemistry, metabolism and inherited defects of the pentose phosphate pathway: a review. *J Inherit Metab Dis*, 31, 703-17.
- WEBER, C., BELGE, K. U., VON HUNDELSHAUSEN, P., DRAUDE, G., STEPPICH, B., MACK, M., FRANKENBERGER, M., WEBER, K. S. & ZIEGLER-HEITBROCK, H. W. 2000. Differential chemokine receptor expression and function in human monocyte subpopulations. *J Leukoc Biol*, 67, 699-704.
- WEIDENBUSCH, M. & ANDERS, H. J. 2012. Tissue microenvironments define and get reinforced by macrophage phenotypes in homeostasis or during inflammation, repair and fibrosis. *J Innate Immun*, 4, 463-77.
- WEST, A. P., BRODSKY, I. E., RAHNER, C., WOO, D. K., ERDJUMENT-BROMAGE, H., TEMPST, P., WALSH, M. C., CHOI, Y., SHADEL, G. S. & GHOSH, S. 2011. TLR signalling augments macrophage bactericidal activity through mitochondrial ROS. *Nature*, 472, 476-80.
- WEST, M. A., WALLIN, R. P., MATTHEWS, S. P., SVENSSON, H. G., ZARU, R., LJUNGGREN, H. G., PRESCOTT, A. R. & WATTS, C. 2004. Enhanced dendritic cell antigen capture via toll-like receptor-induced actin remodeling. *Science*, 305, 1153-7.
- WINTERBOURN, C. C. 2008. Reconciling the chemistry and biology of reactive oxygen species. *Nat Chem Biol*, 4, 278-86.
- WOOD, Z. A., SCHRODER, E., ROBIN HARRIS, J. & POOLE, L. B. 2003. Structure, mechanism and regulation of peroxiredoxins. *Trends Biochem Sci*, 28, 32-40.

- WYNN, T. A. 2008. Cellular and molecular mechanisms of fibrosis. *J Pathol*, 214, 199-210.
- WYNN, T. A. & BARRON, L. 2010. Macrophages: master regulators of inflammation and fibrosis. *Semin Liver Dis*, 30, 245-57.
- WYNN, T. A., CHAWLA, A. & POLLARD, J. W. 2013. Macrophage biology in development, homeostasis and disease. *Nature*, 496, 445-55.
- XIMENES, V. F., KANEGAE, M. P., RISSATO, S. R. & GALHIANE, M. S. 2007. The oxidation of apocynin catalyzed by myeloperoxidase: proposal for NADPH oxidase inhibition. *Arch Biochem Biophys*, 457, 134-41.
- YONA, S., KIM, K. W., WOLF, Y., MILDNER, A., VAROL, D., BREKER, M., STRAUSS-AYALI, D., VIUKOV, S., GUILLIAMS, M., MISHARIN, A., HUME, D. A., PERLMAN, H., MALISSEN, B., ZELZER, E. & JUNG, S. 2013. Fate mapping reveals origins and dynamics of monocytes and tissue macrophages under homeostasis. *Immunity*, 38, 79-91.
- ZANONI, I. & GRANUCCI, F. 2010. Regulation of antigen uptake, migration, and lifespan of dendritic cell by Toll-like receptors. *J Mol Med (Berl)*, 88, 873-80.
- ZHANG, L., YU, L. & YU, C. A. 1998. Generation of superoxide anion by succinate-cytochrome c reductase from bovine heart mitochondria. *J Biol Chem*, 273, 33972-6.
- ZHOU, R., YAZDI, A. S., MENU, P. & TSCHOPP, J. 2011. A role for mitochondria in NLRP3 inflammasome activation. *Nature*, 469, 221-5.
- ZHU, X., MOSE, E. & ZIMMERMANN, N. 2013. Proton channel HVCN1 is required for effector functions of mouse eosinophils. *BMC Immunol*, 14, 24.
- ZIEGLER-HEITBROCK, H. W., FINGERLE, G., STROBEL, M., SCHRAUT, W., STELTER, F., SCHUTT, C., PASSLICK, B. & PFORTE, A. 1993. The novel subset of CD14<sup>+</sup>/CD16<sup>+</sup> blood monocytes exhibits features of tissue macrophages. *Eur J Immunol*, 23, 2053-8.

